Platelet-derived growth factor receptor alpha signaling pathways in development and liver disease

Brian J. Hayes

A dissertation submitted in partial fulfillment of
the requirements for the degree of

Doctor of Philosophy

University of Washington

2014

Reading Committee:
Jean Campbell, Chair
Daniel Bowen-Pope
William Mahoney Jr.

Program Authorized to Offer Degree:
Pathology

University of Washington

Abstract

Platelet-derived growth factor receptor alpha signaling pathways in development and liver disease

Brian J. Hayes

Chair of the Supervisory Committee:

Jean S. Campbell, Assistant Professor

Department of Pathology

Platelet derived growth factor receptor alpha (PDGFRα) signaling is critical for development and disease. Insufficient PDGFRα signal transduction results in developmental anomolies, while excessive signaling results in fibrosis and carcinogenesis. PDGFRα signal transduction is regulated at multiple levels, two of which are ligand binding and *Pdgfrα* expression levels. In my thesis work, I describe a *Pdgfc* mutant mouse, *Pdgfc*^{tm1Lex}, in which only growth factor coding exons are deleted. Viability of *Pdgfc*^{tm1Lex} mice, which express only the complement components C1r/C1s, sea urchin EGF, bone morphogenetic protein 1 (CUB) domain of PDGF-C, depends on the presence of both *Pdgfrα* alleles. Alternative splicing in *Pdgfc*^{tm1Lex} mice gives rise to a truncated transcript that contains the entire coding region of the CUB domain of PDGF-C, but lacks the majority of the exons encoding the growth factor domain (GFD). Contrary to *Pdgfc* knockout (KO) mice, *Pdgfc*^{tm1Lex} mice are viable, suggesting that the CUB domain of PDGF-C contributes to PDGFRα signal transduction. The CUB domain of PDGF-C appears to maintain PDGFRα signal transduction above the minimum level necessary for development.

At the other end of the spectrum, increased PDGFRα signal transduction can contribute to disease. PDGFRα levels are elevated in human liver disease, and after acute and chronic liver injury in mice. These correlative studies indicate that PDGFRα may be important for the

liver's response to injury. Activated hepatic stellate cells (HSCs) produce collagen resulting in fibrosis, which can progress to liver cirrhosis. Cirrhosis is the 12th leading cause of death in the United States, and increases the risk of developing liver cancer. Utilizing a chemical model of fibrosis, chronic carbon tetrachloride (CCl_4) exposure, I found that mice with decreased expression of *Pdgfrα* (*Pdgfrα*$^{WT/nGFP}$) develop less fibrosis, than wild type mice following CCl_4 exposure. These results indicate that elevated *Pdgfrα* expression is associated with chronic liver injury, and suggests excessive PDGFRα signal transduction is detrimental. PDGFRα signal transduction is controlled at the level of ligand binding and gene expression, and needs to be maintained at a balance that allows for proper development, but does not result in fibrotic disease. Therapies targeted to maintain the balance of PDGFRα–specific signaling pathways may provide both sufficient PDGFRα for wound healing and therapeutic benefit for patients with chronic liver disease.

TABLE OF CONTENTS

Page

Abbreviations

BrdU	5-Bromo-2-deoxyuridine
BDL	bile duct ligation
BHK	baby hamster kidney cells
CCl_4	carbon tetrachloride
CRBP-1	cellular retinol binding protein 1
CTGF	connective tissue growth factor
CUB	C1r/C1s sea urchin EGF bone morphogenetic protein 1
ECM	exracellular matrix
EGF	epidermal growth factor
ET-1	endothelin 1
FGF	fibroblast growth factor
GFAP	glial fibrillary acidic protein
GFD	growth factor domain
GFP	green fluorescent protein
Grb2	growth factor receptor-bound protein 2
HCC	hepatocellular carcinoma
HSCs	hepatic stellate cells
IF	immunofluorescence
IHC	immunohistochemistry
KCs	Kupffer cells
LSECs	liver sinusoidal endothelial cells
NAFLD	non-alcoholic fatty liver disease
NPCs	non-parenchymal cells
OPC	oligodendrocyte progenitor cell
Ph	Patch mutant mouse

Abbreviations

PDGF	platelet derived growth factor
PDGFRα	platelet derived growth factor receptor alpha
PDGFRβ	platelet derived growth factor receptor beta
PI3K	phosphoinositol 3-kinase
PLCγ	phospholipase gamma 1
RasGAP	Ras GTPase activating protein
TAA	thioacetamide
TGFβ1	transforming growth factor beta
WT	wild type

List of Figures

List of Figures

Figure Number Page

List of Tables

Chapter 1

Background and Introduction

Summary

This chapter provides background information on 1) the public health burden of liver disease, 2) the functions of parenchymal and non-parenchymal liver cells, 3) mouse models of liver disease, and 4) signaling pathways and molecular components involved in the response to models of hepatotoxic injury and the development of liver fibrosis. A brief synopsis of my thesis project is presented at the end of this chapter.

Liver disease

Chronic liver injury leads to fibrosis, which can progress to cirrhosis and hepatocellular carcinoma (HCC). HCC is the most common type of liver cancer, and develops in cirrhotic liver in 90% of cases (1). The incidence and mortality from liver cancer are both increasing at a rate of around 3% a year (2); five year survival from time of diagnosis is only 16% (2, 3). Underlying cirrhosis in HCC prevents resection, thus the limited therapeutic options for these patients are in part due to the fact that hepatocytes have a reduced capacity to divide in fibrotic livers (4). If cirrhosis progresses to HCC, in most cases transplant is the only effective therapeutic option (5). A better understanding of the molecular mechanisms of fibrosis could lead to therapies to reduce the severity of chronic liver disease, reduce the occurrence of liver failure, make tumor resection a viable option for patients with HCC, or even prevent HCC development.

Liver fibrogenesis occurs when normal injury repair mechanisms, such as fibroblast migration, proliferation, contraction, and extracellular matrix (ECM) deposition, exceed the activity of the pathways that breakdown scar or fibrinolysis. Liver fibrosis most frequently results from alcohol ingestion, hepatitis viruses, and in the increasingly obese population, non-alcoholic fatty liver disease (NAFLD) (6). These conditions cause inflammation, and this chronic

inflammatory state is thought to stimulate the wound healing response of the liver. Fibrosis increases in severity with continued exposure to the injurious agent, and results in liver dysfunction. Cirrhosis is a condition in which severe fibrosis is accompanied by architectural changes in the liver (7). Currently mortality due to cirrhosis in the United States is approximately 30,000 people annually (8). The fact that 40% of patients with cirrhosis are asymptomatic until liver failure occurs decreases the likelihood of lifestyle changes prior to the onset of liver failure (6). Liver failure can systemically affect the body in the form of neurologic disorders, such as hepatic encephalopathy, and cardiovascular effects, such as cardiomyopathies and abnormal regional distribution of blood volume and pressure due to reduced liver functions (9).

The liver performs many essential biological functions, including vitamin A and glycogen storage, bile and blood coagulation factor production, toxin metabolism, iron recycling, lipid transport, and conversion of essential vitamins, such as vitamin D, into usable forms (10-12). Circulation in the liver is unique in that the two-thirds of the blood supply is venous via the portal vein rather than arterial. Because of the unique blood flow through the liver, this organ is exposed to high concentrations of ingested nutrients, toxins, and pathogens. Liver disease inhibits many of the normal functions of the liver.

Liver cell involvement in disease

The liver contains many cell types each with unique functions in homeostasis and disease. Hepatocytes and biliary epithelial cells, parenchymal cells, comprise the majority of the liver. Hepatocytes constitute approximately 52% of the cells in the mouse liver, and perform most of the essential functions of the liver, including glycogen storage and detoxification reactions (13). The remainder of the liver is composed of non-parenchymal cells (NPCs) including liver sinusoidal endothelial cells (LSECs), which make up about 22% of the total cells,

Kupffer cells (KCs, resident macrophages of the liver), which are about 18% of total liver cells, and hepatic stellate cells (HSCs), which are around 8% of the total cells (13). These NPCs together with hepatocytes contribute to proper liver function.

LSECs control blood flow to the hepatocytes and through the liver sinusoids, and are highly fenestrated to allow exchange of solutes and particles from blood to hepatocytes (14). LSECs also play a role in removing soluble particles from blood through receptor-mediated endocytosis (14). Activation of LSECs by inflammatory molecules results in increased portal hypertension due to vasoconstriction, loss of fenestrae, and interaction with HSCs (15). KCs are hematopoietic in origin and comprise 80 to 90% of the body's resident macrophages (16). KCs reside in the sinusoidal space, and identify and remove cell debris and endotoxin from the blood by phagocytosis (14). Activation of KCs by inflammatory stimuli results in the secretion of pro-inflammatory cytokines and eicosanoids, such as tumor necrosis factor alpha, interleukin-6, interleukin-1, and prostaglandin E2, which stimulate hepatocyte proliferation (17-19).

HSCs are normally quiescent and do not divide *in vivo*. HSCs regulate ECM and serve as a major storage site for vitamin A (20). When hepatocytes are injured, HSCs are activated presumably due to cytokines and chemokines produced by KCs and other infiltrating leukocytes. Activation of HSCs is a critical step in the development of liver fibrosis. HSC activation is a state defined by loss of vitamin A, proliferation, and production of ECM (21). The ECM secreted from HSCs is composed mostly of collagen I, collagen III, sulfated proteoglycans, and glycoproteins (22). HSCs respond to signals from LSECs and KCs that lead to wound healing in the liver, and HSC proliferation, contraction, and secretion of ECM subside upon resolution of the injury. Sustained hepatocyte injury leads to prolonged activation of HSCs, which is thought to be the major driver of hepatic fibrosis. Thus manipulation of HSCs should affect the onset, extent and resolution of fibrosis.

Mouse models of chronic liver disease

Liver failure takes decades to develop in humans (6), but can be modeled experimentally over a shorter time frame in rodents. Both rats and mice have been used as preclinical models, given that they recapitulate many aspects of human liver disease (23). Given that murine liver fibrosis develops in weeks to months, this allows a more rapid assessment of the molecular mechanisms that lead to liver disease. Other types of liver disease can be modeled in mice, including chronic inflammation, fatty liver, and hepatocellular carcinogenesis.

In mice damage to hepatocytes, which leads to fibrosis, can be achieved by surgical methods such as bile duct ligation (BDL), or chemical methods such as injection of thioacetamide (TAA) or carbon tetrachloride (CCl_4) (23). BDL is a surgical manipulation induces proliferation of biliary epithelial cells, which in turn induce proliferation of bile ductules, cholestasis, and portal inflammation, which causes fibrosis (23). TAA induces liver fibrosis when it is metabolized to a reactive oxygen species within hepatocytes, but fibrosis development is minimal during the first 6 weeks of exposure (23, 24). The injury resulting from CCl_4 exposure involves central lobular necrosis, and repeated exposure to CCl_4 induces liver fibrosis over the course of weeks (Figure 1.1) (25). The cytochrome P450 enzyme, CYP2E1 is primarily expressed in hepatocytes, and responsible for metabolizing CCl_4 into intermediate products that are toxic to hepatocytes (26). CCl_4 causes waves of hepatocyte death directly following each injection, which indirectly causes fibrosis due to infiltrating neutrophils and KCs, which release cytokines and growth factors that activate HSCs. The fibrosis that develops in the CCl_4 rodent model is fully reversible, in contrast to cirrhosis in humans, in whom most forms of late stage fibrosis and cirrhosis only partially regress with cessation of injury (27, 28). It is important to note that chronic administration of CCl_4 in rats or mice has yet to be associated with an increased risk of HCC, as is the relationship between cirrhosis and carcinogenesis in humans.

Much of our understanding of key regulators of fibrogenesis comes from the use of these models. Many inflammatory cytokines and growth factors are released during liver injury. These include platelet derived growth factors (PDGFs), transforming growth factors (TGFs), epidermal growth factor (EGF), fibroblast growth factors (FGFs), connective tissue growth factor (CTGF) endothelin 1 (ET-1), and interleukins -6, -8, and -10 among others (25, 29). These cytokines and growth factors stimulate liver cell populations to initiate or dampen repair mechanisms. Initially these repair associated proteins are required to respond to injury, however when injury persists these growth factors and cytokines can induce fibrosis. Surgical and chemical models of fibrogenesis correlate increased expression of growth factors and cytokines with fibrogenesis, but genetic manipulation more directly defines the roles of individual pathways to fibrogenesis *in vivo*.

One of the most useful aspects of mice as a preclinical model is the ability to engineer genes for mechanistic and functional studies. Multiple transgenic and knock out mouse models have been used to study liver fibrosis (30); most of these transgenic or knockout mice were combined with surgical or chemical liver injury to uncover a phenotype. Overexpression of TGFβ1 induces liver fibrosis without additional liver injury. TGFβ1 has been over-expressed using albumin, c-reactive protein, and liver-enriched activator protein, all hepatocyte specific promoters (31-35). TGFβ1 transgenic animals often have significant extrahepatic pathologies in addition to liver fibrosis such as early mortality from kidney fibrosis (33, 34). Conditional expression of TGFβ1 in hepatocytes results in activation of HSCs and subsequent fibrosis, thus these mice have not yet been used in long-term studies (35).

Overexpression of PDGF ligands in the liver results in liver fibrosis albeit with subtle phenotypic differences. Transgenic mice expressing PDGF-A or PDGF-B under hepatocyte specific promoters develop liver fibrosis, but do not develop HCC (36, 37). While transgenic mice have not been develop to overexpress PDGF-D in the liver, increased expression of

PDGF-D has been reported to increase macrophage accumulation in the skin and skeletal muscles (38). Therefore PDGF-D has the potential to affect the KC component of the liver. PDGF-C overexpression under control of the albumin promoter, induces progressive fibrosis that leads to HCC (39). This model is unique in its ability to recapitulate this aspect of human liver disease (Figure 1.2). The liver pathology is so severe in this mouse model that the median survival is only 16 months, as opposed to 24 months for wild type animals (Figure 1.3, (40)). The cause of death in these transgenic mice is difficult to determine, however upon necropsy the majority of these animals had liver tumors and hepatomegaly with hemoperitoneum (40). This model highlights the contribution of PDGF-C to development of fibrosis in the liver, and suggests that the PDGF pathway is an attractive potential target to modulate liver fibrosis.

Platelet-derived growth factor ligands and receptors

PDGFs are thought to be the main mitogens for HSCs that are released during liver injury (29, 41). The PDGF family of ligands and receptors play a central role in the development of connective tissue and in repair after injury (42, 43). Enhanced PDGF signal transduction has been reported in multiple human pathologies, including thymoma, pancreatic cancer, ovarian cancer, glioblastoma, dermatofibrosarcoma protuberans, myelodysplastic syndrome, chronic myelomonocytic leukemia and gastrointestinal stromal tumors (44-50).

The PDGF family consists of five ligand dimers, -AA, -AB, -BB, -CC, and –DD, and two receptor tyrosine kinases, PDGF receptor alpha (PDGFRα) and PDGF receptor beta (PDGFRβ) (Figure 1.4) (51). PDGF was originally described as a component present in serum and absent in platelet free plasma that stimulates proliferation in fibroblasts, smooth muscle cells, and glial cells (52-54). The original PDGFs identified were named PDGF-A and PDGF-B (55, 56), and were soon found to be important proteins in the modulation of mesenchymal cell activity. These ligands have similar properties, as both are small (less than 20 kilodaltons), cationic, heat stable,

and form dimers (57). The sequence of PDGF-A and PDGF-B are composed almost entirely of the PDGF growth factor domain (GFD). More recently, PDGF-C and PDGF-D, were identified expanding the ligand family to 4 separate genes (58-61). These two new ligands contain the same domain as PDGF-A and PDGF-B in the C-terminus of the protein, a conserved 110 amino acid sequence, but have an additional N-terminal complement components C1r/C1s, sea urchin epidermal growth factor, and bone morphogenetic protein 1 (CUB) domain (62). Despite their sequence and structural similarities, these four ligands have different receptor binding affinities *in vitro* (58-61, 63, 64). PDGF-AA, -AB, -BB, and -CC bind to the α-receptor and induce PDGFRαα dimerization. PDGF-BB and PDGF-DD induce dimerization of PDGFRββ, and -AB, -BB, and -CC induce αβ-receptor dimerization (65).

The major structural difference between PDGF-C and PDGFs -A and -B is the presence of the N-terminal CUB domain. CUB domains were first recognized by sequence homology comparing extracellular proteins involved in fertilization, development, and proteolysis (66, 67). Since their discovery, they have been shown to be important for interacting with developmentally important ligands, such as sonic hedgehog, bone morphogenetic protein 4, and semaphorin (68-71), as well as for binding substrates for proteases (72, 73). Additionally proteins with CUB domains have been shown to be important for absorption and reabsorption of essential vitamins and plasma proteins (74). At present, the contributions of the CUB domain to PDGF signaling are unknown. Cleavage of the CUB domain from the GFD of PDGF-C is thought to be required to allow GFD binding to PDGFRα and subsequent signal transduction events (58, 59). In this model the CUB domain acts in an inhibitory capacity. Interestingly, bacterially expressed PDGFC CUB domain has been reported to stimulate proliferation of human coronary artery smooth muscle cells, suggesting a possible additional role for the CUB domain (75). Tissue specific overexpression of the CUB domain in the mouse heart, however, has no obvious phenotype (76).

The PDGF signal transduction pathway is precisely regulated, and slightly increasing or decreasing PDGFR activity leads to significant abnormalities in mice. PDGFRs dimerize upon ligand binding, resulting in autophosphorylation of the intracellular receptor domain, which initiates activation of downstream kinases including Src, phosphoinositol 3-kinase (PI3K), SHP-2, and phospholipase gamma 1 (PLCγ) (77, 78). PDGFRβ additionally phosphorylates growth factor receptor-bound protein 2 (Grb2) and Ras GTPase activating protein (RasGAP) (Figure 1.4) (78). Removing only the PI3K phosphorylation site of PDGFRβ significantly reduces the number of vascular pericytes (78), while removing the PI3K phosphorylation site from PDGFRα causes lethality in all homozygous mice by P16 (77). These data indicate that the PDGFRs have independent functions despite phosphorylating the same intracellular kinase.

Deletion of one allele of either receptor has also been shown to have detrimental effects, but appears to be cell-specific (79-82). Chimerism analysis measures the contribution of embryonic stem cells to the embryo after injection into a blastocyst. By this method, it has been show that *Pdgfrβ* is important for the development of smooth muscle cells in the aorta, renal arteries, stomach, and intestines as well as capillary pericytes and cardiac and skeletal muscle (79). Deletion of one allele of *Pdgfrα*, and the resultant heterozygosity, reveals that some cell types are more sensitive to loss of one *Pdgfrα* allele than others. In *Pdgfrα*$^{+/-}$ chimeras, tail biopsies and germline transmission show expected levels of chimerism. Contribution to coat color in *Pdgfrα*$^{+/-}$ chimeras is low however, suggesting that the cells with a *Pdgfrα*$^{+/+}$ genotype are more fit to contribute to coat color than are heterozygous *Pdgfrα* cells (80). Another *Pdgfrα* sensitive cell type is the oligodendrocyte progenitor cell (OPC). The number of OPCs is decreased in mice with reduced copy number of *Pdgfrα,* and differentiation of OPCs into oligodendrocytes is increased (81, 82). When heterozygous *Pdgfrα* mice are bred to mice with mutations in PDGF ligands that bind PDGFRα (83), or mutations in immediate early genes directly downstream of PDGFRα (84), there is an additive effect on development.

Deleting PDGF ligands individually in mice results in severe developmental deficiencies, suggesting a lack of redundancy between PDGFs despite their overlapping receptor binding affinities (85-87). Deleting PDGF-A has an effect on lung development that results in lethality (85), while deletion of PDGF-B affects the vascular and hematopoietic systems (86). Deletion of PDGF-C affects the migration of the neural crest cells that form the palate (87). Deleting multiple ligands, such as PDGF-A and PDGF-C, results in an additive effect on development (87). Of the four PDGF ligands, most research has been focused on the dimer PDGF-BB, due to its similarity to the oncogene v-sis and its ability to bind and activate both PDGFRα and PDGFRβ (88, 89). As mentioned above, increasing the expression of PDGF-B in the liver causes fibrosis, but does not result in HCC (37), similar to the phenotype of increased PDGF-A expression in the liver (36). In contrast, increasing expression of PDGF-C leads to progressive fibrosis followed by HCC (39). The PDGF-C transgenic mouse model suggests that the CUB domain and PDGF-C's receptor, PDGFRα, have important functions in induction of severe liver fibrosis and progression to HCC.

Hypothesis

This chapter highlights the importance of PDGF signal transduction in the activation of HSCs in response to hepatocyte injury. However, why PDGF-C elicits a different response than PDGF-A, and the specific contribution of PDGFRα to liver fibrosis remain to be determined. My first hypothesis is that the CUB domain of PDGF-C functions to amplify PDGFRα signal transduction. I addressed this hypothesis with experiments described in chapter 2. I utilized two mouse models; one in which the growth factor domain of PDGF-C is removed systemically, and one in which one allele of PDGFRα is replaced with GFP systemically. My second hypothesis is that PDGFRα signal transduction is a primary cause of liver fibrosis. For the experiments described in chapter 3, I again used the mouse model in which one allele of PDGFRα is

replaced with GFP, this time in combination with CCl_4-induced liver injury to investigate the role of PDGFRα in liver fibrosis.

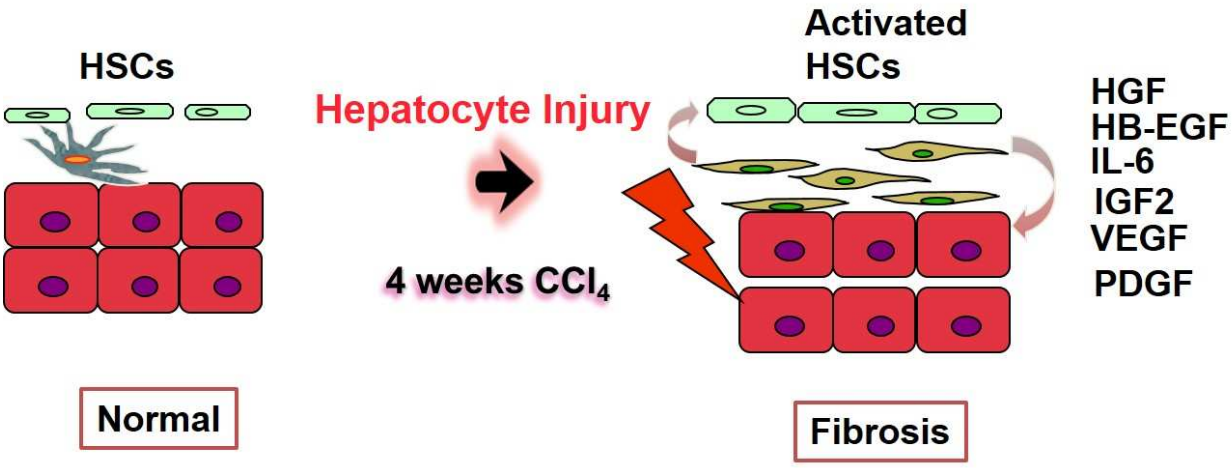

Figure 1.1. Carbon tetrachloride mouse model of liver fibrosis. Mice are injected with the hepatotoxin carbon tetrachloride (CCl_4) twice weekly for 4 weeks to induce liver injury and fibrosis

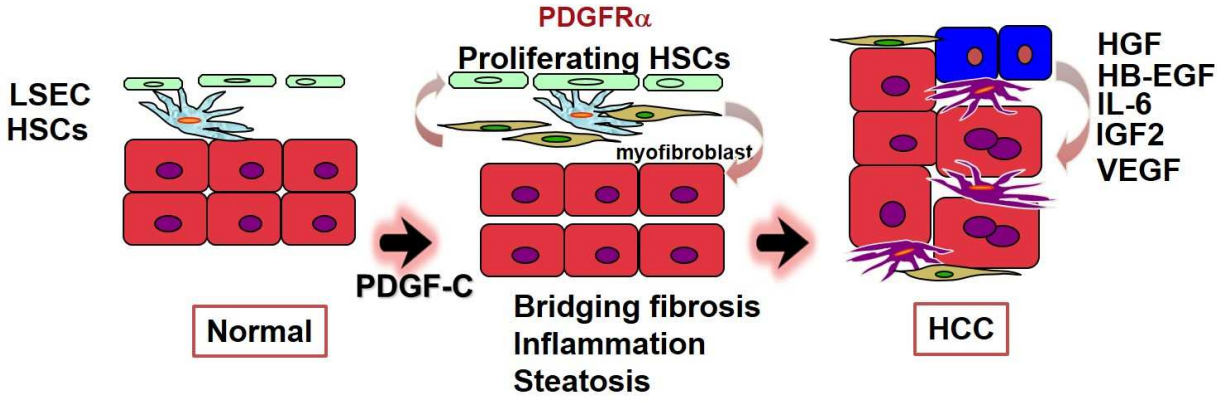

Figure 1.2. PDGF-C transgenic mouse model of liver fibrosis. Expression of human PDGF-C under the albumin promoter/enhancer induces progressively severe fibrosis which eventually develops into HCC.

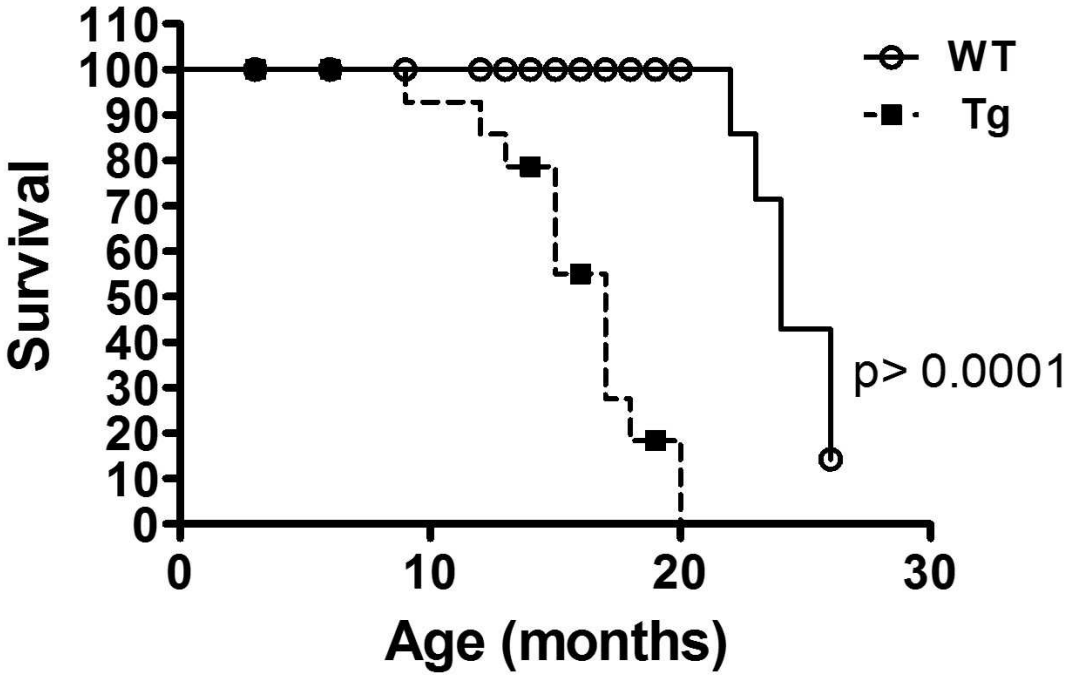

Figure 1.3. PDGF-C transgenic mouse Kaplan-Meyer survival curve. Mice expressing human PDGF-C transgene (dashed line) have a median survival of 16 months (n=10), while wild type mice had an approximate median survival of 24 months (n=16). Note: wild type mice were killed at 24 months (40).

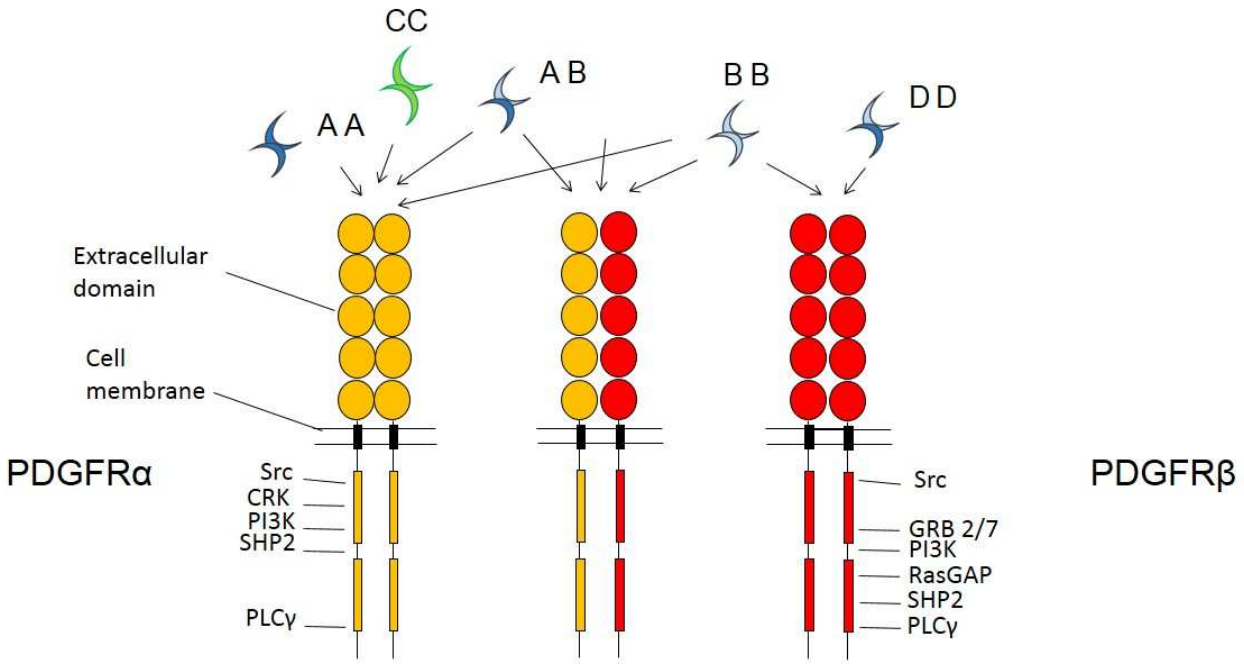

Figure 1.5. PDGFR induced intracellular kinase phosphorylation. PDGFRαα dimerization phosphorylates Src, Crk, PI3K, SHP2, and PLCγ, while PDGFRββ does not phosphorylate Crk and does phosphorylate GRB2 and RasGAP.

Chapter 2

Function of the CUB domain in PDGF-C knockout mice

Abstract

Platelet derived growth factors (PDGFs) are necessary for normal development. Here we report a *Pdgfc* mutant mouse in which only growth factor coding exons are deleted. Alternative splicing gives rise to a truncated transcript that contains the entire coding region of the complement components C1r/C1s sea urchin EGF bone morphogenetic protein 1 (CUB) domain of *Pdgfc,* but lacks the majority of the exons encoding the growth factor domain (GFD). This mutant *Pdgfc* mouse is viable, and a mutant protein is translated from the truncated sequence *in vitro.* Viability of mice expressing only the PDGF-C CUB domain depends on the presence of both *Pdgfrα* alleles, however.

Introduction

The platelet derived growth factor (PDGF) family has important functions in development, as evidenced by the fact that mice lacking PDGF receptor (PDGFR) -α or –β are embryonic lethal (80, 90). PDGFRα is important for skeletal development and neural crest migration (80, 91), while PDGFRβ is vital for kidney and hematologic development (90). The four ligands, PDGF-A, -B, -C, and –D, are secreted as dimers and induce homo- or hetero-dimerization of PDGFRs. *In vitro* studies demonstrate that PDGF-AA, -BB, and -CC have high affinities for PDGFRα and induce αα dimerization. PDGF-BB and PDGF-DD induce dimerization of PDGFRβ; -AB, -BB, and -CC induce αβ-receptor dimerization (92). Mutation of *Pdgf –a, -b,* or *–c* results in perinatal lethality in homozygous knockout (KO) animals, though live births are seen in *Pdgfa* and *Pdgfc* KO mice (85-87). As predicted by *in vitro* binding studies, *Pdgfb* KO mice have a phenotype similar to *Pdgfrβ* KO mice (86). Mice lacking PDGFA, however, have a defect in lung development (85), while *Pdgfrα* KO mice show skeletal abnormalities (80). The previously described *Pdgfc* KO animals, termed $Pdgfc^{tm1Nagy}$, have a defect in palate formation, which may

interfere with feeding and contribute to perinatal demise (87); this phenotype depends on genetic background (93-95). Further, *Ding et al.* reported that *Pdgfa* and *Pdgfc* double KO mice have a phenotype similar to *Pdgfrα* KO mice (87).

PDGF-AA, PDGF-BB, and PDGF-AB are secreted as active dimers (96), while PDGF-CC and PDGF-DD are secreted as inactive homodimers requiring extracellular cleavage of an N-terminal complement components C1r/C1s sea urchin EGF bone morphogenic protein 1 (CUB) domain to allow receptor binding (Figure 2.1a)(58-61). All PDGFs share a common growth factor domain (GFD), which is 110 amino acids long and contains 8 conserved cysteines that facilitate intra- and intermolecular disulfide bonds (62). Mutations of these cysteines cause loss of disulfide bonds and thus a lack of PDGFR signal transduction (97, 98). Furthermore, mutations in loops I, II, or III of the GFD decrease its ability to bind PDGFRs (99-101). Effective signal transduction by PDGF-CC thus should require the conserved cysteines and loops I-III, as well as cleavage of the CUB domain. We describe a *Pdgfc* mutant mouse wherein only the GFD is deleted, and show that expression of the CUB domain alone is sufficient for viability.

Materials and Methods

Mouse Models

The *Pdgfc* locus was isolated from a 129S5/SvEvBrd genomic BAC library. The targeting construct replaced a 5 kb genomic region on chromosome 3 with an IRES LacZ MC1 Neo cassette. The homologous arms consisted of a 3 kb 5' fragment and a 2.1 kb 3' fragment. Lex-1 129S5/SvEvBrd ES cells were transfected with the targeting construct and injected into C57BL/6 blastocysts to generate chimeras. Chimeras were bred to albino C57BL/6J-*Tyr*$^{c\text{-}2J}$ mice (The Jackson Laboratory) to generate F1 progeny. F1 hybrids were crossed to generate initial Mendelian ratios (shown in Table 1). Mice were further backcrossed to a C57BL/6 background

six times to generate the Mendelian ratio for C57BL/6 (Table 1). These mice can be obtained from the Mutant Mouse Regional Resource Centers (http://www.mmrrc.org/index.php) supported by the NIH. Hemizygous *Pdgfrα* mice, *Pdgfra*$^{tm11(EGFP)Sor}$, were purchased from The Jackson Laboratory (stock # 007669). Animals were housed at the University of Washington, which is an Association for the Assessment and Accreditation of Laboratory Animal Care approved facility, and all experiments were performed with University of Washington Institutional Animal Care and Use Committee approval.

Necropsy and Histology

Homozygote *Pdgfc*^{tm1Lex} mice (n=4) and WT C57BL/6 littermates (n=4) aged 5 and 8 weeks were euthanized by CO_2 asphyxiation followed by complete necropsy. Blood was collected for chemistry and complete blood counts performed by Phoenix Central Laboratories (Everett, WA). Tissues were collected for histological analysis with immersion fixation in 10% phosphate-buffered formalin, 4-6µm sections were made and stained with hematoxylin and eosin. Tissues examined included: lungs, esophagus, trachea, liver, kidneys, heart and great vessels, adrenal glands, gallbladder, brown and white adipose tissue, exocrine and endocrine pancreas, spleen, thyroid, submandibular, parotid and sublingual salivary glands, mesenteric lymph nodes, mesentery, preputial or clitoral glands, skeletal muscle, bladder, male accessory sex glands, testes or ovaries, haired skin, large and small intestine, glandular and non-glandular stomach, uterus and cross section of the head (eyes, middle and internal ears, oral and nasal cavities, cerebrum, cerebellum, olfactory lobes, brain stem, pituitary, tongue and teeth). All tissues were examined by a board-certified veterinary pathologist (PMT) and given a morphological diagnosis where applicable. Skeletons were processed by eviscerating, removing the brain and as much muscle tissue and fat as possible, followed by immersion in 95% ethanol for at least 72 hours, placed in acetone overnight, and stained the next night at 37℃ with a solution of 70% ethanol, 5%

glacial acetic acid, 11.6 µM Alcian blue, and 14.6 µM Alizarin red. The following day the skeletons were washed in 95% ethanol and cleared in 2% KOH for 2 days and transferred to 1% KOH until fully cleared, with the solution refreshed every 2 to 3 days until soft tissues were cleared, at which point the skeletons were transferred to 100% glycerol.

Genotyping

Genomic DNA was extracted from mouse tails by incubation overnight at 55℃ in 20µg/ml Proteinase K (Invitrogen) in lysis buffer (200mM NaCl, 1% W/V SDS, 10mM Tris-HCl, 1mM EDTA pH 8.0). Phenol chloroform extraction was performed, followed by ethanol precipitation and resuspension in Tris-HCl 10mM EDTA 1mM pH7.4 (TE). Polymerase chain reaction was carried out with 0.5 U Gemtaq (MGQuest), supplied 5x buffer, and dNTPs to a final concentration of 0.2mM with primers 5' CCTGGTCAAGCGCTGTGG 3'(200nM), 5' TCTGGATTCATCGACTGTGG 3'(200nM), 5' ACGGCTAACATGGAGCACG 3' (100nM). All primers were designed using Oligo Calc (102). Cycling conditions were 95℃ for 3 min, and 35 cycles of 95℃ for 20 sec, 60℃ for 30 sec, and 72° C for 30 sec with a final extension at 72℃ for 10 min.

Southern blotting

The targeting construct was verified using standard methods as described (103). Briefly, genomic DNA was extracted as described above, and purified DNA was restriction digested using EcoR1 HF (New England Biolabs) at 37℃ overnight. 10µg of DNA from *Pdgfc*^{tm1Lex} homozygous, heterozygous, and wild type (WT) mice was loaded onto a Tris-acetate-EDTA (TAE) gel. Following electrophoresis the gel was denatured in 0.4M NaOH, 1.5 M NaCl for 10min followed by neutralization in Tris HCl with 1.5M NaCl, pH 7.4. DNA was transferred to Hybond N+ (GE Healthcare) nylon membrane in 10x SSC and cross-linked in a Stratalinker

1800 (Stratagene). Exonic DNA including exon 6 and the 3' UTR was used as a probe amplified by 5' CCTTTTAGGTCCTTCAGTTGAGACC 3' and 5' ATCTATGCAAACAGGTTGGAGAAATCC 3'. The probe was labeled with 50µCi [α-^{32}P] dCTP using random decamers (DECAprime II, Ambion) to a specific activity >10^8dpm/µg. The blot was prehybridized with Quickhyb (Stratagene) at 68℃ for 30 min and then incubated with denatured probe (10^6dpm/ml) at 68℃ for 2 hr. Labeled membranes were then washed in 2x SSC with 0.1% SDS and 0.2x SSC with 0.1% SDS at 60℃ for 30 min each. The sizes of the digested genomic DNA were confirmed by comparison with ^{32}P-dCTP end-labeled λ Hind III DNA marker (Fermentas).

RT-PCR analysis

Tissues were collected and flash frozen immediately in liquid nitrogen. RNA was extracted with Trizol (Invitrogen) per the manufacturer's instructions, and cDNA synthesized from 0.5µg RNA. Primers (F1) 5' CTCACGTGTGCTGCTACGAAGG 3' and (R3) 5' CCCTGCGATTCTCTGCTGCC 3' were used with the following conditions; 95℃ for 3 min, and 35 cycles of 95℃ for 15 sec, 58℃ for 15 sec, and 72℃ for 30 sec with a final extension at 72℃ for 10min.

Cloning

WT and *Pdgfc*^{tm1Lex} mouse cDNA was amplified with primers 5' GCCCTCGCCCCAGTCAGC 3' and 5' CTCACGTGTGCTGCTACGAAGG 3' to generate *Pdgfc* and *Pdgfc*^{tm1Lex} sequences, and WT cDNA was amplified with primers 5' ATGGTGGTGAATCTAAATCTCCTC 3' and 5' CTCACGTGTGCTGCTACGAAGG 3' to generate the *GFD* alone. Additionally, a sequence containing a Kozak sequence and the *Pdgfc* signal peptide for secretion was added to the 5'

end of the *GFD* by amplification (*i.e.* 5' GCAGAATTGCCACCATGCTCCTCCTCGGCCT-CCTCCTGCTGACATCTGCCCTGGCCGGCCAAAGAACGGGGACTCGGGCTGAGTCC 3')

The *Pdgfc, Pdgfc*^{tm1Lex}, and *GFD* sequences were cloned separately into pEF1/*myc*-His B (Life Technologies) plasmids, but retained the termination codons which prevent translation of the myc-His tag. The plasmids were linearized with Mlu I (New England Biolabs).

Transfection

Cells [HEK293](ATCC® CRL1573™) were maintained at 37℃ 95 % humidity with 5% CO_2. Transfections were performed using the calcium phosphate method as described (104), and the cells were subjected to 500 µg/ml G418 (Life Technologies) for two weeks to select for cells expressing the following constructs: empty vector (pEF1empty), pEF1Pdgfc^{GFD} , pEF1Pdgfc^{mut}, or pEF1Pdgfc^{FL} to produce untagged proteins, PDGF-C^{GFD}, PDGF-C^{mut} and PDGF-C^{FL} respectively. Confluent cultures were allowed to condition media for 24 hours, at which point media were collected and frozen at -80℃.

Immunoblot analysis

SDS-PAGE and immunoblotting were carried out as described (105). Membranes were incubated with goat anti-mouse PDGF-C antibody (1:1,000, AF1447 R&D Systems) followed by incubation with an anti-goat horseradish peroxidase (HRP) conjugated secondary antibody and detection performed with ECL (Pierce).

Results

Homologous recombination targeting strategy

We examined a *Pdgfc* knockout mouse that was generated using a targeting strategy, in which only the GFD exons 4 and 5 are deleted, *Pdgfc*^{tm1Lex} (Figure 2.1b). Surprisingly, a viable mouse

resulted from this approach in contrast to the aforementioned *Pdgfc* KO mice with perinatal lethality (*Pdgfc*^{tm1Nagy}, Figure 2.1c). Figure 1a shows the protein domain structure of PDGF-C and, compares the two different targeting approaches used to generate knockout mice. *Pdgfc*^{tm1Lex} mice were derived from a 129S5/SvEvBrd embryonic stem cell line (Lex1) targeted by homologous recombination to replace exons 4 and 5. This strategy eliminates transcription of the GFD. *Pdgfc*^{tm1Nagy} mice were derived from R1 embryonic stem cells targeted by homologous recombination to replace exon 2 of *Pdgfc* with a SA-IRES-β-geo-pA cassette (87). This strategy prevents transcription downstream of β-geo, including the CUB and GFD.

Anatomic characterization

Originally derived on a 129S5/SvEvBrd background, *Pdgfc*^{tm1Lex} mice were backcrossed to a C57BL/6 background. Homozygous F1 C57BL/6 x 129S5/SvEvBrd Pdgfc^{tm1Lex} progeny had a hunched appearance, and gross skeletal analysis demonstrated spina bifida (Figure 2.2a and 2.2b), which was confirmed by histology (data not shown). All other organs were grossly normal. After six backcrosses, no overt anatomical differences were noted between homozygous *Pdgfc*^{tm1Lex} mice and WT C57BL/6 littermates, *i.e.* the spina bifida phenotype was rescued. Comprehensive histological analyses (see methods) conducted on 5 and 8-week old *Pdgfc*^{tm1Lex} homozygous mice were unremarkable or showed incidental lesions, such as dermatitis or mild multifocal extramedullary hematopoiesis in the liver, which are known to be associated with the C57BL/6 background (106). Brains of *Pdgfc*^{tm1Lex} mice were examined histologically and did not differ from those of WT littermates; clinical chemistry and blood counts were also unremarkable (data not shown).

Verification of recombination

To confirm that our selection cassette was targeted correctly, we performed Southern blotting on genomic DNA isolated from homozygous *Pdgfc*^{tm1Lex}, heterozygous *Pdgfc*^{tm1Lex}, and WT littermates. EcoRI digestion should produce a 12.4 kb band encompassing exons 4, 5, 6, and the 3' untranslated region (UTR) from WT mice, and a 6.5 kb band including exon 6 and the 3' UTR in correctly targeted *Pdgfc*^{tm1Lex} mice (Figure 2.2c). A ^{32}P labeled DNA probe with a complementary sequence to exon 6 and the 3' UTR of *Pdgfc* was used to detect these 12.4 and 6.5 kb bands by hybridization (Figure 2.2d).

Pdgfc^{tm1Lex} transcription and translation

Given our Southern blotting results, we next verified production of the expected Pdgfc^{tm1Lex} transcript, which should lead to transcription of exons 1, 2, and 3 of *Pdgfc* (Figure 2.1c). Attempts to amplify a transcript containing exon 3 and the internal ribosomal entry site (IRES) (Figure 2.3a, primers F1 and R1) or *lacZ* (Figure 2.3a, F1 and R2) did not produce a product (data not shown), suggesting the targeting construct may have facilitated skipping the splice acceptor in the KO cassette. RT-PCR of *Pdgfc*^{tm1Lex} cDNA using primers F1 and R3 (Figure 2.3a), however, generated a 296 bp band consistent with a transcript in which exons 4 and 5 are skipped, but exon 6 remains (Figure 2.3b). Sequencing this amplicon confirmed that the region corresponding to WT exons 4 and 5 was removed, and exon 6 was spliced in frame to the 3' end of exon 3 to create a truncated transcript (Figure 2.4). To detect the full-length coding region of *Pdgfc*, we designed primers to anneal to the 5' and 3' UTRs, and found that the *Pdgfc*^{tm1Lex} transcript retains the endogenous 5' and 3' UTRs (Figure 2.3a, F2 and R4) and associated regulatory elements (data not shown).

The mutant transcript is expected to have an expression pattern similar to WT *Pdgfc*, given that the selection cassette was targeted to avoid *Pdgfc* 5' and 3' regulatory elements. The protein product of *Pdgfc*^{tm1Lex} is expected to contain the entire CUB domain and the C-terminal 38

amino acids of the GFD with a predicted molecular weight of 22.5 kDa. HEK293 cells transfected with plasmids that express the coding regions for *Pdgfc* (PDGF-C^{FL}), *Pdgfc^{tm1Lex}* (PDGF-C^{mut}), or *GFD* (PDGF-C^{GFD}) secrete proteins of the predicted molecular weights into culture media, as determined by immunoblot analysis (Figure 2.3c).

Genotype ratios

We observed normal Mendelian ratios in the offspring of heterozygote *Pdgfc^{tm1Lex}* breeding pairs on two genetic backgrounds (Table 1). We did not observe premature death in Pdgfc^{tm1Lex} mice up to 12 months of age, and did not see sex-dependent differences in viability on the C57BL/6 background, as has been reported for *Pdgfc^{tm1Nagy}* mice (94). Similar to Fredriksson *et al.*, we observed a statistically significant decrease in body mass in C57BL/6 Pdgfc^{tm1Lex} mice at 3 and 7 months (a 17 to 24% decrease, data not shown). To determine whether PDGFRα is necessary for normal development of *Pdgfc^{tm1Lex}* mice, we intercrossed hemizygous *Pdgfrα* mice with heterozygous *Pdgfc^{tm1Lex}* mice. Progeny resulting from this cross did not include mice that were homozygous *Pdgfc^{tm1Lex}*; hemizygous *Pdgfrα* (Table 2). Neonatal mice homozygous for *Pdgfc^{tm1Lex}* and hemizygous for *Pdgfrα* were born, but failed to thrive and 100% died prior to the age of weaning. Histological and gross anatomical analysis of these neonatal animals revealed severe spina bifida encompassing a region from vertebrae T11 to L1. In contrast to reports for *Pdgfc^{tm1Nagy}* mice these homozygous *Pdgfc^{tm1Lex}*; hemizygous *Pdgfrα* mice had a macroscopically normal palate. Palatoschisis in these mice was only detected upon microscopic analysis. This result is surprising, as hemizygous *Pdgfrα* mice are phenotypically normal (80, 107); we thus conclude that *Pdgfc^{tm1Lex}* viability requires two alleles of *Pdgfrα*. These genetic data indicate that PDGF-C^{mut} interacts with PDGFRα in some novel way, as *Pdgfc^{tm1Nagy}* mice have reduced viability, while *Pdgfc^{tm1Lex}* mice have lethality only in conjunction with hemizygous *Pdgfrα*.

Discussion

PDGF signaling is essential for normal development. In this study we characterized a new PDGF-C mutant mouse strain and demonstrate that *Pdgfc*^{tm1Lex} mice are viable in two backgrounds, C57BL/6 x 129S5/SvEvBrd and C57BL/6. The targeting strategy in this mouse results in alternative splicing to generate a mutant form of *Pdgfc* that lacks over 60% of the GFD, but expresses the entire CUB domain. Two alleles of PDGFRα are necessary for viability of *Pdgfc*^{tm1Lex} mice as mice that are homozygous for *Pdgfc*^{tm1Lex} and hemizygous for PDGFRα die within days of birth. Our results suggest that the CUB domain of PDGF-C performs a function in PDGFRα signaling.

Given that the paralogs PDGF-A and PDGF-B require cysteines for dimerization and intramolecular and intermolecular folding (97, 98), we hypothesize that the *Pdgfc*^{tm1Lex} product (PDGF-C^{mut}), lacking 6 of the 8 conserved cysteines, would have compromised GFD activity. PDGF-C^{mut} is also missing the paralogous loop I of the GFD, which is necessary for receptor binding by PDGF-B (99). Loop I has been shown to be critical for receptor activation by the PDGF orthologs placental growth factor (PlGF) and vascular endothelial growth factor B (VEGFB), as well as the viral protein VEGFE$_{NZ-7}$ (108, 109). Loop III remains in PDGF-C^{mut}, but is not expected to bind PDGFRα in the absence of loop I. Additionally, PDGF-C^{mut} lacks arginine 231, which has specifically been shown to be critical for cleavage of the CUB domain (58, 59). All of these structural differences suggest that PDGF-C^{mut} would not interact with PDGFRα in the same manner as does PDGF-CC.

Genetic background has a profound effect on PDGF signaling. For example, the Patch mutant mouse (*Ph*), in which *Pdgfrα* is deleted, has a phenotype that varies with background. C57BL/6 homozygous *Ph* mice die earlier in development than do *Ph* mice on a CBA, BALB/C, or DBA background (80, 81). Though our observations may be due in part to strain differences,

Pdgfc^{tm1Lex} and *Pdgfc*^{tm1Nagy} mice appear to have different viabilities and phenotypes. *Pdgfc*^{tm1Nagy} shows developmental abnormalities on a 129S1/Sv*129X/SvJ background, specifically palate formation defects resulting in lethality, but is viable on a C57BL/6 background (93, 94). Future experiments are needed to determine whether *Pdgfc*^{tm1Nagy} mice on C57BL/6 background require two PDGFRα alleles.

Our conclusion that the CUB domain of PDGF-C has a function is consistent with reports that the PDGF-C CUB domain stimulates proliferation in human coronary artery smooth muscle cells (75), and that CUB domains of other proteins are involved in a diverse range of functions, including complement activation, developmental patterning, tissue repair, axon guidance and angiogenesis, cell signaling, fertilization, hemostasis, inflammation, neurotransmission, receptor-mediated endocytosis, and tumor suppression (69, 110-113). The availability of *Pdgfc*^{tm1Lex} mice will facilitate genetic screens, alone or in conjunction with *Pdgfc*^{tm1Nagy} mice or other mutants, to determine the biological functions of the PDGF-C CUB domain.

Acknowledgments

Grant support: NHLBI, Cardiovascular Pathology training grant (NIH-HL007312) and HHMI program in Molecular Medicine (BJH), Herbert Coe Foundation, American Surgical Association Foundation, and the American College of Surgeons (KJR), Drug Metabolism Transport and Pharmacogenetics Research Fund in the School of Pharmacy, University of Washington (EJK), NCI, Mechanisms of PDGF-C induced HCC (NIH-CA127228) (JSC).

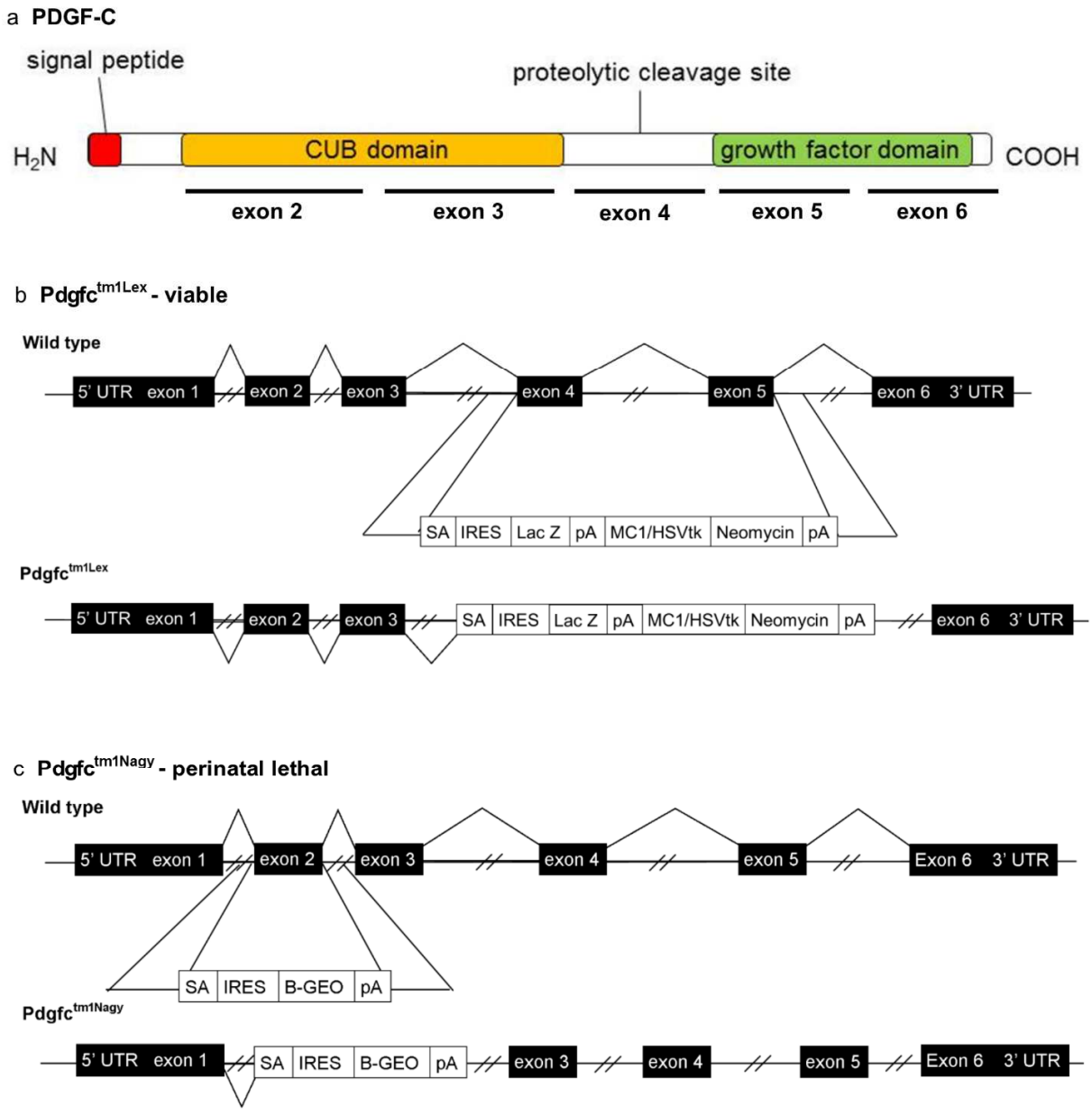

Figure 2.1 Design of targeting constructs to inactivate PDGF-C. a) A linear diagram of the PDGF-C protein showing the CUB (orange) and GFD (green) above the exons that that correspond to these protein domains. b) The targeting strategy for *Pdgfc*^{tm1Lex} mice, which removes exons 4 and 5. c) The targeting strategy for the *Pdgfc*^{tm1Nagy} strain, which removes exon 2 (Ding *et al.*, 2004). Abbreviations : splice acceptor (SA), internal ribosomal entry site (IRES), complement components C1r/C1s sea urchin EGF bone morphogenic protein 1 (CUB), beta galactosidase neomycin fusion protein (βGEO), poly (A) tail (pA), Lac Z gene encoding beta galactosidase (Lac Z), the enhancer, promoter, and neomycin phosphotransferase (MC1/ HSVtk and Neomycin).

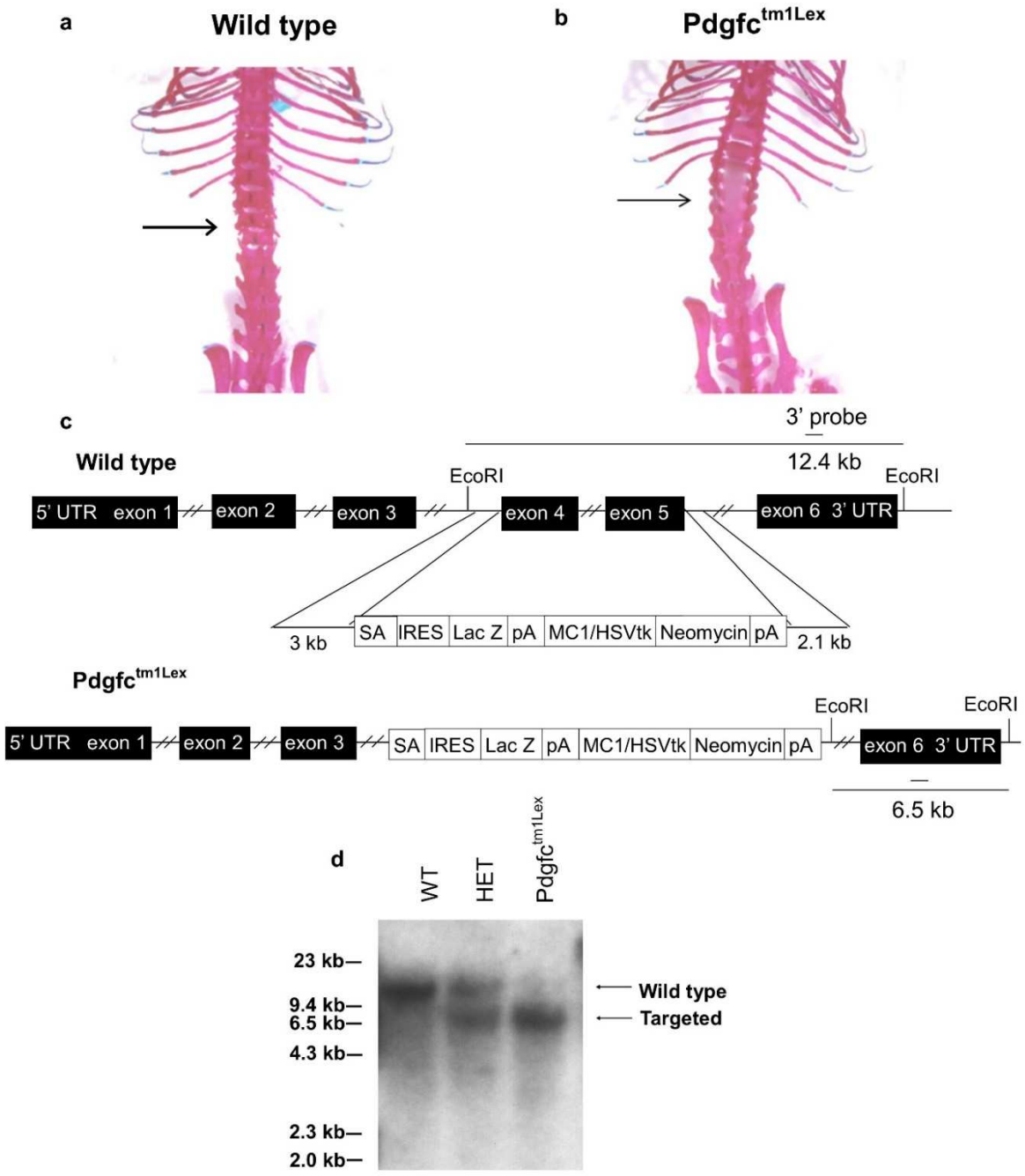

Figure 2.2 Recombination at the *Pdgfc* locus in the Pdgfc^{tm1Lex} mouse. a) 129Sv/EvBrd x C57BL/6 F1 cross results in normal thoracic and lumbar vertebrae in wild type. b) Spina bifida in the thoracic and lumbar region (arrow) of Pdgfc^{tm1Lex} Homozygous mice. c) The anticipated results from EcoR1 digestion of genomic DNA from a wild type mouse and a *Pdgfc*^{tm1Lex} mouse. Genomic DNA from wild type mice is expected to result in a 12.4 kb band, and *Pdgfc*^{tm1Lex} DNA is expected to produce a 6.5 kb band after digestion with Eco RI. d) Southern blot of genomic DNA digested with EcoRI from wild type, heterozygous, and homozygous *Pdgfc*^{tm1Lex} mice.

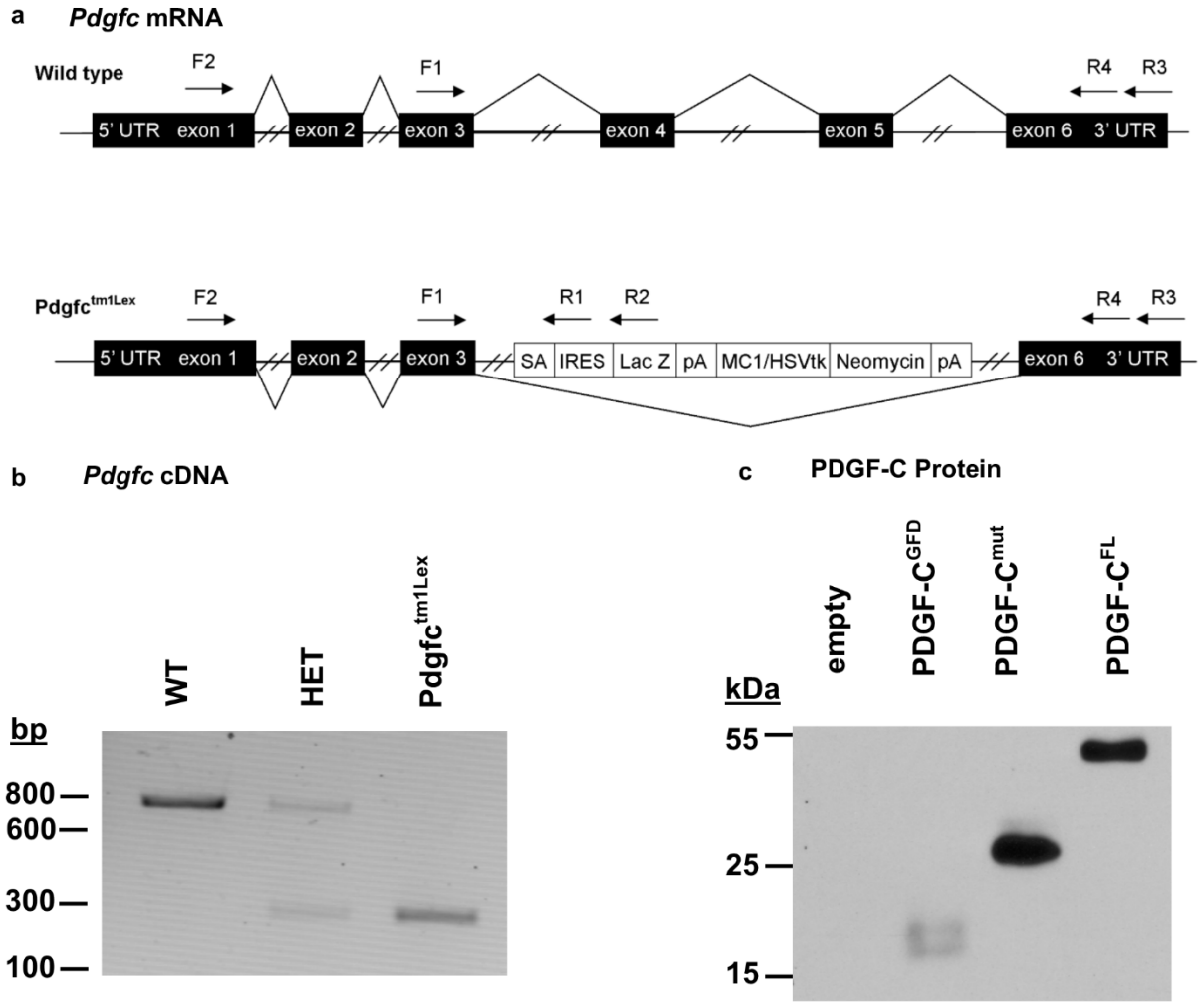

Figure 2.3 Alternative mRNA transcribed from the *Pdgfc* locus in *Pdgfc*^{tm1Lex} mice. a) Diagram of the splicing of wild type and mutant *Pdgfc* with various PCR primers (F1, F2, R1, R2, R3, and R4) used to detect transcripts. b) Amplicons generated by RT-PCR of RNA from kidneys of wild type, heterozygous, and homozygous Pdgfc^{tm1Lex} mice are shown, producing products of 722 bp for *Pdgfc* and 296 bp for *Pdgfc*^{tm1Lex}. c) Immunoblot of media from transfected HEK 293 cells expressing the coding sequences for an empty vector (empty), the *GFD* (PDGF-C^{GFD}), *Pdgfc*^{tm1Lex} (PDGF-C^{mut}), or *Pdgfc* (PDGF-C^{FL}). The size of DNA ladder (b) and protein standards (c) are shown to the left of each image.

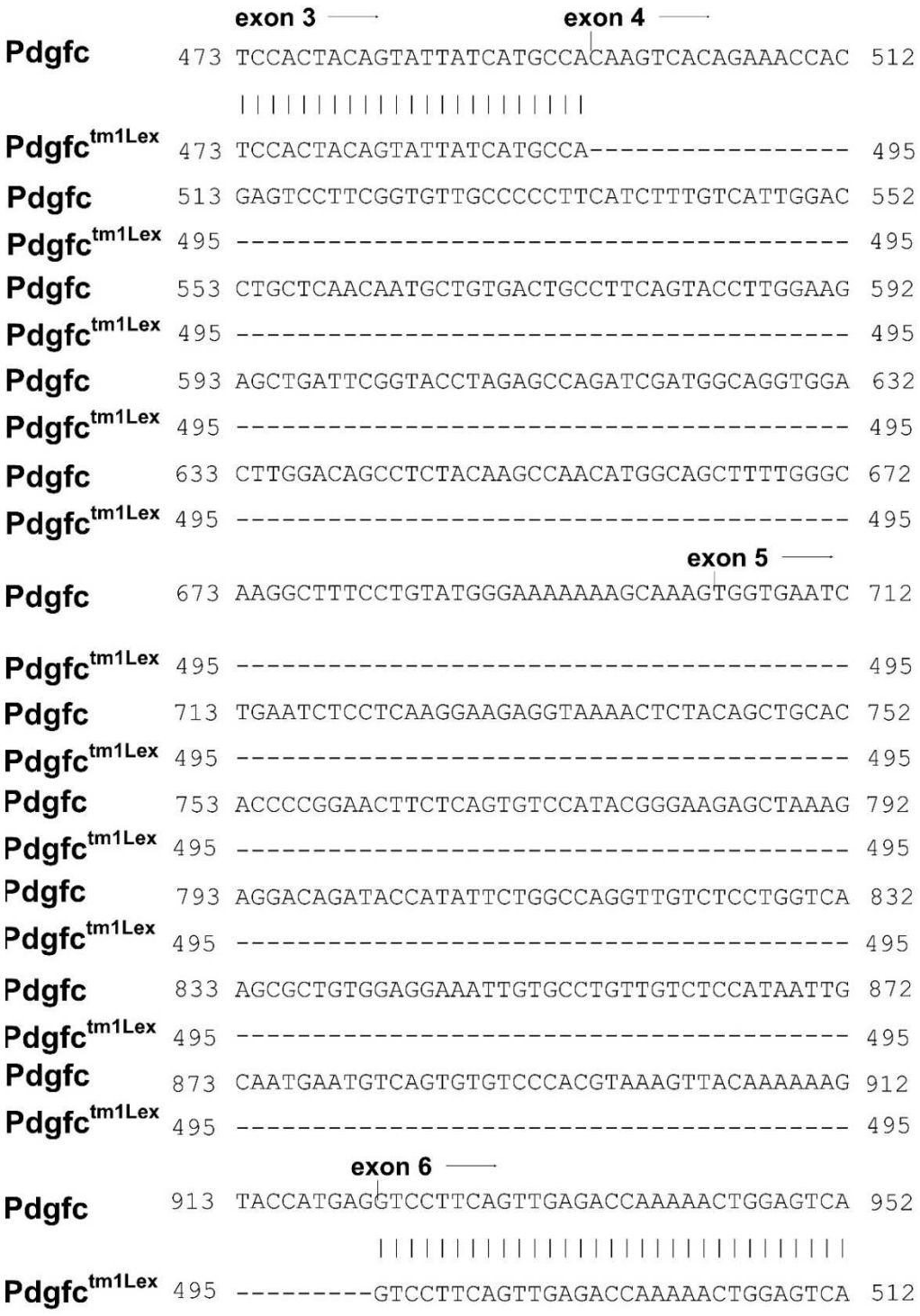

Figure 2.4 Sequence of cDNA from Pdgfc^{tm1Lex} mice. *Pdgfc^{tm1Lex}* from exons 3 to 6 compared to the consensus mouse sequence for *Pdgfc*, CCDS17425.1. Exon junctions are indicated above the consensus sequence.

Table 2.1. Heterozygous *Pdgfc*^{tm1Lex} breeding pairs in two backgrounds produce offspring with normal Mendelian distribution.

Cohort	No. of animals	+/+	*Pdgfc*^{tm1Lex}/+	*Pdgfc*^{tm1Lex} / *Pdgfc*^{tm1Lex}	Chi sq value
129Sv/EvBrd					
observed	99	26	50	23	0.19
expected		*25*	*50*	*25*	
C57BL/6					
observed	265	55	147	63	3.7
male					
observed	146	29	83	34	3.1
expected		*37*	*73*	*37*	
female					
observed	119	26	64	29	0.83
expected		*30*	*59*	*30*	

Male and female heterozygous *Pdgfc*^{tm1Lex} /+ mice were bred and the genotypes of the resulting offspring were determined from DNA extracted from tail snips by PCR. Two different genetic backgrounds, 129SvBrd and C57BL/6, were analyzed. The expected number of pups with a specific genotype was calculated based on the total number of pups analyzed. Analysis of normal Mendelian distribution was determined by Chi square analysis with two degrees of freedom. A Chi square number greater than 5.99 is statistically significant.

Table 2.2. **Heterozygous *Pdgfc*^{tm1Lex} breeding pairs with one copy of Pdgfrα do not produce *Pdgfc*^{tm1Lex} homozygous and hemizygous Pdgfrα offspring.**

Cohort	No. of animals	Pdgfc +/+ Pdgfrα +/-	Pdgfc +/- Pdgfrα +/-	Pdgfc -/- Pdgfrα +/-	Pdgfc +/+ Pdgfrα +/+	Pdgfc +/- Pdgfrα +/+	Pdgfc -/- Pdgfrα +/+	Chi sq value
observed	127	14	27	0	20	50	16	30
expected		16	32	16	16	32	16	

Male and female heterozygous *Pdgfc*^{tm1Lex} /+ mice, with a single copy of *Pdgfrα*, were bred, and the genotypes of the resulting offspring were determined from DNA extracted from tail snips by PCR. The expected number of pups with a specific genotype was calculated based on the total number of pups analyzed. Analysis of normal Mendelian distribution was determined by Chi squared analysis with five degrees of freedom. A Chi square number greater than 11.07 is statistically significant. Pdgfc -/- represents *Pdgfc*^{tm1Lex} / ^{tm1Lex} mice.

Chapter 3

Activation of platelet-derived growth factor receptor alpha contributes to liver fibrosis

Abstract

Chronic liver injury leads to fibrosis, cirrhosis, and loss of liver function. Liver cirrhosis is the 12th leading cause of death in the United States, and it is the primary risk factor for developing liver cancer. Fibrosis and cirrhosis result from activation of hepatic stellate cells (HSCs), which produce collagen. Here, we show that platelet-derived growth factor receptor α (PDGFRα) is expressed by human HSCs, and PDGFRα expression is elevated in human liver disease. Using a green fluorescent protein (GFP) reporter mouse strain, we evaluated the role of PDGFRα in liver disease in mice and found that mouse HSCs express PDGFRα and expression is upregulated during carbon tetrachloride (CCl_4) induced liver injury and fibrosis injection. This fibrotic response is reduced in *Pdgfrα* heterozygous mice, consistent with the hypothesis that liver fibrosis requires upregulation and activation of PDGFRα. These results indicate that *Pdgfrα* expression is important in the fibrotic response to liver injury in humans and mice, and suggest that blocking PDGFRα–specific signaling pathways in HSCs may provide therapeutic benefit for patients with chronic liver disease.

Introduction

Chronic liver injury is a major cause of morbidity and mortality in the US and worldwide, due to complications of liver fibrosis, cirrhosis, and hepatocellular carcinoma (HCC) (114). To date, there are no effective treatments for patients with liver fibrosis, so a better understanding of pathways that regulate fibrosis has great clinical potential (41). Many inflammatory cytokines and growth factors are released during liver injury, including platelet derived growth factors (PDGFs), which are potent mitogens for hepatic stellate cells (HSCs) (29, 41). The PDGF

family of ligands and receptors plays a central role in repair after injury, and are key regulators of the formation of connective tissue (43, 115). Elevated platelet-derived growth factor receptor (PDGFR) expression is detected in human heart disease, pulmonary fibrosis, and kidney fibrosis (116-118), and blocking PDGFR signaling decreases collagen deposition after myocardial infarct, in pulmonary fibrosis, and in kidney fibrosis (119-121). Thus, targeting the PDGF pathway may modulate liver fibrosis.

There are five known functional ligand dimers in the PDGF family, -AA, -AB, -BB, -CC, and –DD, which bind cell surface receptor tyrosine kinases comprised of PDGFRα and PDGFRβ subunits (51). PDGFs stimulate the migration and proliferation of mesenchymal cells during development (122). Loss of PDGFRs leads to significant abnormalities in mice (80, 90). PDGFRβ is critical to vascular and hematopoietic development, and cell specific deletion or activation of PDGFRβ results in failure or increased pericyte and vascular smooth muscle cell coverage of blood vessels in mice (90, 123, 124). PDGFRα is required for migration and survival of neural crest cells and for skeletal system development, and cell specific deletion of PDGFRα decreases β-cell proliferation in the pancreas and ventricular septation of the heart (80, 91, 125). Systemic activation of PDGFRα causes fibrosis that is particularly noticeable in intestine, skin, muscle and heart, but activation has to be conditionally induced in late prenatal or adult animals, as constitutive PDGFRα activation causes lethality (115). Deleting one allele of *Pdgfrα* in mice does not affect development, unlike the observed phenotype in homozygous knockout mice (80, 107). PDGF signal transduction pathways play a prominent role in fibrosis (126). It has been suggested that PDGFRα signaling is more likely to induce fibrosis than PDGFRβ (127), however this notion has not been conclusively demonstrated in the liver. In summary, PDGF signaling is tightly regulated by abundance and degree of signal transduction, and perturbing either results in developmental defects and organ dysfunction.

In the present study we analyzed *PDGFR* in pathologic human liver tissue sections, human liver cell lines, and a mouse model of liver injury and fibrosis. We found increased detectable PDGFRα in human liver disease. Mouse experiments revealed that PDGFRα is primarily expressed in HSCs, and *Pdgfrα* expression increased in injured mouse livers. We investigated the role of PDGFRα in liver fibrosis using mice with only one allele of *Pdgfrα*, and found that reducing *Pdgfrα* copy number inhibits liver fibrosis in mice. Together our data suggest that PDGFRα inhibitors could be an effective means to reduce liver fibrosis in patients.

Materials and Methods

Animals

Mice were housed in a specific pathogen-free environment overseen by the Department of Comparative Medicine at the University of Washington. Mice that express nuclear localized green fluorescent protein (GFP) driven by the endogenous *Pdgfrα* promoter, *Pdgfrα*^{nGFP}, were purchased from the Jackson Laboratory (007669) (107). Either wild type (WT) littermates that retain both *Pdgfrα* alleles, or control mice, *i.e.* male C57BL/6 mice purchased from the Jackson Laboratory (000664), were used as experimental controls. To induce fibrosis, mice were injected (*i.p.*) with 10µl/g body weight CCl_4 (Sigma-Aldrich) diluted in olive oil 10% (v/v), either one time (acute injury) or twice weekly for four or six weeks (chronic injury). Olive oil-injected animals served as controls for CCl_4-injected mice. Animals were sacrificed using CO_2 inhalation. The Institutional Animal Care and Use Committee of the University of Washington, which is certified by the Association for Assessment and Accreditation of Laboratory Animal Care International, approved all experiments.

Human Liver Samples

Human liver and HCC specimens were obtained from the University of Washington Medical Center after IRB-approval (MMY and RSY). All samples were de-identified of any patient information. Specimens were either fixed in formalin or frozen at -80℃ until use.

Immunohistochemistry (IHC) and Histological staining

Formalin-fixed liver tissue was processed and embedded in paraffin using standard protocols, and IHC was performed as previously described (128), using the primary antibodies listed in Supplementary Table 3.1. A board-certified clinical liver pathologist (MMY) reviewed all human samples and determined the presence of cirrhosis and/or tumor and assessed for PDGFRα and PDGFRβ immunoreactivity. To quantify fibrosis, formalin-fixed liver tissue was stained with picrosirius red. For morphometric analysis, picrosirius red area was imaged under polarized light (129). Images were analyzed using NIH image J software to convert pixels to binary values and determine the relative number of positive and negative pixels.

Immunoblotting

Tissues were homogenized in a 1% Triton-x 100 lysis buffer and processed as described (105). Membranes were incubated with primary antibodies overnight at 4℃, and then with the appropriate horseradish peroxidase (HRP)-conjugated secondary antibodies. Primary antibodies used in this study are listed in Supplementary Table 3.1

Immunofluorescence (IF) and *ex-vivo* imaging

Livers were fixed in 4% paraformaldehyde overnight, and tissues were frozen in optimum cutting temperature compound for cryosectioning. IF was performed using standard techniques, with liver sections incubated overnight with the primary antibodies listed in Supplementary Table 3.1. Immune complexes were detected with goat Alexa 633 conjugated anti-rat IgG (A-21094, Life

Technologies) and goat Alexa 546 conjugated anti-rabbit IgG (A-11010, Life Technologies) antibodies. Sections were mounted with SlowFade Gold (S36936, Life Technologies) and imaged with a Leica SL confocal microscope (Leica Microsystems, Keck Center UW). For *ex-vivo* imaging, freshly harvested livers were analyzed as previously described (40). Images were captured using a Zeiss 510 Meta confocal microscope. In *Pdgfra*$^{WT/nGFP}$ mice, GFP fluorescence was used to report PDGFRα positive cells (107).

Cell culture and Proliferation assay

Liver cell lines (Supplementary Table 3.2) were grown in a 37℃ incubator with 95% humidity and 5% CO2 in DMEM (Life Technologies) with 10% FBS. Confluent cells were split and allowed to attach to plates as described (130). Cells were serum-starved for 24 hours then stimulated with 10ng/ml PDGF-AA, -AB,-BB, or –CC (R&D systems) for 24 hours. [^{3}H]Thymidine (1 µCi/ml final concentration) was added to the media for the final 3 hours of stimulation. Unincorporated [^{3}H] thymidine was removed from the cells, and trichloroacetic acid was used to precipitate protein-bound DNA. DNA was solubilized in NaOH, quantified using a scintillation counter, and measured in triplicate.

RNA expression analysis

RNA was extracted from cells or liver tissue using Trizol (15596-018, Life Technologies) as described by the manufacturer. Reactions contained cDNA synthesized from 0.5µg RNA using MMLV (28025-013, Life Technologies), and Taqman Universal Mastermix II (4440040, Life Technologies). Cycling conditions were 95℃ for 10 min, and 49 cycles of 95℃ for 15 sec, 60℃ for 60 sec with a final extension at 72℃ for 1 min. Data are represented as delta delta Ct values after normalization to *Gapdh* mRNA levels. Primers used in this experiment are listed in Supplementary Table 3.3.

Statistical analysis

Statistical significance was analyzed using Prism software (Graphpad), either with Kruskal-Wallis non-parametric ANOVA with significance $p<0.05$, or Mann-Whitney U test with significance $p<0.05$, as indicated in the figure legends.

Results

Expression of PDGFRα in human cirrhosis and HCC

Previous studies have demonstrated that over expression of PDGF ligands induces fibrosis in mice (36, 37, 39), and elevated expression of *PDGFRβ* in chronic liver disease has been reported (131-133). As PDGF ligands can activate both PDGFRα and PDGFRβ, we sought to investigate the role of PDGFRα in chronic liver injury. 80-90% of human HCC arise in the setting of a cirrhotic liver, in which HSCs have been activated (134), so we first performed IHC analysis to determine whether PDGFRα and PDGFRβ levels are elevated in human cirrhosis and HCC. While normal adult liver has relatively little PDGFRα immunoreactivity, fibrotic and cirrhotic liver tissue was characterized by focal, perisinusoidal immunoreactivity for PDGFRα, which was stronger in steatotic and cirrhotic livers (Figure 3.1 A-D). PDGFRβ immunoreactivity was also increased in the fibrotic and cirrhotic areas compared to un-injured liver (data not shown). Supplementary Table 4 summarizes PDGFRα and PDGFRβ immunoreactivity in diseased human liver specimens, 77% of which demonstrated increased PDGFRα immunoreactivity and 56% of which demonstrated increased PDGFRβ immunoreactivity. Using a separate set of specimens, we compared PDGFR protein levels in grossly dissected HCC tumors to adjacent non-tumor tissue from the same patient by immunoblot analysis. PDGFRα protein was frequently detected in the non-tumor tissue (Supplementary Figure 3.8, Supplementary Table 3.5). One specimen, patient 5, had detectable PDGFRα protein by

immunoblot in the tumor (Supplementary Table 3.5). IHC analysis of this specimen demonstrated PDGFRα immunoreactive cells within the tumor (Figure 3.1 E, F), but these cells do not have the histological appearance of hepatocytes, suggesting that non-parenchymal cells (NPCs) had invaded the parenchymal tumor and account for PDGFRα immunoreactivity observed in the tumor by immunoblot analysis. Taken together, our data suggest that PDGFRα is expressed primarily in fibrotic and cirrhotic livers, predominantly in NPCs.

Expression of PDGFRα and PDGFRβ in human liver and stellate cell lines.

We next analyzed mRNA transcripts from human liver cell lines, and found that both *PDGFRα* and *PDGFRβ* mRNA are expressed in non-diseased human liver (Figure 3.2). The human HSC line LX-1 has higher relative expression of *PDGFRα* than human liver (Figure 3.2A). LX-2 cells, a LX-1 subclone, express *PDGFRβ,* albeit to variable levels*,* and LX-1 cells express little to no *PDGFRβ* (Figure 3.2B). Transcription of both PDGFRs is reduced in human hepatoma cell lines compared to whole liver, suggesting that PDGFRs are predominantly expressed in NPCs. We next stimulated various liver cell lines with PDGF ligands, and found that PDGF –AA, -AB, -BB, and –CC lead to robust proliferation in stellate cells, but these ligands had little effect on the hepatocyte or hepatoma cell lines tested (Supplementary Table 3.6).

Increased expression of Pdgfrα and Pdgfrβ in mice after CCl_4 induced hepatocyte injury.

To investigate the role of PDGFRα in liver injury and fibrosis, we used the well-established model of CCl_4 injection, in which HSCs are activated in response to necrotic inflammatory injury to hepatocytes, leading to liver fibrosis (25). CCl_4 injury to rats has been shown to induce *Pdgfrs* mRNA in the liver (135). To determine whether *Pdgfr* expression is induced after liver injury in mice, WT mice were injected with a single dose of CCl_4. We found that *Pdgfrα* expression increased during 72 hours after injury (Figure 3.3A). CCl_4 injection also induced

expression of *Pdgfrβ*, although to a differing extent and with a different time course than *Pdgfrα* (Figure 3.3B). Thus, acute CCl_4 exposure induces *Pdgfr* expression in the liver.

Cells expressing Pdgfrα and Pdgfrβ respond to CCl_4 injury.

To determine the liver cell type that expresses PDGFRα in response to liver injury, we used transgenic *Pdgfrα*$^{WT/nGFP}$ mice, in which the endogenous *Pdgfrα* promoter initiates transcription of nuclear-restricted GFP reporter in place of the *Pdgfrα* gene (107). These mice have one copy of *Pdgfrα* replaced by GFP and are thus heterozygous for *Pdgfrα*. While a single injection of CCl_4 induces necrosis and injury that is repaired within seven days, repeated injection of CCl_4 induces liver fibrosis (25). Vehicle-injected *Pdgfrα*$^{WT/nGFP}$ mice have histologically normal liver (Figure 3.4A). CCl_4 injection increases the density of small cells with a high nuclear to cytoplasmic ratio, similar to inflammatory cells around central veins 72 hours after acute injection, while chronic injection increases the density of cells between portal veins (Figure 3.4B, C). As shown in Figure 3.4D, vehicle-injected *Pdgfrα*$^{WT/nGFP}$ mice have an even distribution of PDGFRα-positive cells throughout the liver lobule. 72 hours after a single injection of CCl_4, however, PDGFRα-positive cells have a higher density around central veins at areas of hepatocyte injury (Figure 3.4E). We found that after six weeks of twice weekly CCl_4 injections, PDGFRα positive cells are detected around and between portal veins, where fibrotic bands form (Figure 3.4F). As PDGFRβ is expressed in quiescent and activated HSCs (136), we next determined whether both PDGF receptors were expressed in the same cell type. PDGFRα positive cells in chronic CCl_4 injected *Pdgfrα*$^{WT/nGFP}$ mouse livers (Figure 3.5A, D) co-localize with PDGFRβ immunoreactive cells (Figure 3.5B, E), indicating that activated HSCs express both receptors (Figure 3.5C, F) after chronic CCl_4 injection.

Data from human tissue using IHC (Figure 3.1) and from mice using a GFP reporter (Figure 3.5) indicated that HSCs are the predominant liver cell type that expresses PDGFRα. In order to

confirm which cells express *Pdgfrα*, we stained for specific liver cell epitopes using immunofluorescence in combination with nuclear-GFP expression in *Pdgfrα*$^{WT/nGFP}$mice (107). Images of livers from *Pdgfrα*$^{WT/nGFP}$mice indicate that PDGFRα and PDGFRβ are co-localized in the same cells (Figure 3.5, Supplementary Figure 3.9A), and that these cells also express desmin (Supplementary Figure 3.9B) and cellular retinol binding protein 1 (CRBP-1, Supplementary Figure 3.9C), proteins expressed in HSCs. Furthermore, GFP is not detected in Kupffer cells that express F4/80 expression (Supplementary Figure 3.9D), or endothelial cells as identified by CD31 expression (Supplementary Figure 3.9E). Hepatocytes, identified morphologically by fluorescence as described (137), were also negative for GFP (Supplementary Figure 3.9F). Taken together, these data suggest that HSCs are the primary liver cell type which express PDGFRα and PDGFRβ.

Reducing PDGFRα expression reduces fibrosis in mice

After confirming that *Pdgfrα* expression increases with CCl_4-induced liver injury, and that PDGFRα-positive HSCs respond to CCl_4 injection, we utilized *Pdgfrα*$^{WT/nGFP}$mice to evaluate the functional significance of *Pdgfrα* expression during liver fibrosis. *Pdgfrα*$^{WT/nGFP}$mice, which are heterozygous for *Pdgfrα* expression, are phenotypically normal, and have normal cell composition (107). Uninjured and CCl_4-injected *Pdgfrα*$^{WT/nGFP}$ and C57BL/6 mice were analyzed for transcriptional changes in genes associated with chronic liver injury. At baseline and after 4 weeks of twice weekly injections of CCl_4, *Pdgfrα* expression is decreased in *Pdgfrα*$^{WT/nGFP}$ mice compared to C57BL/6 mice (Figure 3.6A). *Pdgfrβ* expression was equivalently expressed in both genotypes of uninjured and chronic CCl_4 injected mice (Figure 3.6B). Smooth muscle α-actin (*Acta2*) expression, an epitope expressed when HSCs are activated (138, 139), increased when C57BL/6 mice were injected with CCl_4 for 4 weeks, but *Pdgfrα*$^{WT/nGFP}$ mice had greatly reduced *Acta2* expression in after chronic liver injury (Figure 3.6C). Fibrillar collagen 1a1

(*Col1a1*) expression was equivalent in uninjured mice of the two genotypes, but significantly reduced in chronically injured *Pdgfrα*$^{WT/nGFP}$ mice (Figure 3.6D). Conversely, collagen 4 (*Col4,* Figure 3.6E), and tissue inhibitor of metalloproteinase 1 (*Timp1,* Figure 3.6F) expression was comparable between both genotypes both in uninjured mice and after chronic injury.

Reduced mRNA expression of *Col1a1* in *Pdgfrα*$^{WT/nGFP}$ mice after chronic CCl_4 injection was accompanied by a reduction in fibrosis, as assessed by picrosirius red staining, a histochemical assay for tissue fibrosis. C57BL/6 mice injected with vehicle for 4 weeks had little to no fibrosis (Figure 3.7A, D), but developed periportal fibrosis after 4 weeks of twice weekly CCl_4 injections (Figure 3.7B, D). Significantly less collagen was deposited in chronically injured *Pdgfrα*$^{WT/nGFP}$ mice (Figure 3.7C, D). These results demonstrate that liver fibrosis, in response to chronic CCl_4 injection, is dependent on normal expression of PDGFRα, and are consistent with the hypothesis that liver fibrosis is regulated in part by PDGFRα ligands.

Discussion

PDGFRs stimulate proliferation, migration, and survival of mesenchymal cells, and increased activation of PDGFRs leads to organ fibrosis (126, 140). Elevated expression of PDGFRs is associated with liver fibrosis and cirrhosis, so we sought to determine whether PDGFRα regulates liver fibrogenesis using mice that have one allele of *Pdgfrα (Pdgfrα*$^{WT/nGFP}$). We found that mice with decreased *Pdgfrα* expression have less liver fibrosis after chronic CCl_4 injury. In addition, and consistent with the notion that PDGFRα regulates the liver's response to injury, patients with liver disease have elevated PDGFRα and PDGFRβ. In conjunction, hepatic GFP localization in *Pdgfrα*$^{WT/nGFP}$ mice indicates that PDGFRα positive HSCs migrated to sites of injury following CCl_4 injection. These data all suggest that PDGFRα is involved in the activation of HSCs after hepatocyte injury.

PDGFRs are thought to play a central role in activating HSCs and promoting liver fibrosis and cirrhosis (132, 133, 141); whether *Pdgfrα* and *Pdgfrβ* play independent roles in fibrogenesis is not known. We and others observe that *Pdgfrβ* expression increases in WT mice after acute liver injury by CCl_4, implicating PDGFRβ in HSC activation. Thus it is surprising that mice which systemically express a hyperactive PDGFRβ allele do not develop more liver fibrosis than WT mice after 4 weeks of CCl_4 injections (142). Our data indicate that hepatocyte injury induces *Pdgfrα* above uninjured liver in both mice and humans, corroborating previously published studies (133, 135). Our results demonstrate that expression of *Pdgfrα* and *Pdgfrβ* are both increased after chronic CCl_4 liver injury, while reducing *Pdgfrα* copy number reduced *Pdgfrα* expression, but not *Pdgfrβ* expression in $Pdgfr\alpha^{WT/nGFP}$ mice. Reduced *Pdgfrα* expression in $Pdgfr\alpha^{WT/nGFP}$ mice is correlated with reduced picrosirius red staining even though *Pdgfrβ* expression remains high. PDGFRα and PDGFRβ appear to affect HSC differentially, despite being co-localized in the same liver cell type. Further studies will be necessary to dissect the receptor-specific contributions of PDGF signaling pathways in HSCs and in liver fibrosis.

Small perturbations in the PDGF pathway, whether due to expression of ligand or receptor, appear to have a large impact on disease. Support for this notion is found in genetic evidence from rodents, which suggests that small changes in PDGFR activity *in vivo* are capable of significantly affecting a cell's function. For example in development, chimerism studies show that both $Pdgfr\beta^{+/-}$ and $Pdgfr\alpha^{+/-}$ embryonic stem cells are deficient in contributing cells to the embryo (79, 80), and adults have a decreased number of progenitor cells in mice heterozygous for *Pdgfrs* (81, 143). Heterozygous *Pdgfrα* mice have been bred to mice with mutations in PDGF ligands (83), or mutations in immediate early genes directly downstream of PDGFRα (84), resulting in additive effects. However, deletion of one allele of *Pdgfrα* and the resultant heterozygosity does not affect development (80, 107). These studies suggest that a single copy

of *Pdgfrα* is usually sufficient for development, although under certain circumstances two alleles of *Pdgfrα* are required. In the current studies, we found that *Pdgfrα*$^{WT/nGFP}$ have reduced fibrosis and reduced expression of profibrotic genes *Acta2* and *Col1a1* compared to C57BL/6 mice, after chronic CCl_4 injury. Our data indicate that in chronic liver injury, PDGFRα plays a critical role in the development of fibrosis.

We also sought to better define the role of PDGFRα in liver fibrosis by utilizing both human specimens and mouse models. Using a variety of experimental approaches, increased PDGFRα was seen in cirrhotic human livers, and in mice with chemically-induced liver fibrosis. Although no preclinical rodent model fully recapitulates human liver fibrosis, there appears to be comparable molecular pathophysiology between human and mouse. We chose to utilize a knock-in mouse model expressing nuclear-GFP driven by the *Pdgfrα* promoter in order to discriminate between cells located in close proximity to each other, specifically different NPC populations in liver sinusoids (107). We did not observe nuclear-GFP expression in hepatocytes, Kupffer cells, or LSECs, thus we conclude that the majority of PDGFRα is expressed in HSCs in the mouse liver, consistent with our observation that human liver specimens express PDGFRα primarily in NPCs. Our IHC data are further supported by data from the Human Protein Atlas (http://www.proteinatlas.org/ENSG00000134853/cancer), which demonstrates that NPCs are positive for PDGFRα by IHC in both normal liver and HCC (144).

We and others posit that selectively targeting PDGFRα in liver fibrosis and cirrhosis could reduce the proliferation, migration, and survival of the activated HSCs cells that contribute to collagen deposition. Therapeutic blockade of PDGFRα signaling may have a broad impact in the treatment of liver fibrosis, as four out of the five PDGF ligands, PDGF-AA, -AB, -BB, and -CC bind and activate PDGFRα (51). Targeting PDGFRβ, on the other hand, would completely inhibit only signal transduction induced by PDGF-DD, and could disrupt necessary functions of

PDGFRβ in the liver. Targeting both PDGFRs with multi-kinase inhibitors, such as imatinib or sorafenib, leads to severe off target effects (145, 146). The breadth of multi-kinase inhibitor activity thus likely leads to inhibition of beneficial signal transduction, either via PDGFRβ or other kinases. In summary, our data suggest that PDGFRα has a specific role in liver fibrosis in mice and in humans, and suggest that further mechanistic evaluation of PDGFRα function in the liver has the potential to uncover new anti-fibrotic therapies.

Acknowledgments and notes: The authors would like to thank Dan Bowen-Pope for critically reviewing this manuscript. Melissa Johnson and Jagadambika Gunaje for experimental assistance and Dr. Nelson Fausto for valuable input in the early stages of this project. The authors also thank Dr. Scott L. Friedman for generously sharing the LX1 and LX2 cells. This work was supported by grants R01CA127228 (to JS Campbell), the Herbert S. Coe Foundation, American College of Surgeons Louis C. Argenta Fellowship, the American Surgical Association Foundation Fellowship (to KJ Riehle), and the Howard Hughes Medical Institute program in Molecular Medicine and T32HL007312 (to BJ Hayes).

The content is solely the responsibility of the authors and does not represent the official views of the National Institutes of Health.

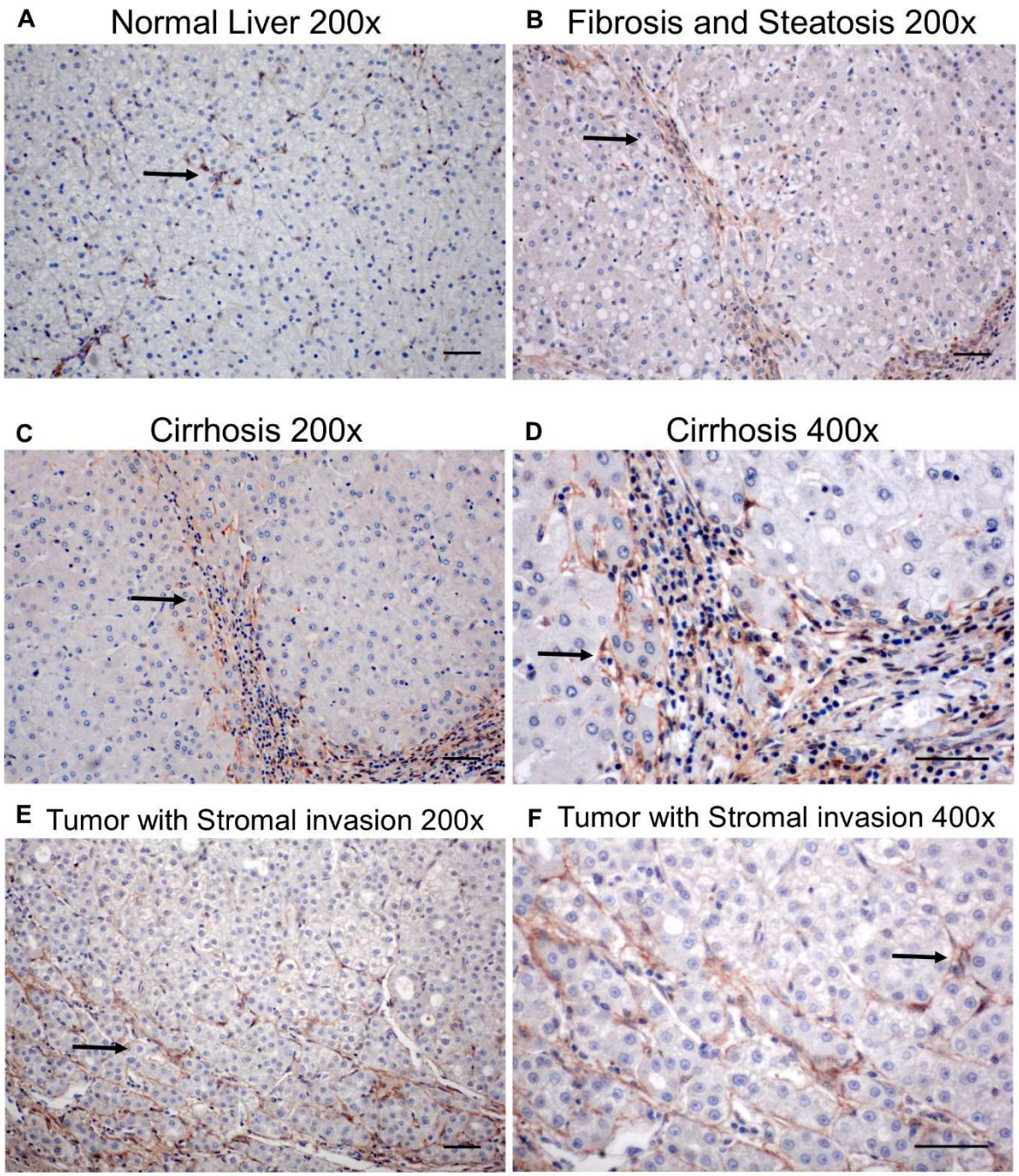

Figure 3.1. Perisinusoidal PDGFRα expression is localized to fibrotic or cirrhotic areas in tumor specimens by IHC. A) Uninjured (non-diseased) human liver demonstrate focal PDGFRα immunoreactivity (arrow) in NPCs but not hepatocytes. Resected tumor specimens show PDGFRα positive cells within fibrotic areas (arrow) (B), and cirrhotic areas (C), with sinusoidal PDGFRα immunoreactivity (arrows) within fibrotic septa (D). E and F) A resected tumor specimen shows stromal PDGFRα immunoreactivity (arrows). All scale bars are 50 µm.

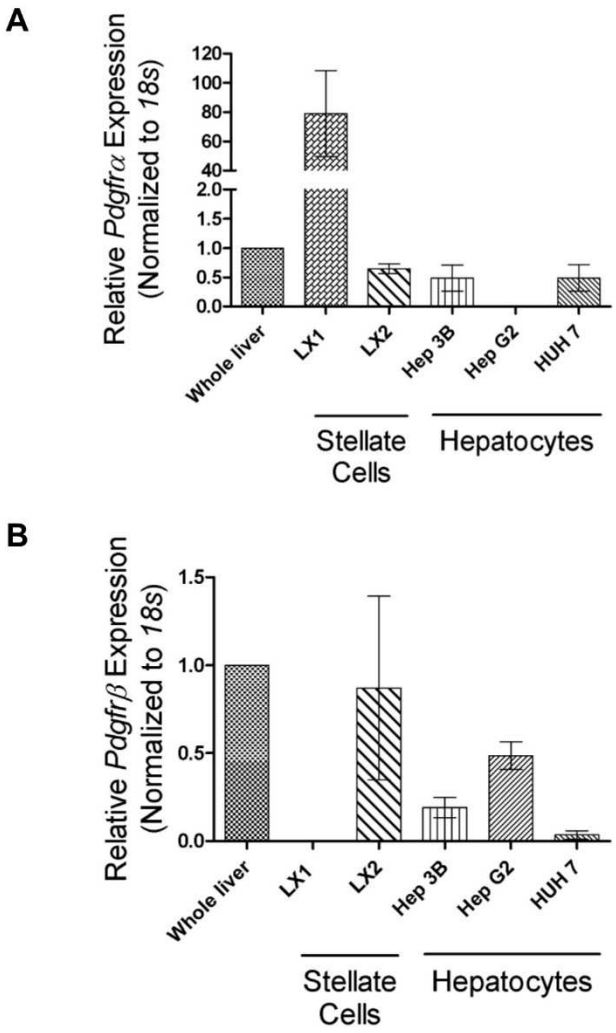

Figure 3.2. PDGF receptors are expressed in hepatic stellate cell lines. A) Relative *PDGFRα* mRNA expression is greater in LX1 HSCs compared to LX2 and hepatocyte cell lines. B) *PDGFRβ* mRNA expression in LX2 HSC is variable, but similar to whole liver and hepatocyte cell lines. *PDGFR* expression was normalized to 18S ribosomal RNA and reported as fold increase by the ΔΔCt method, normalized to adult human liver. Error bars indicate standard error of the mean, n=3 separate cultures.

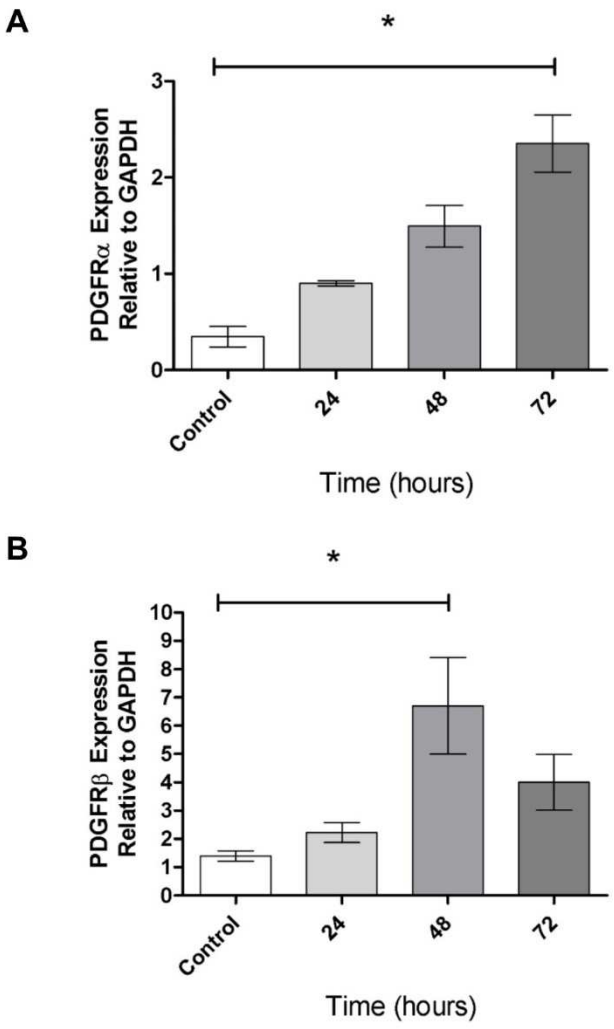

Figure 3.3. PDGFR mRNA expression increases in response to acute CCl_4 exposure. Expression of *Pdgfrα* (A) and *Pdgfrβ* (B) increases after a single injection of CCl_4 in C57BL/6 mice. Values are represented as means with SEM; n=3 mice per group; and data was analyzed by Kruskal-Wallis non-parametric ANOVA *=p<0.05.

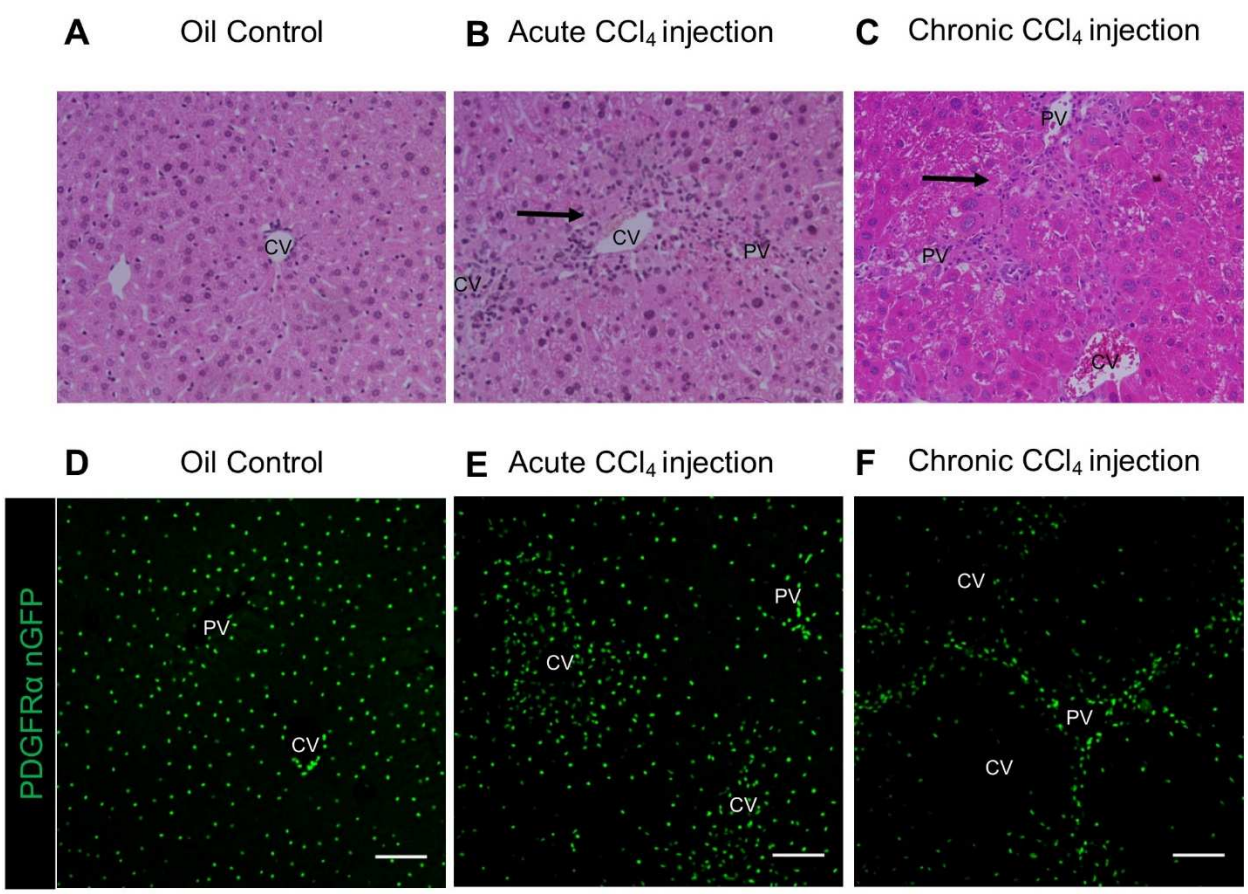

Figure 3.4. PDGFRα positive cells form fibrotic bands after chronic CCl_4 injection in *Pdgfra*$^{WT/nGFP}$ mice. Oil injection A) does not lead to necrosis around central veins (CV), while areas of necrosis are visible (arrow) 72 hrs after CCl_4 injection (B) as determined by H&E. C) NPCs are visible in areas between portal veins (PV, arrow). D) PDGFRα positive cells (green nuclei) are evenly distributed throughout the liver after oil injection. E) PDGFRα positive cells localize around the CV 72 hr after CCl_4 injury. F) PDGFRα positive cells align with fibrotic bands that develop between portal triads after chronic CCl_4 injury. Scale bars are 100 µm.

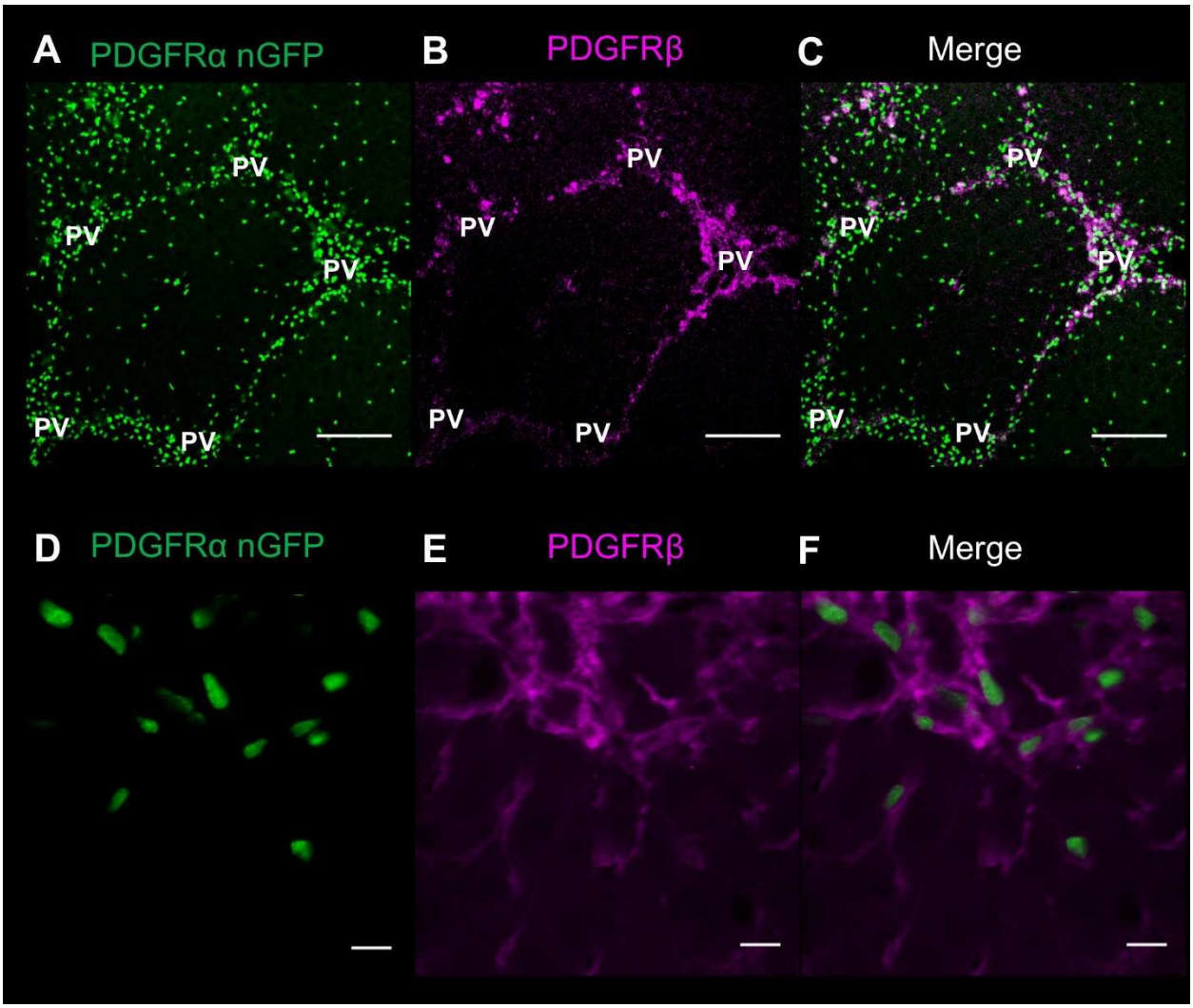

Figure 3.5. PDGFRα-positive cells co-localize with PDGFRβ-positive cells in chronic CCl_4 injured liver. *Pdgfrα*$^{WT/nGFP}$ mice were injected with CCl_4 twice weekly for six weeks. PDGFRα-expressing cells are identified by nuclear-localized GFP (green). PDGFRβ-expressing cells are identified by IF (PDGFRβ; magenta). A) PDGFRα-positive cells are aligned between portal veins (PV). B) PDGFRβ is expressed in the same periportal area as PDGFRα-positive cells, as shown in the merged image (C). A-C) Scale bars are 100 µm. D-F) Higher magnification shows that PDGFRα and PDGFRβ co-localize in the same cell, based upon co-localization of the GFP and PDGFRβ signal. Scale bars are 10 µm.

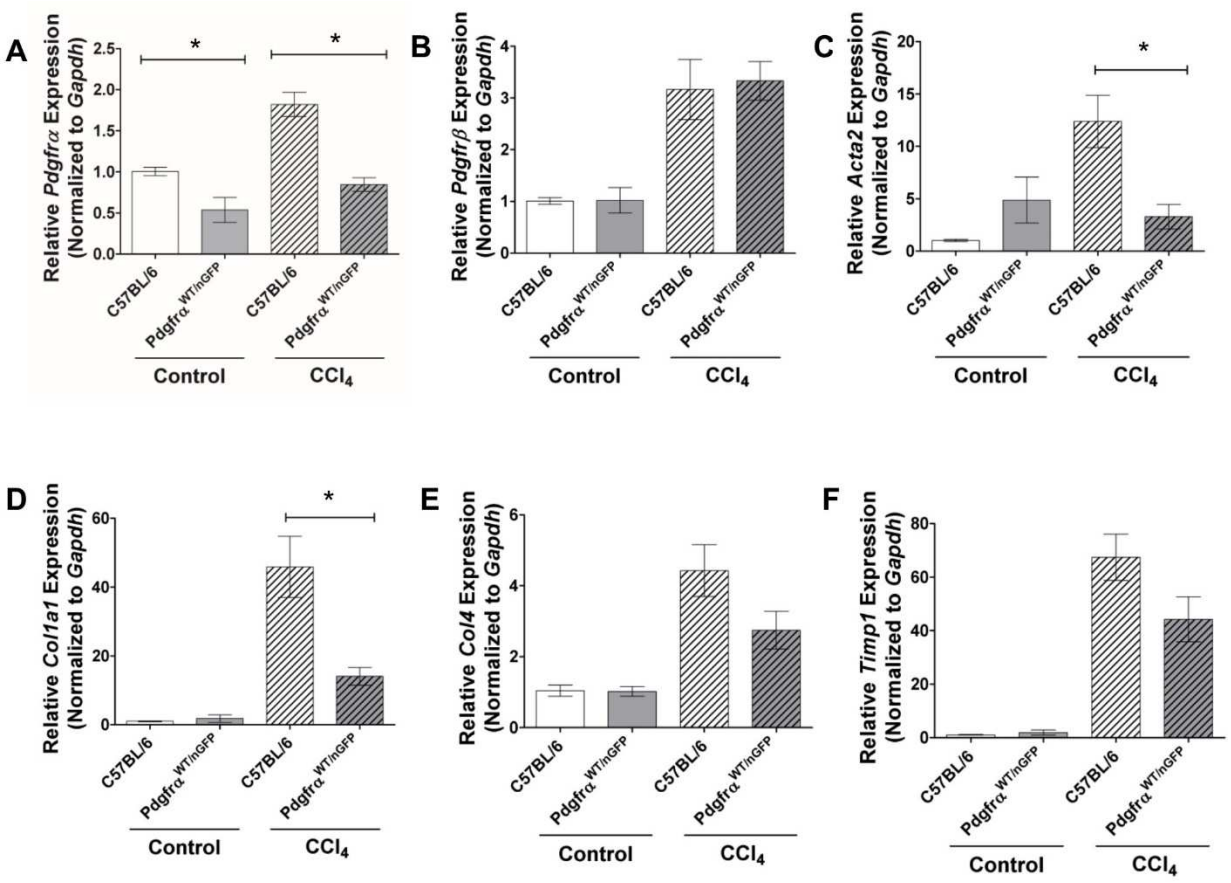

Figure 3.6. Compared to C57BL/6 mice, chronically CCl_4 injured *Pdgfrα*$^{WT/nGFP}$ mice have reduced transcription of fibrotic genes. Livers from *Pdgfrα*$^{WT/nGFP}$ and C57BL/6 mice that were either uninjured (controls) or treated for 4 weeks with CCl_4 were used to prepare total liver RNA. A) Compared to C57BL/6 mice, expression of *Pdgfrα* is decreased in *Pdgfrα*$^{WT/nGFP}$ mice in uninjured mice and after chronic CCl_4. B) Expression of *Pdgfrβ* does not differ between C57BL/6 and *Pdgfrα*$^{WT/nGFP}$ mice. C) Expression of *Acta2* is increased in uninjured *Pdgfrα*$^{WT/nGFP}$ mice compared to C57BL/6 and decreased after chronic CCl_4 between *Pdgfrα*$^{WT/nGFP}$ and C57BL/6 mice. D) Expression of *Col1a1* is similar in uninjured *Pdgfrα*$^{WT/nGFP}$ mice compared to C57BL/6 and decreased after chronic CCl_4 between *Pdgfrα*$^{WT/nGFP}$ and C57BL/6 mice. E) Expression of *Col4* is similar in *Pdgfrα*$^{WT/nGFP}$ mice compared to C57BL/6 in both uninjured and chronic CCl_4 injected mice. F) Expression of *Timp1* is increased to a similar level in both genotypes. Samples were analyzed as described in figure 3.2. Values are represented as means with SEM, and were analyzed by Mann-whitney non-parametric U test *=$p<0.05$, n=3-6 mice per time point.

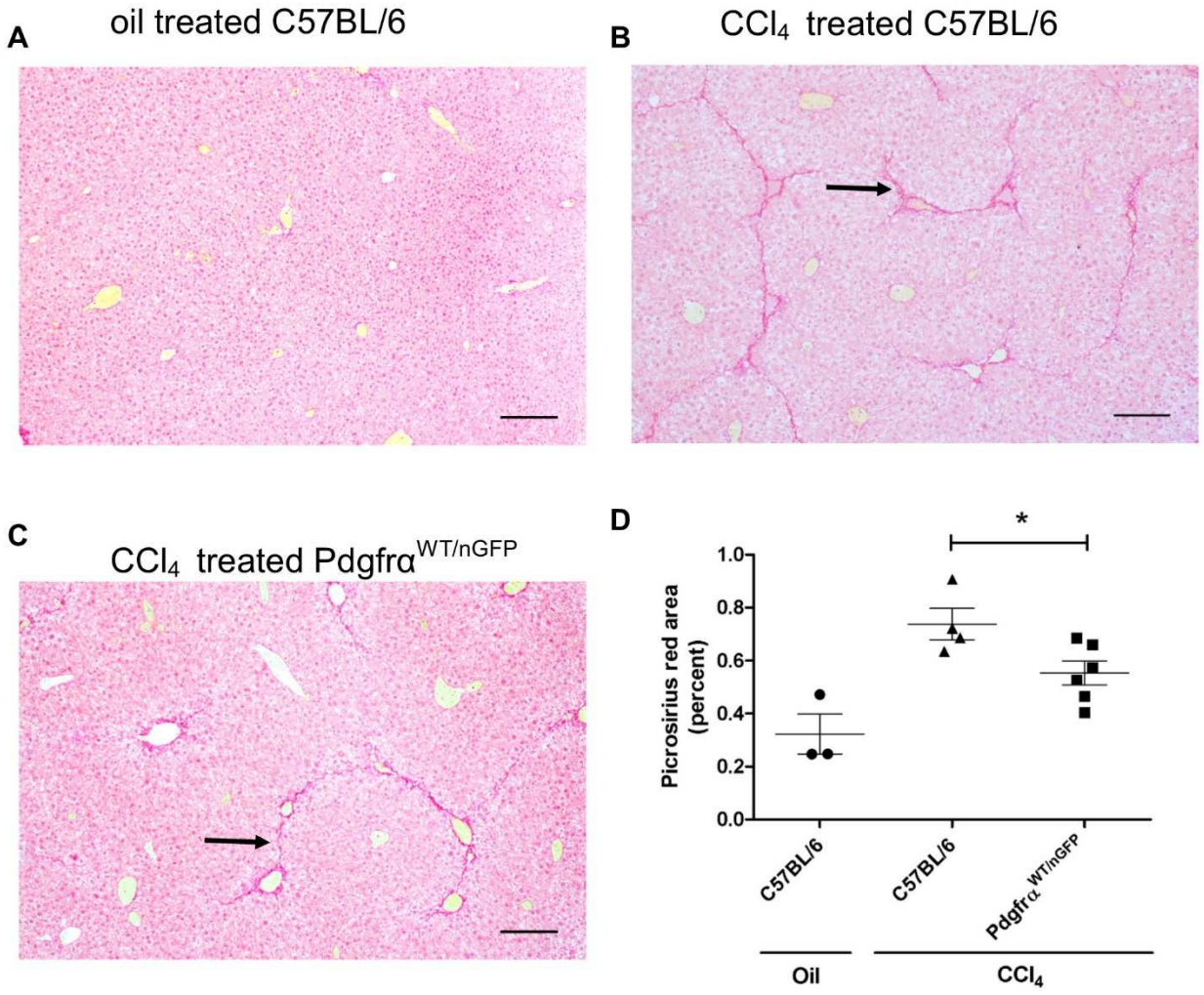

Figure 3.7. Chronically injured *Pdgfrα*$^{WT/nGFP}$ mice have less collagen deposition than C57BL/6 mice. Mice were injected with olive oil or CCl_4 twice weekly for 4 weeks and collagen was detected in liver tissue by picrosirius red staining. A) Liver from a mouse injected with oil shows little collagen deposition. B) C57BL/6 mice develop fibrosis (arrow) after 4 weeks of CCl_4 injections. C) *Pdgfrα*$^{WT/nGFP}$ mice develop less fibrosis (arrow) than C57BL/6 mice after 4 weeks of CCl_4 injections. D) Quantification of picrosirius red positive area. Values are represented as means with SEM, and were analyzed by Mann-Whitney non-parametric U test *=$p<0.05$, n=3-6 mice per time point. Scale bars are 100 µm.

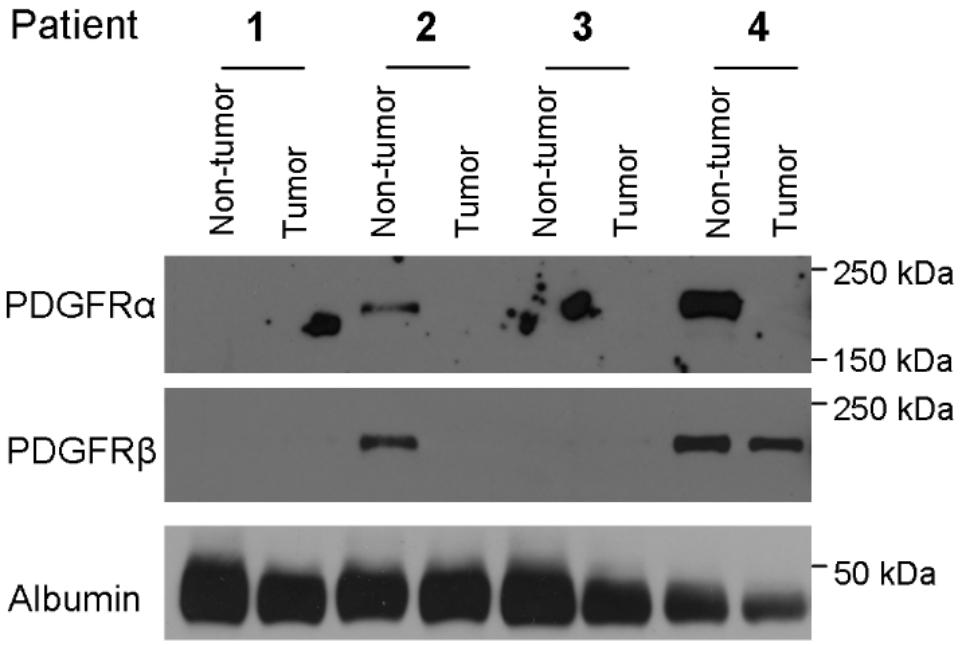

Supplementary Figure 3.8. Expression of PDGFRs in human liver tumor and non-tumor tissue. An immunoblot of PDGFRα detects PDGFRα in non-tumor tissue while an immunoblot for PDGFRβ shows protein in both tumor and surrounding tissue. Albumin was used as a loading control.

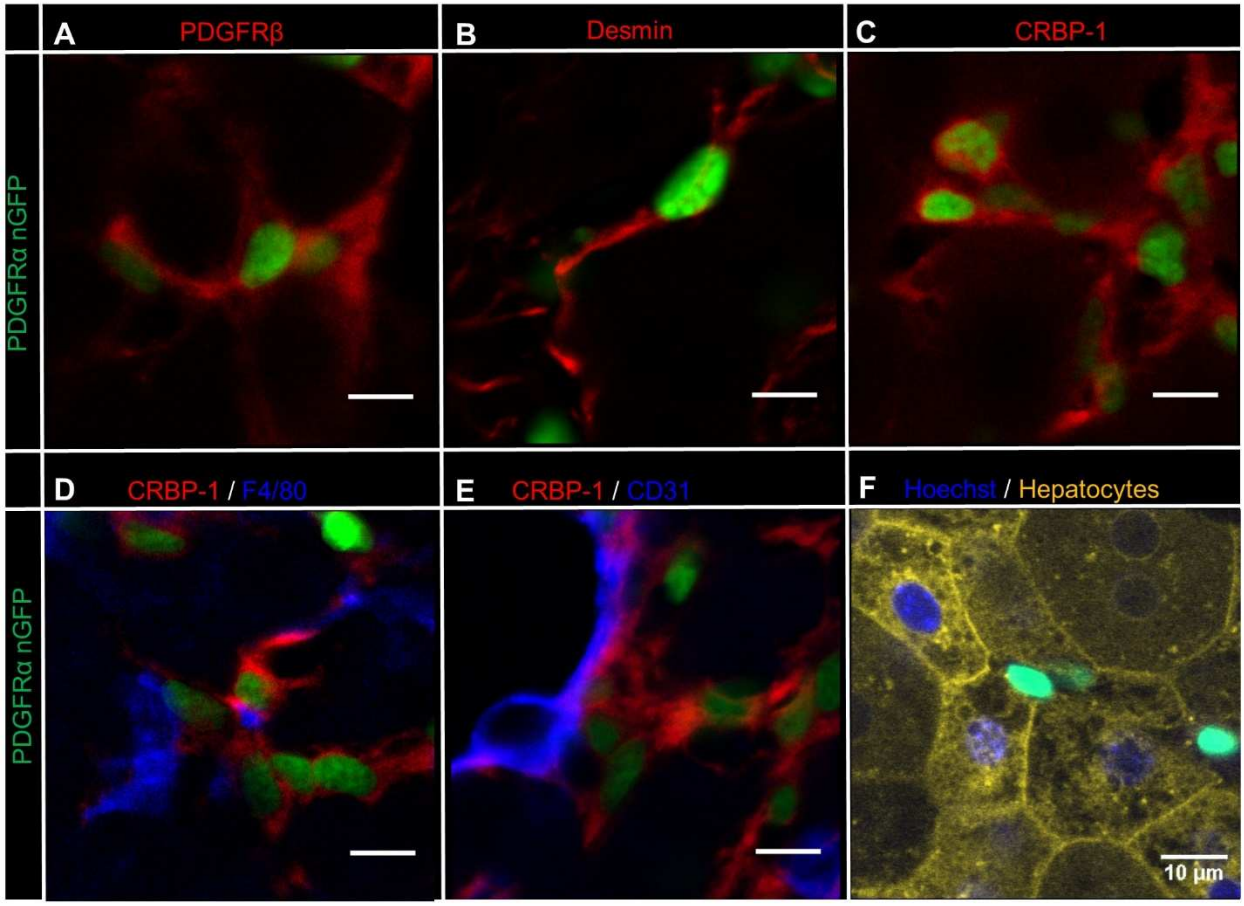

Supplementary Figure 3.9. C57BL/6 HSCs express PDGFRα. PDGFRα, nuclear GFP, is expressed in liver cells that are immunoreactive for common HSC markers: A) PDGFRβ (red), B) Desmin (red), and C) cellular retinol binding protein 1 (CRBP-1) (red). PDGFRα and CRBP-1 are not expressed in cells that stain for D) Kupffer cells F4/80 (blue) or E) endothelial cells CD31(blue). F) PDGFRα positive cells are distinct from hepatocytes (yellow). Scale bars are 10 µm.

Supplementary Table 3.1: Antibodies used for immunohistochemistry and immunofluorescence

Antibodies			
Antigen	**Manufacturer**	**catalog number**	**Use**
PDGFRα	Cell Signaling Technologies	3164	Western Blot, Immunohistochemistry
PDGFRα	Santa Cruz Biotechnology	sc-338	Western Blot
PDGFRβ	Epitomics	APB5	Immunofluorescence
PDGFRβ	Cell Signaling Technologies	3169	Western Blot, Immunohistochemistry
Desmin	Epitomics	1466-1	Immunofluorescence
CRBP-1	Santa Cruz Biotechnology	sc-30106	Immunofluorescence
F4/80	Abd Serotec	MCA497A647	Immunofluorescence
CD-31	BD Biosciences	553370	Immunofluorescence
Gapdh	Genscript	A00192	Western Blot
Albumin	MP Bio	55235	Western Blot

Supplementary Table 3.2: Human and mouse hepatocyte and stellate cells used in this study

Human Stellate Cells			
Cell line	**Origin**	**Source**	**PMID**
LX-1	SV40 large T immortalized hepatic stellate cell	Dr. S. L. Friedman	15591520
LX-2	low serum adapted subclone of LX-1	Dr. S. L. Friedman	15591520

Rat Stellate Cells			
Cell line	**Origin**	**Source**	**PMID**
CFSC-2G	CCl_4 treated rat		8394478

Human Hepatocytes			
Cell line	**Origin**	**Source**	**PMID**
Hep 3B	8 year old male hepatocellular carcinoma hepatitis B positive	ATCC: HB-8064	233137
Hep G2	15 year old male hepatocellular carcinoma hepatitis B negative	ATCC: HB-8065	233137
HuH-7	57 year old male differentiated hepatocellular carcinoma (well differentiated) hepatitis B negative	JCRB0403	6286115
HH4	Normal human hepatocytes immortalized by HPV E6/E7	Dr. N. Fausto	17991716
SK-Hep cells	Hepatocellular carcinoma	ATCC: HTB-52	327080

Mouse Hepatocytes			
Cell line	**Origin**	**Source**	**PMID**
AML12	hTGFα transgene driven by MT1	ATCC: CRL-2254	7904757
NMH	Normal BALB/c liver		7775596

*references as PMID number.

Supplementary Table 3.3: Oligonucleotide primers used for real time analysis.

Taqman primers	
Target Gene	**catalog number**
PDGFRA (human)	Hs00183486_m1
PDGFRB (human)	Hs01019589_m1
18S (human)	Hs99999901_s1
Gapdh (mouse)	Mm99999915_g1
Pdgfra (mouse)	Mm01211694_m1
Pdgfrb (mouse)	Mm00435546_m1
Acta2 (mouse)	Mm01546133_m1
Col1a1 (mouse)	Mm00801666_g1
Col4 (mouse)	Mm01210125_m1
Gfap (mouse)	Mm00441818_m1

Supplementary Table 3.4: Summary of PDGFRα and PDGFRβ immunoreactivity in human liver specimens

Patient	Tumor present	Cirrhosis	Stromal PDGFRα	Stromal PDGFRβ	Other
1	no	yes	+++	+	
5	yes		++	+	No non-tumor
9	yes	no	+	N.D.	
13	yes	yes	+	0	
14	yes		+	+	No non-tumor
15	yes	yes	+	0	
16	yes		N.D.	+	
17	yes		N.D.	0	
18	yes	yes	N.D.	0	
19	yes		N.D.	0	
20	yes	yes	+	0	
21	yes	yes	+++	0	
22	no	yes	+	0	
23	yes	no	++	+	
24	yes		+		
25	no	yes	+	0	
26	yes	yes	+		
27	yes	yes	+	+	
28	yes		+	++	No non-tumor
29	yes	no	++	0	
30	yes		+	+	
31	yes	yes	+	+	
32	yes	yes	+	+	
33	yes	yes	+	N.D.	
34	yes	yes	+++	N.D.	
35	yes	yes	+	N.D.	
36	yes		+	N.D.	
37	yes	yes	++	+	
38	yes	no	+	+	
39	yes	yes	+	++	
40	yes	yes	+	+	
41	yes	yes	+++	+	
42	yes	yes	+	+	
43	yes	yes	+++	0	
44	no		+	+	
45	yes		N/A		No non-tumor
46				+	
47	yes			N.D.	
48	yes	no	+	N.D.	
49	yes	no		N.D.	
50	yes	yes	+++	N.D.	
51	yes	no	0	N.D.	
52	yes	no	0	N.D.	
53	yes		+++	N.D.	

Resected liver specimens with HCCs were formalin-fixed paraffin embedded and evaluated for cirrhosis and HCCs. IHC for PDGFRα and PDGFRβ was performed as described in methods. Relative staining intensity is indicated as weak (+), moderate (++), strong (+++), or absent (0).

Supplementary Table 3.5: Immunoblot detection of PDGFR expression in macroscopically dissected human tumors and surrounding liver

Patient	Tissue	PDGFRα	PDGFRβ
1	Non-tumor	0	+
1	Tumor	0	+
2	Non-tumor	+	+
2	Tumor	0	0
3	Non-tumor	0	+
3	Tumor	0	+
4	Non-tumor	+	+
4	Tumor	0	+
5	Non-tumor	0	0
5	Tumor	+	+
6	Non-tumor	0	0
6	Tumor	0	0
7	Non-tumor	0	0
7	Tumor	0	0
8	Non-tumor	0	0
8	Tumor	0	0
9	Non-tumor	+	+
9	Tumor	0	0
10	Non-tumor	0	0
10	Tumor	0	0
11	Non-tumor	+	0
11	Tumor	0	0
12	Non-tumor	0	0
12	Tumor	0	0

HCCs (Tumor) and surrounding liver (Non-Tumor) macrodissected from patients were frozen and processed for immunoblot analysis as described in Methods. Intensity is indicated as present (+) or absent (0).

Supplementary Table 3.6: PDGF stimulates proliferation[1] in stellate cell lines, but not primary hepatocytes or hepatoma cell lines

	PDGF-AA	PDGF-AB	PDGF-BB	PDGF-CC	Positive control [2]
Human stellate cells (LX-2)	3 fold increase*	3 fold increase*	3 fold increase*	3 fold increase*	3 fold increase*
Rat stellate cells (2G)	5 fold increase*	5 fold increase*	5 fold increase*	5 fold increase*	10 fold increase*
Primary hepatocytes (mouse)	No stimulation	No stimulation	No stimulation	No stimulation	2.5 fold increase
AML12 hepatocytes (mouse)	No stimulation	No stimulation	No stimulation	No stimulation	5 fold increase*
NMH hepatocytes (mouse)	No stimulation	No stimulation	No stimulation	No stimulation	10 fold increase*
HH4 hepatocytes (human)	No stimulation	No stimulation	No stimulation	No stimulation	5 fold increase*
SK-Hep cells (human)	No stimulation	No stimulation	No stimulation	No stimulation	10 fold increase*

1 Cell proliferation was measured by DNA synthesis using tritiated thymidine incorporation (130). The data is the average of three different experiments that were each done in triplicates. Fold change represents the increase when compared to unstimulated cells for each cell line.

2 "Positive control" indicates that DNA synthesis was stimulated in each cell line or primary culture with a growth factor previously reported to simulate proliferation. Growth factors used for each cell and the concentrations are as follows: mouse hepatocytes, EGF (20 ng/mL); AML12 cells, EGF (20ng/mL); NMH cells, HB-EGF (20 ng/mL); rat stellate cells (2G), 1% fetal calf serum; human stellate cells (LX-2), 1% FCS; SK-Hep (human hepatoma cells of endothelial origin), 10% fetal calf sera.

Chapter 4

Conclusions and Future Directions

Understanding the mechanisms underlying liver fibrosis is critical to mitigating the growing healthcare burden of chronic liver disease and hepatocellular carcinoma. The PDGFRα pathway has been implicated in the development of fibrosis, as PDGF signal transduction is important in activation of HSCs in response to hepatocyte injury. Evidence from *in vitro* experiments indicates that PDGF-C elicits a different response via PDGFRα signal transduction than does PDGF-A (59). CUB domains have been reported to influence signaling pathways (68, 71, 147). As PDGF-C contains a CUB domain, we speculate that the CUB domain maybe one reason PDGF-A and PDGF-C have independent roles in fibrosis or biology. For my thesis work, my first hypothesis was that the CUB domain of PDGF-C functions to amplify PDGFRα signal transduction. My second hypothesis was that PDGFRα signal transduction is a primary driver of liver fibrosis. To my knowledge my studies are the first to directly addressed PDGFRα's function in the liver's response to injury. In this chapter, I will discuss the implications of my thesis research and propose possible future studies of PDGF signal transduction in liver fibrosis and the broader significance of this work.

Major Findings

1. PDGF-C CUB domain contributes to PDGFRα signal transduction

We found that in the context of development, both domains of PDGF-C, the CUB and GFD, seem to contribute to PDGFRα signal transduction. Our findings are in contrast to earlier reports that the CUB domain interferes with the ability of the GFD to activate PDGFRα when PDGF-C is in its full length form (58). In my studies we utilized a mouse model that produces only the CUB domain of PDGF-C, *Pdgfc*^{tm1Lex}, to evaluate this question. We found that the PDGF-C CUB domain induces sufficient PDGFRα signal transduction to prevent some of the

developmental defects seen in PDGF-C KO mice (*Pdgfc*^{tm1Nagy}) (87, 95, 148). Furthermore, when *Pdgfc*^{tm1Lex} mice were intercrossed with hemizygous *Pdgfrα* (*Pdgfrα*$^{WT/nGFP}$) mice, we observed peri-natal lethality in pups that expressed the CUB domain of PDGF-C and one allele of *Pdgfra.* These results suggest that PDGFRα activity is important to the mechanism(s) used by the CUB domain of PDGF-C to prevent lethality. The precise biochemical mechanism(s) of the PDGF-C CUB domain influencing PDGFRα signal transduction remain unknown.

2. PDGFRα is a major contributor to liver fibrosis

PDGFRα has been reported to induce systemic fibrosis in mice (115), but its contribution to liver fibrosis has not been extensively investigated. When the ligands that activate PDGFRα are overexpressed in the liver, fibrosis results; implicating PDGFRα as an important mechanism of liver fibrosis (36, 37, 39). PDGF-B can activate both PDGFRα and PDGFRβ, but expression of a constitutively active form of PDGFRβ in the liver did not result in increased liver fibrosis (142). We thus hypothesized that PDGFRα is a driver of fibrosis in liver, and data presented in this thesis support this hypothesis. Increased expression of PDGFRα correlates with human liver disease, and *Pdgfrα* expression is increased in injured mouse liver (Chapter 3). We also localized PDGFRα expression to NPCs in both mouse and human. Finally, genetic deletion of one copy of *Pdgfrα* decreases collagen deposition in chronically injured mouse livers, as well as the expression of fibrotic markers *Col1a1, Pdgfrα,* and *αSMA.* These results suggest that PDGFRβ may have a different role in liver fibrosis than the PDGFRα/ PDGF-A PDGF-C axis.

Future Directions

My work demonstrates that PDGFRα drives liver fibrosis, but raises a number of questions that require further investigation. These questions, and potential experimental approaches that would address them are discussed in this section.

1. Does the CUB domain of PDGF-C physically interact with PDGFRα?

My thesis work suggests the PDGF-C CUB domain interacts directly or indirectly with PDGFRα or a protein in the PDGFRα pathway (Chapter 2). CUB domains have been identified in a number of proteins and thought to facilitate binding to other proteins (69, 110-113). Not much is known about which proteins might interact with the CUB domain of PDGF-C. Based on the cDNA sequence of *Pdgfc* in *Pdgfc*^{tm1Lex} mice (Figure 2.4), the amino acid sequence of the *Pdgfc*^{tm1Lex} protein product (PDGF-C^{mut}) (Figure 4.1) would lack the proteolytic cleavage site and two-thirds of the growth factor domain, suggesting an absence of GFD activity.

A hypothetical model based on a combination of the protein crystal structure of the a2 CUB domain of neurophilin 1 (PDB 2QQM) and the PDGF-B growth factor domain (PDB 3MJK) indicates that the PDGF-C^{mut} monomer is expected to have a dramatically altered structure compared to wild type PDGF-C (Figure 4.2). Further, the dimer of PDGF-C is expected to require cysteines to form intra- and inter-chain disulfide bonds like other PDGF dimers (122). The cysteines that form the disulfide bonds are lacking in the PDGF-C^{mut} sequence (Figure 4.3). Thus the tertiary structure necessary for receptor interaction in PDGF paralogs PDGF-A and PDGF-B is not present in PDGF-C^{mut} (99, 101).

Multiple techniques could be employed to interrogate the direct interaction between the CUB domain of PDGF-C and PDGFRα. Molecular cloning would allow us to add peptide tags to the N and C termini of the CUB domain that would allow the use of tagged CUB domains to co-immunoprecipitate PDGFRα in cells that over express PDGFRα such as baby hamster kidney (BHK) cells (149). Additionally these proteins could be used in analysis of direct binding between PDGFRa and CUB domain using surface plasmon resonance. ,In such experiments, the tagged CUB domain would be attached to a surface and PDGFRα in solution would flow over the surface. Interactions between the two proteins are detected by changes to the surface

tension. The results will identify whether the PDGF-C CUB domain physically interacts with PDGFRα.

A complementary approach would be to perform saturation binding assays and Scatchard analyses. We would express and label the CUB domain with radioactivity, and ligand binding studies can be carried out with BHK cells expressing PDGFRα, PDGFRβ, or the parental BHK cell line (149, 150) and excess 'cold' CUB domain. Specific binding constants would be calculated for CUB binding to PDGFRα in BHK cells, which would indicate a PDGF-C CUB/ PDGFRα interaction. Typically, radioactivity is measured after washing cells either in the presence or absence of a non-labeled competitor. The measurement of cell associated radioactivity can define the dissociation constant, receptor binding sites, and quantify the CUB domain binding sites on the cell surface (151). Additionally, use of non-labeled PDGF ligands would determine whether any PDGF ligands interfere with CUB domain binding to PDGFRα. These studies would provide biochemical evidence of direct interaction with the PDGF-C CUB domain with PDGFRα.

The results of the proposed experiments should identify whether the CUB domain physically interacts with PDGFRα. If the CUB domain binds to PDGFRα, it suggests that the CUB domain has a function in PDGFRα signal transduction. My own work (Chapter 2) suggests that the CUB domain of PDGF-C amplifies the PDGFRα signal. This could be due to an interaction in which PDGF-C is secreted in a latent form, the CUB domain binds to PDGFRα, and brings the GFD in close proximity to the PDGFRα IgG domains to directly bind following cleavage of the two domains. On the other hand The PDGF-C CUB domain could associate after cleavage with the GFD as PDGF-A non-covalently associates with a furin cleaved segment of PDGF-A (152). In support of this hypothesis PDGFA associated protein 1 (PDAP1), a soluble protein with an affinity for PDGFA, has been reported to amplify the proliferative response

induced by PDGF-AA (153). Alternatively, the PDGF-C CUB domain could bind to and facilitate an interaction between PDGFRα and co-receptor, as has been reported for PDGFRβ and tissue trans glutaminase (Tgm2) (154). An interaction between the CUB domain and the PDGFRα would add nuance to PDGFRα signaling as it is becoming increasingly apparent that PDGFRα signaling is a gradient of intensity rather than a binary on/off signal.

2. Does PDGF-C growth factor domain (GFD) enhance liver fibrosis?

PDGF-C overexpression causes liver fibrosis and development of HCC in mice (39). In my thesis work, I have also shown that reduction of PDGFRα decreases fibrosis caused by CCl_4 injection. I have also shown that the PDGF-C CUB domain plays a role in development (Chapter2), but the individual contributions of either the GFD or the CUB domain of PDGF-C to liver fibrosis is unknown. Using *Pdgfc*^{tm1Lex} mice (expressing PDGF-C CUB in the absence of GFD), we can test whether twice weekly injections of CCl_4 for 4 weeks induces liver fibrosis to the same extent as control mice. If we compare CCl_4-induced liver fibrosis in the *Pdgfc*^{tm1Lex} to control animals with endogenous *Pdgfc*, we would anticipate decreased liver fibrosis in *Pdgfc*^{tm1Lex} compared to control mice. In the context of this hypothesis it is important to note that other investigators found that liver fibrosis induced by BDL was unaffected by loss of PDGF-C, introducing the possibility that the method of injury is important to the formation of fibrosis(155).

Another approach to determine whether the PDGF-C GFD enhances liver fibrosis is to engineer a transgenic mouse analogous to the PDGF-C transgenic mouse already described by our lab (39). Overexpression of just the GFD of PDGF-C would indicate the contribution of the GFD to liver fibrosis. Full length PDGF-C overexpression in the liver induces liver fibrosis that increases in severity with time. Inserting the DNA sequence for exons 1, 5, and 6 of *Pdgfc* into a plasmid vector under the control of the albumin enhancer promoter would result in a transcriptional product containing only the coding region for the PDGF-C signal peptide and the

PDGF-C GFD. Injecting this construct into the pronucleus of a mouse zygote should result in a transgenic mouse that over expresses only the PDGF-C GFD. The PDGF-C GFD mice can then be analyzed for liver fibrosis and compared to the severity of liver disease in PDGF-C Tg mice and wild type mice at multiple time points. The results should determine the effect of the PDGF-C GFD on liver fibrosis and indicate whether overexpression of the GFD is similar to overexpression of PDGF-A, PDGF-B, or full length PDGF-C.

3. What are the cell specific contributions of PDGFRα activation to liver injury?

My work suggests that PDGFRα expression in HSCs is required for liver fibrosis, through the use of *Pdgfrα*$^{WT/nGFP}$ mice. However, *Pdgfrα*$^{WT/nGFP}$ mice cannot be used to address the effect of cell-specific expression of PDGFRα on liver fibrosis because they carry a mutation that affects every cell in the mouse. To demonstrate a liver cell-specific role for PDGFRα in fibrosis, cell specific gene ablation is required. Our approach will be to use mice engineered to express a tamoxifen-inducible Cre recombinase fused to a mutated human estrogen receptor under the human GFAP promoter (156), and similar human GFAP promoter constructs have been shown to be active in HSCs (157). Intercrossing these mice to mice with both alleles of *Pdgfrα* flanked by *loxp* sites, *Pdgfrα*$^{fl/fl}$ mice, should result in offspring from which *Pdgfrα* can be removed from *GFAP* expressing cells after mice are exposed to tamoxifen. Deletion of *Pdgfrα* from *GFAP* positive liver cells targets some or all populations of HSCs. If PDGFRα signaling is critical in *GFAP* expressing HSC populations, we would expect a decreased fibrotic response to chronic injury or genetically induced fibrosis, and a reduction of activated HSCs.

Another approach to demonstrate a role for PDGFRα would be to use mice engineered to express conditionally active PDGFRα (115); these mice have normal PDGFRα expression until a Cre recombinase excises the transcriptional stop cassette 5' of a mutated D849V PDGFRα. Once the stop codon is removed constitutively active *Pdgfrα* is expressed from the

endogenous *Pdgfrα* locus, hence only cells that normally express *Pdgfrα* will have increased PDGFRα activation. Breeding PDGFRα D849V mice to mice expressing Cre recombinase under the human *GFAP* promoter would allow for inducible activation of PDGFRα in HSCs. As HSCs normally express PDGFRα, they should express constitutively active D849V-PDGFRα after exposure to tamoxifen. Constitutive activity of PDGFRα in HSCs is expected to induce severe liver fibrosis, which would increase in severity with the number of *GFAP* positive HSCs that removed the stop cassette. Evidence from mice overexpressing the PDGFRα ligand PDGF-C suggest that the activated HSC population persists over time and increases the severity of liver fibrosis (39). The results of these experiments would determine the contribution of *GFAP* positive cells to liver fibrosis. The severity of fibrosis in these genetic models will also indicate whether a GFAP negative population of cells contributes to liver fibrosis.

My thesis work together with other published data from the Campbell lab clearly show that PDGFRα is expressed in HSCs. The work described so far does not exclude any contribution of *Pdgfrα* expression by other liver cell types, such as hepatocytes, endothelial cells, or Kupffer cells. Combining Cre-lox technology with available mouse models could illuminate any potential cell-specific contribution of other liver cell types expressing PDGFRα to liver disease. To demonstrate the hepatocyte contribution of PDGFRα, mice have been engineered to express Cre recombinase fused to a mutated human estrogen receptor under the endogenous albumin locus in the mouse (158). If these mice were crossed with PDGFRα D849V mice, any PDGFRα transcribed after exposure to tamoxifen would be constitutively active in hepatocytes. If hepatocyte-specific expression of PDGFRα is important to liver tumor formation, as suggested by others, then constitutively active PDGFRα should decrease the time to form liver tumors or induce larger liver tumors in response to carcinogens, for example. Likewise promoters specific for endothelial cells, such as Vegfr2, or Kupffer cells, such as Lyz2, could drive Cre-recombinase and confirm or refute a PDGFRα contribution to fibrosis in these

cell types (159, 160). These approaches would be expected to induce liver fibrosis if there is endogenous expression of PDGFRα. On the other hand, if these cell types do not express PDGFRα, they will not express constitutively active PDGFRα D849V and there will be no difference in liver disease between experimental and control mice. These approaches could also be coupled with chemical and genetic fibrosis models.

Discussion

PDGF signaling affects biology in a highly cell specific manner, and some cell lineages express only one of the receptors. Figure 4.4 summarizes a number of studies performed in mice and the effect of manipulating PDGFRα on development and ECM production (87, 95, 115, 148). Proliferation and differentiation are sensitive to *Pdgfra* expression in oligodendrocyte progenitor cells (OPCs), which exclusively express PDGFRα (81, 82). When cells express both receptors however, it is more difficult to discern the relative effects of one PDGFR or the other. *In vitro* migration of cells has been reported to be directly related to the relative number of PDGFRs expressed on the cell surface. When PDGFRα or PDGFRβ are expressed at similar levels in smooth muscle cell cultures PDGF ligands -AA, -AB, and -BB all stimulate the same level of migration and proliferation (161). However, when PDGFRβ is expressed at three to five times the expression level of PDGFRα ligands -AB, and -BB stimulate significantly more migration and proliferation than –AA (161).

The PDGF signal transduction pathway is strictly regulated, such that a modest increase or decrease in PDGFR activation leads to significant abnormalities in mice. PDGFRα is important for migration and survival of neural crest cells and for skeletal development, and cell specific deletion of PDGFRα affects the function of the pancreas and development of the heart (80, 91, 125). PDGFRβ is critical to development, particularly for the hematopoietic and vascular systems, and cell specific deletion of PDGFRβ in the epicardium results in immature

coronary arteries with fewer vascular smooth muscle cells than wild type mice (90, 123). Embryonic stem cells hemizygous for PDGFRβ cannot compete with wild type PDGFRβ cells to produce capillary pericytes (79). Systemic constitutive activation of PDGFRβ is also detrimental in that it increases the number of undifferentiated adipose and mural cell progenitors (124). PDGFRα causes systemic fibrosis that is particularly noticeable in intestine, skin, muscle and heart, however activation has to be conditionally induced in late prenatal or adult animals as constitutive PDGFRα activation causes lethality (115). PDGFRα and PDGFRβ activation stimulate transcription of similar immediate early genes (162), and the intracellular domains of the PDGF receptors are interchangeable (163). We suggest that the different phenotypes observed in mice with increased or decreased PDGFRα compared to PDGFRβ signaling are due to cell specific expression of either PDGFRα or PDGFRβ.

As mentioned, PDGF signaling affects biology in a highly cell specific manner both spatially and temporally. PDGFRs are detected in ischemic cardiomyopathy, pulmonary fibrosis, and kidney fibrosis (116-118), and blocking PDGFRs decreases collagen deposition after myocardial infarction, in pulmonary fibrosis, and in kidney fibrosis (119-121). These results suggest that the PDGFRα signal transduction pathway plays a prominent role in fibrosis in multiple organs. Thus, deviation from wild type activity of PDGFRα by increasing or decreasing signal transduction leads to developmental phenotypes and disease.

Another level of complexity is added by the different PDGF ligands. The ligands PDGF-A,-B, and –C all bind PDGFRα, and are all found in alpha granules of platelets (164, 165). A number of other cells express PDGF-A,-B, and –C, including HSCs, smooth muscle cells and monocytes/macrophages (166, 167). Redundant binding affinities for PDGFRs and expression of multiple PDGF ligands by a single type of cell suggest that there might be some flexibility to the PDGF signal transduction pathway. This notion is not supported by reports that individual

deletion of PDGF -A, -B, or -C cause developmental deficiencies, however (85, 86, 168). Furthermore, deletion of just the heparin binding exon of *Pdgfa,* while leaving the rest of the *Pdgfa* sequence intact, has subtle effects on organ development, but these effects are amplified by decreasing expression of *Pdgfrα* or *Pdgfc* (148). In light of this information, it is not surprising that deletion of only part of the *Pdgfc* gene results in a different phenotype than a complete *Pdgfc* deletion. Our observation that Pdgfc^{tm1Lex} mice, which express mRNA encoding the PDGF-C CUB domain alone, have increased viability compared to Pdgfc^{tm1Nagy} mice suggests that the CUB domain of PDGF-C has a signaling function. The CUB domain in thus has the potential to enhance normal development in the absence of the GFD. Wild type levels of *Pdgfrα* are required as *Pdgfrα*$^{WT/nGFP}$ mice are not viable without the PDGF-C GFD (Figure 4.4). This *in vivo* evidence suggests that altering the activity of PDGFRs in either direction can be detrimental, and there is a narrow range of activation that promotes normal development.

We have shown that HSCs express both PDGFRs, though PDGFRα activation seems to be a more potent activator of fibrosis than PDGFRβ. I propose a model in which cell-specific PDGFRα is a key factor in development of liver fibrosis. Thus small perturbations in PDGFRα activity via increased ligand expression or increased HSC activation initiates a loop of fibrosis. PDGFRα expression induces HSC proliferation, migration, and PDGFRα-stimulated PDGFRα expression (Figure 4.5). Autocrine stimulated transcription of *PDGFRα* continues the cycle of PDGFRα induced proliferation and migration, and leads to fibrosis.

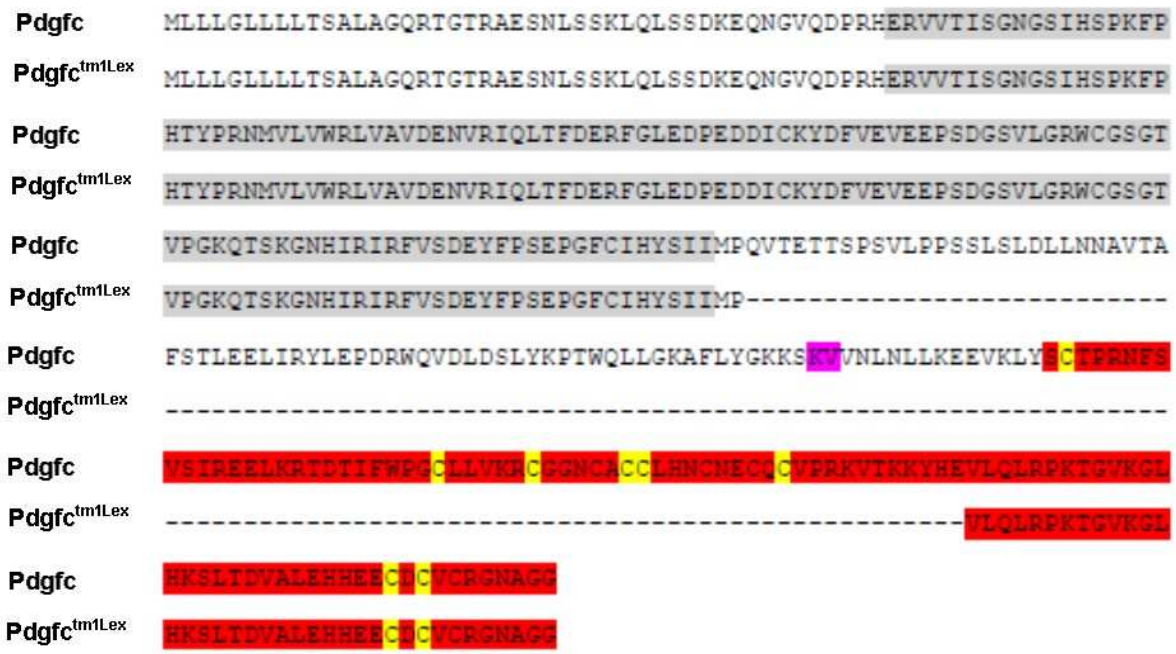

Figure 4.1. Amino acid sequence of wild type PDGFC and PDGF-C^{mut}. Both wild type (PDGFC) and PDGF-C^{mut} (Pdgfc^{tm1Lex}) sequences contain the CUB domain (grey). Only the wild type PDGFC has the proteolytic cleavage site (pink) and all eight cysteines (yellow) required for disulfide bond formation. Pdgfc^{tm1Lex} PDGFC contains some of the GFD sequence, but only two cysteines.

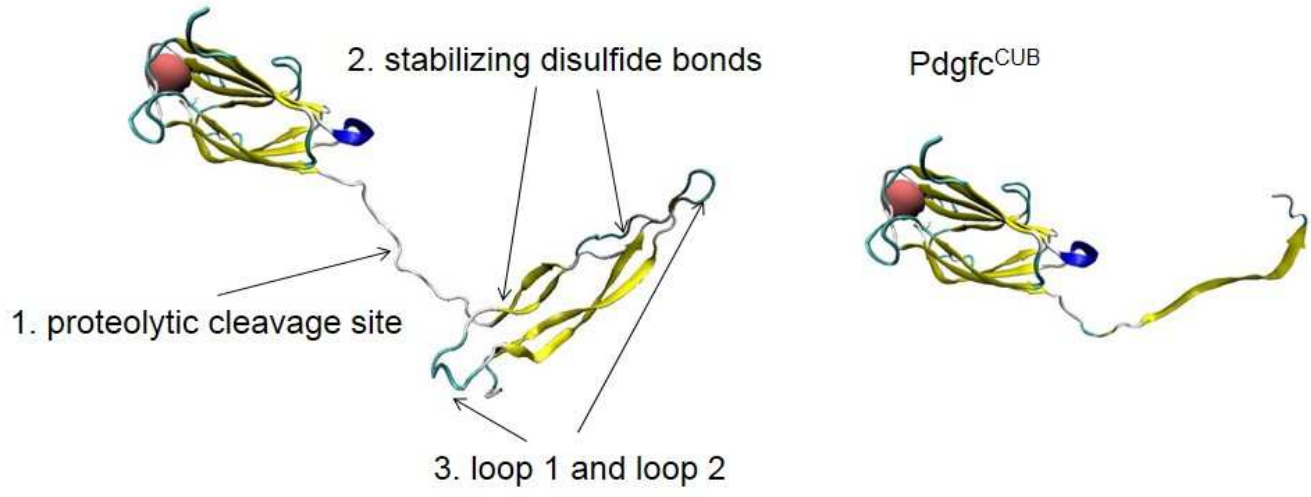

Figure 4.2. Hypothetical model of a monomer of wild type PDGFC and PDGF-C^{mut}. Both wild type and PDGF-C^{mut} sequences contain the CUB domain. Only the wild type PDGFC (left) has the proteolytic cleavage site and the disulfide bond formation required for the cysteine knot motif. PDGF-C^{mut} contains some of the GFD sequence, but only two cysteines.

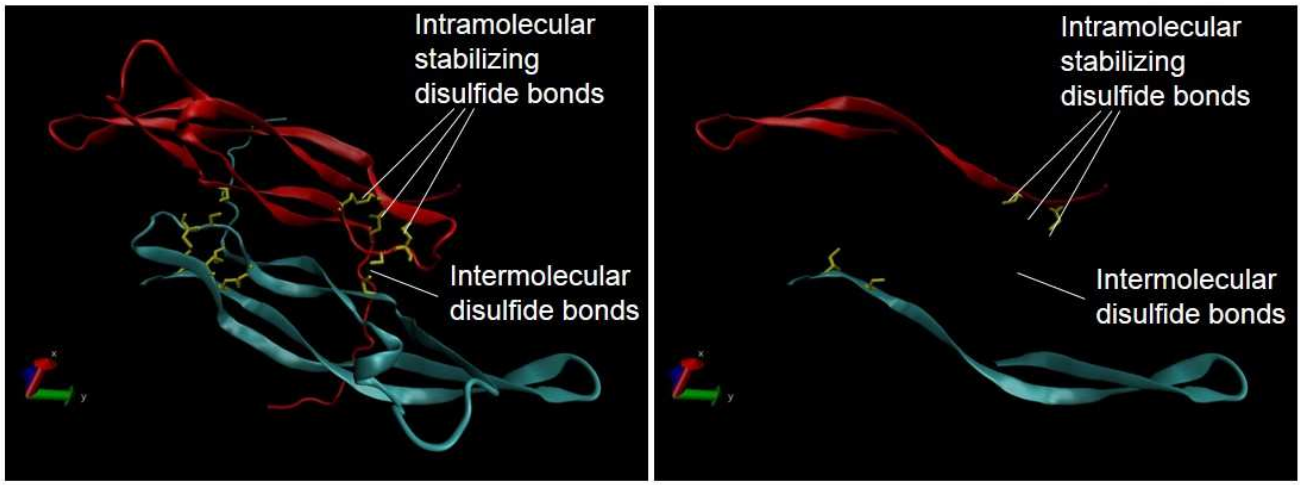

Figure 4.3. Hypothetical model of a dimer of wild type PDGF-CC and PDGF-C^{mut}. Only the wild type PDGFC (left) has the cysteines that form disulfide bonds for both the cysteine knot motif and intermolecular bond formation between two PDGF GFDs. PDGF-C^{mut} contains some of the GFD sequence, but only two cysteines which do not have the endogenous paired cysteines for disulfide bond formation.

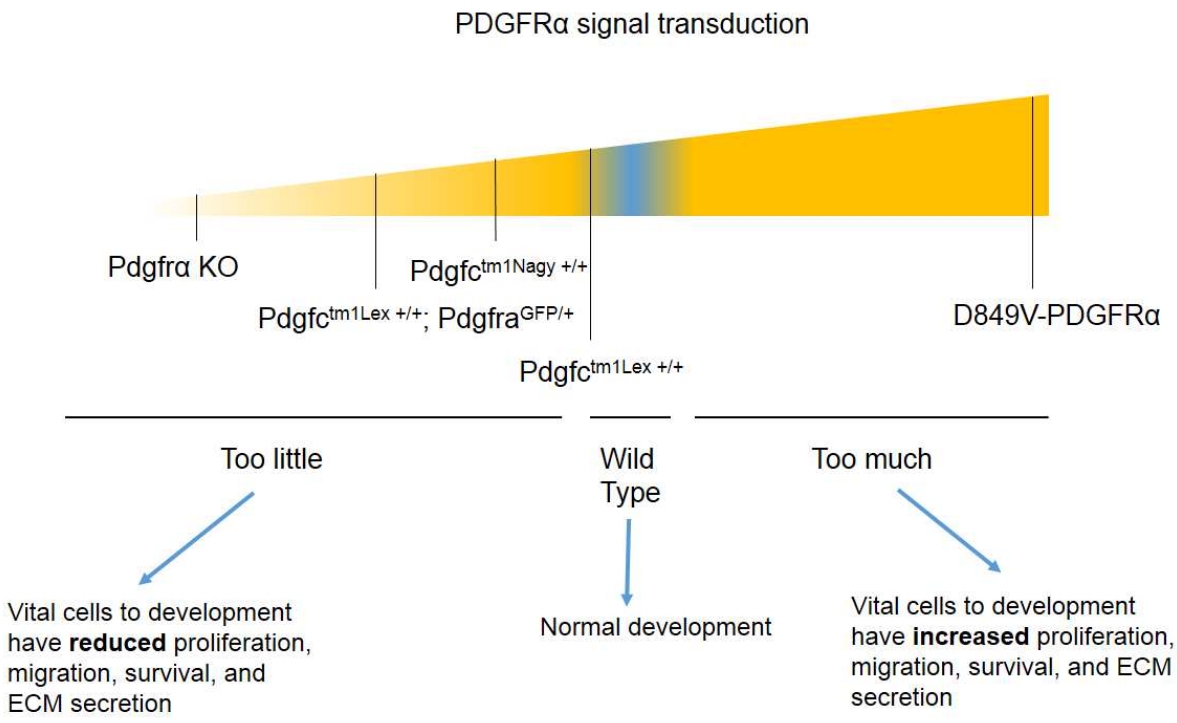

Figure 4.4. PDGFRα Activity has a narrow range compatible with developmental viability. Mouse models altering PDGFRα activity decrease viability in developing embryos. Pdgfc^{tm1Lex} mice are on the edge of the viable range (blue), but decreasing *Pdgfra* copy number (Pdgfc^{tm1Nagy}; Pdgfra$^{GFP/+}$) decreases the viability of mice without the PDGF-C GFD. Pdgfc^{tm1Nagy} mice fall just outside the viable range.

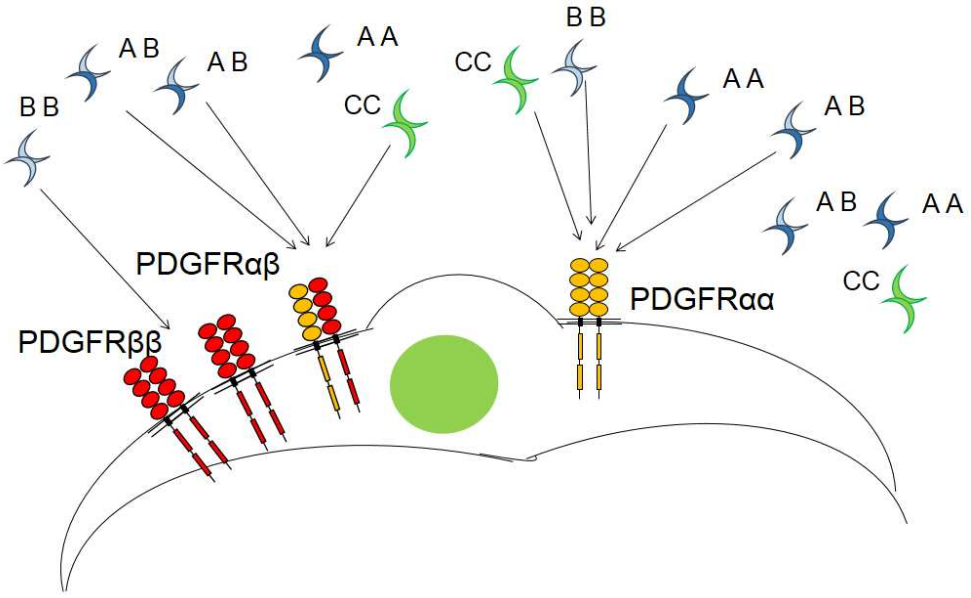

Figure 4.5. PDGFRα as the limiting PDGF pathway component in the liver environment. High endogenous expression of PDGFRβ and expression of PDGF ligands -AA, -AB, -BB, and –CC coupled with low endogenous levels of PDGFRα lead to cells primed to react to PDGFRα stimulation. Activation of PDGFRα induces increased expression of *Pdgfrα*.

References:

1. El-Serag HB. Epidemiology of viral hepatitis and hepatocellular carcinoma. Gastroenterology. 2012;142(6):1264-73.e1. doi: 10.1053/j.gastro.2011.12.061. PubMed PMID: 22537432; PubMed Central PMCID: PMCPMC3338949.
2. Howlader N NA, Krapcho M, Garshell J, Neyman N, Altekruse SF, Kosary CL, Yu M, Ruhl J, Tatalovich Z, Cho H, Mariotto A, Lewis DR, Chen HS, Feuer EJ, Cronin KA (eds). SEER Cancer Statistics Review, 1975-2010, National Cancer Institute. Bethesda, MD, http://seer.cancer.gov/csr/1975_2010/, based on November 2012 SEER data submission, posted to the SEER web site, April 2013.
3. Jemal A, Ward E, Thun M. Declining death rates reflect progress against cancer. PLoS One. 2010;5(3):e9584. doi: 10.1371/journal.pone.0009584. PubMed PMID: 20231893; PubMed Central PMCID: PMCPMC2834749.
4. Clavien PA, Petrowsky H, DeOliveira ML, Graf R. Strategies for safer liver surgery and partial liver transplantation. N Engl J Med. 2007;356(15):1545-59. doi: 10.1056/NEJMra065156. PubMed PMID: 17429086.
5. Jelic S, Sotiropoulos GC, Group EGW. Hepatocellular carcinoma: ESMO Clinical Practice Guidelines for diagnosis, treatment and follow-up. Ann Oncol. 2010;21 Suppl 5:v59-64. doi: 10.1093/annonc/mdq166. PubMed PMID: 20555104.
6. Friedman SL. Liver fibrosis -- from bench to bedside. J Hepatol. 2003;38 Suppl 1:S38-53. PubMed PMID: 12591185.
7. Anthony PP, Ishak KG, Nayak NC, Poulsen HE, Scheuer PJ, Sobin LH. The morphology of cirrhosis: definition, nomenclature, and classification. Bull World Health Organ. 1977;55(4):521-40. PubMed PMID: 304393; PubMed Central PMCID: PMCPMC2366674.
8. Murphy SL XJ, Kochanek KD. Deaths: Final Data for 2010. National vital statistics reports; vol 61 no 4. Hyattsville, MD: National Center for Health Statistics. 2013.
9. Findlay JY, Fix OK, Paugam-Burtz C, Liu L, Sood P, Tomlanovich SJ, Emond J. Critical care of the end-stage liver disease patient awaiting liver transplantation. Liver Transpl. 2011;17(5):496-510. doi: 10.1002/lt.22269. PubMed PMID: 21506240.
10. Bikle DD. The vitamin D endocrine system. Adv Intern Med. 1982;27:45-71. PubMed PMID: 7041549.
11. Zhang AS, Enns CA. Iron homeostasis: recently identified proteins provide insight into novel control mechanisms. J Biol Chem. 2009;284(2):711-5. doi: 10.1074/jbc.R800017200. PubMed PMID: 18757363; PubMed Central PMCID: PMCPMC2613612.
12. Spector AA. Plasma lipid transport. Clin Physiol Biochem. 1984;2(2-3):123-34. PubMed PMID: 6386279.
13. Baratta JL, Ngo A, Lopez B, Kasabwalla N, Longmuir KJ, Robertson RT. Cellular organization of normal mouse liver: a histological, quantitative immunocytochemical, and fine structural analysis. Histochem Cell Biol. 2009;131(6):713-26. doi: 10.1007/s00418-009-0577-1. PubMed PMID: 19255771; PubMed Central PMCID: PMCPMC2761764.
14. Aird WC. Phenotypic heterogeneity of the endothelium: II. Representative vascular beds. Circ Res. 2007;100(2):174-90. doi: 10.1161/01.RES.0000255690.03436.ae. PubMed PMID: 17272819.
15. Iwakiri Y. Endothelial dysfunction in the regulation of cirrhosis and portal hypertension. Liver Int. 2012;32(2):199-213. doi: 10.1111/j.1478-3231.2011.02579.x. PubMed PMID: 21745318; PubMed Central PMCID: PMCPMC3676636.
16. Billiar TR, Curran RD. Kupffer cell and hepatocyte interactions: a brief overview. JPEN J Parenter Enteral Nutr. 1990;14(5 Suppl):175S-80S. PubMed PMID: 2232101.

17. Roland CR, Goss JA, Mangino MJ, Hafenrichter D, Flye MW. Autoregulation by eicosanoids of human Kupffer cell secretory products. A study of interleukin-1, interleukin-6, tumor necrosis factor-alpha, transforming growth factor-beta, and nitric oxide. Ann Surg. 1994;219(4):389-99. PubMed PMID: 8161265; PubMed Central PMCID: PMCPMC1243156.
18. Dajani OF, Meisdalen K, Guren TK, Aasrum M, Tveteraas IH, Lilleby P, Thoresen GH, Sandnes D, Christoffersen T. Prostaglandin E2 upregulates EGF-stimulated signaling in mitogenic pathways involving Akt and ERK in hepatocytes. J Cell Physiol. 2008;214(2):371-80. doi: 10.1002/jcp.21205. PubMed PMID: 17654493.
19. Ledda-Columbano GM, Curto M, Piga R, Zedda AI, Menegazzi M, Sartori C, Shinozuka H, Bluethmann H, Poli V, Ciliberto G, Columbano A. In vivo hepatocyte proliferation is inducible through a TNF and IL-6-independent pathway. Oncogene. 1998;17(8):1039-44. doi: 10.1038/sj.onc.1202018. PubMed PMID: 9747883.
20. Geerts A. History, heterogeneity, developmental biology, and functions of quiescent hepatic stellate cells. Semin Liver Dis. 2001;21(3):311-35. doi: 10.1055/s-2001-17550. PubMed PMID: 11586463.
21. Friedman SL. Hepatic stellate cells: protean, multifunctional, and enigmatic cells of the liver. Physiol Rev. 2008;88(1):125-72. doi: 10.1152/physrev.00013.2007. PubMed PMID: 18195085; PubMed Central PMCID: PMCPMC2888531.
22. Schuppan D, Ruehl M, Somasundaram R, Hahn EG. Matrix as a modulator of hepatic fibrogenesis. Semin Liver Dis. 2001;21(3):351-72. doi: 10.1055/s-2001-17556. PubMed PMID: 11586465.
23. Liu Y, Meyer C, Xu C, Weng H, Hellerbrand C, ten Dijke P, Dooley S. Animal models of chronic liver diseases. Am J Physiol Gastrointest Liver Physiol. 2013;304(5):G449-68. doi: 10.1152/ajpgi.00199.2012. PubMed PMID: 23275613.
24. Salguero Palacios R, Roderfeld M, Hemmann S, Rath T, Atanasova S, Tschuschner A, Gressner OA, Weiskirchen R, Graf J, Roeb E. Activation of hepatic stellate cells is associated with cytokine expression in thioacetamide-induced hepatic fibrosis in mice. Lab Invest. 2008;88(11):1192-203. doi: 10.1038/labinvest.2008.91. PubMed PMID: 18794850.
25. Weber LW, Boll M, Stampfl A. Hepatotoxicity and mechanism of action of haloalkanes: carbon tetrachloride as a toxicological model. Crit Rev Toxicol. 2003;33(2):105-36. doi: 10.1080/713611034. PubMed PMID: 12708612.
26. Wong FW, Chan WY, Lee SS. Resistance to carbon tetrachloride-induced hepatotoxicity in mice which lack CYP2E1 expression. Toxicol Appl Pharmacol. 1998;153(1):109-18. doi: 10.1006/taap.1998.8547. PubMed PMID: 9875305.
27. Bonis PA, Friedman SL, Kaplan MM. Is liver fibrosis reversible? N Engl J Med. 2001;344(6):452-4. doi: 10.1056/NEJM200102083440610. PubMed PMID: 11172184.
28. Acharya SK, Batra Y. Is cirrhosis of the liver reversible? The ultimate that a hepatologist wishes. Trop Gastroenterol. 2003;24(1):1-2. PubMed PMID: 12974205.
29. Hernandez-Gea V, Friedman SL. Pathogenesis of liver fibrosis. Annu Rev Pathol. 2011;6:425-56. doi: 10.1146/annurev-pathol-011110-130246. PubMed PMID: 21073339.
30. Hayashi H, Sakai T. Animal models for the study of liver fibrosis: new insights from knockout mouse models. Am J Physiol Gastrointest Liver Physiol. 2011;300(5):G729-38. doi: 10.1152/ajpgi.00013.2011. PubMed PMID: 21350186; PubMed Central PMCID: PMCPMC3094136.
31. Sanderson N, Factor V, Nagy P, Kopp J, Kondaiah P, Wakefield L, Roberts AB, Sporn MB, Thorgeirsson SS. Hepatic expression of mature transforming growth factor beta 1 in transgenic mice results in multiple tissue lesions. Proc Natl Acad Sci U S A. 1995;92(7):2572-6. PubMed PMID: 7708687; PubMed Central PMCID: PMCPMC42260.

32. Kopp JB, Factor VM, Mozes M, Nagy P, Sanderson N, Böttinger EP, Klotman PE, Thorgeirsson SS. Transgenic mice with increased plasma levels of TGF-beta 1 develop progressive renal disease. Lab Invest. 1996;74(6):991-1003. PubMed PMID: 8667617.
33. Clouthier DE, Comerford SA, Hammer RE. Hepatic fibrosis, glomerulosclerosis, and a lipodystrophy-like syndrome in PEPCK-TGF-beta1 transgenic mice. J Clin Invest. 1997;100(11):2697-713. doi: 10.1172/JCI119815. PubMed PMID: 9389733; PubMed Central PMCID: PMCPMC508473.
34. Kanzler S, Lohse AW, Keil A, Henninger J, Dienes HP, Schirmacher P, Rose-John S, zum Büschenfelde KH, Blessing M. TGF-beta1 in liver fibrosis: an inducible transgenic mouse model to study liver fibrogenesis. Am J Physiol. 1999;276(4 Pt 1):G1059-68. PubMed PMID: 10198351.
35. Ueberham E, Löw R, Ueberham U, Schönig K, Bujard H, Gebhardt R. Conditional tetracycline-regulated expression of TGF-beta1 in liver of transgenic mice leads to reversible intermediary fibrosis. Hepatology. 2003;37(5):1067-78. doi: 10.1053/jhep.2003.50196. PubMed PMID: 12717387.
36. Thieringer F, Maass T, Czochra P, Klopcic B, Conrad I, Friebe D, Schirmacher P, Lohse AW, Blessing M, Galle PR, Teufel A, Kanzler S. Spontaneous hepatic fibrosis in transgenic mice overexpressing PDGF-A. Gene. 2008;423(1):23-8. doi: S0378-1119(08)00218-7 [pii] 10.1016/j.gene.2008.05.022. PubMed PMID: 18598744.
37. Czochra P, Klopcic B, Meyer E, Herkel J, Garcia-Lazaro JF, Thieringer F, Schirmacher P, Biesterfeld S, Galle PR, Lohse AW, Kanzler S. Liver fibrosis induced by hepatic overexpression of PDGF-B in transgenic mice. J Hepatol. 2006;45(3):419-28. doi: S0168-8278(06)00245-5 [pii] 10.1016/j.jhep.2006.04.010. PubMed PMID: 16842882.
38. Uutela M, Wirzenius M, Paavonen K, Rajantie I, He Y, Karpanen T, Lohela M, Wiig H, Salven P, Pajusola K, Eriksson U, Alitalo K. PDGF-D induces macrophage recruitment, increased interstitial pressure, and blood vessel maturation during angiogenesis. Blood. 2004;104(10):3198-204. doi: 10.1182/blood-2004-04-1485. PubMed PMID: 15271796.
39. Campbell JS, Hughes SD, Gilbertson DG, Palmer TE, Holdren MS, Haran AC, Odell MM, Bauer RL, Ren HP, Haugen HS, Yeh MM, Fausto N. Platelet-derived growth factor C induces liver fibrosis, steatosis, and hepatocellular carcinoma. Proc Natl Acad Sci U S A. 2005;102(9):3389-94. doi: 0409722102 [pii] 10.1073/pnas.0409722102. PubMed PMID: 15728360; PubMed Central PMCID: PMCPMC552940.
40. Wright JH, Johnson MM, Shimizu-Albergine M, Bauer RL, Hayes BJ, Surapisitchat J, Hudkins KL, Riehle KJ, Johnson SC, Yeh MM, Bammler TK, Beyer RP, Gilbertson DG, Alpers CE, Fausto N, Campbell JS. Paracrine activation of hepatic stellate cells in platelet-derived growth factor C transgenic mice: Evidence for stromal induction of hepatocellular carcinoma. Int J Cancer. 2013. doi: 10.1002/ijc.28421. PubMed PMID: 23929039.
41. Bataller R, Brenner DA. Liver fibrosis. J Clin Invest. 2005;115(2):209-18. doi: 10.1172/JCI24282. PubMed PMID: 15690074; PubMed Central PMCID: PMCPMC546435.
42. Ross R, Raines EW, Bowen-Pope DF. The biology of platelet-derived growth factor. Cell. 1986;46(2):155-69. PubMed PMID: 3013421.
43. Pierce GF, Tarpley JE, Tseng J, Bready J, Chang D, Kenney WC, Rudolph R, Robson MC, Vande Berg J, Reid P. Detection of platelet-derived growth factor (PDGF)-AA in actively healing human wounds treated with recombinant PDGF-BB and absence of PDGF in chronic nonhealing wounds. J Clin Invest. 1995;96(3):1336-50. doi: 10.1172/JCI118169. PubMed PMID: 7657809; PubMed Central PMCID: PMCPMC185756.
44. Cimpean AM, Ceauşu R, Encică S, Gaje PN, Ribatti D, Raica M. Platelet-derived growth factor and platelet-derived growth factor receptor-α expression in the normal human thymus and

thymoma. Int J Exp Pathol. 2011;92(5):340-4. doi: 10.1111/j.1365-2613.2011.00777.x. PubMed PMID: 21645144; PubMed Central PMCID: PMCPMC3193148.
45. Rahbari NN, Schmidt T, Falk CS, Hinz U, Herber M, Bork U, Büchler MW, Weitz J, Koch M. Expression and prognostic value of circulating angiogenic cytokines in pancreatic cancer. BMC Cancer. 2011;11:286. doi: 1471-2407-11-286 [pii]10.1186/1471-2407-11-286. PubMed PMID: 21729304; PubMed Central PMCID: PMCPMC3144458.

46. Verhaak RG, Hoadley KA, Purdom E, Wang V, Qi Y, Wilkerson MD, Miller CR, Ding L, Golub T, Mesirov JP, Alexe G, Lawrence M, O'Kelly M, Tamayo P, Weir BA, Gabriel S, Winckler W, Gupta S, Jakkula L, Feiler HS, Hodgson JG, James CD, Sarkaria JN, Brennan C, Kahn A, Spellman PT, Wilson RK, Speed TP, Gray JW, Meyerson M, Getz G, Perou CM, Hayes DN, Network CGAR. Integrated genomic analysis identifies clinically relevant subtypes of glioblastoma characterized by abnormalities in PDGFRA, IDH1, EGFR, and NF1. Cancer Cell. 2010;17(1):98-110. doi: S1535-6108(09)00432-2 [pii]10.1016/j.ccr.2009.12.020. PubMed PMID: 20129251; PubMed Central PMCID: PMCPMC2818769.

47. Cools J, DeAngelo DJ, Gotlib J, Stover EH, Legare RD, Cortes J, Kutok J, Clark J, Galinsky I, Griffin JD, Cross NC, Tefferi A, Malone J, Alam R, Schrier SL, Schmid J, Rose M, Vandenberghe P, Verhoef G, Boogaerts M, Wlodarska I, Kantarjian H, Marynen P, Coutre SE, Stone R, Gilliland DG. A tyrosine kinase created by fusion of the PDGFRA and FIP1L1 genes as a therapeutic target of imatinib in idiopathic hypereosinophilic syndrome. N Engl J Med. 2003;348(13):1201-14. doi: 348/13/1201 [pii]10.1056/NEJMoa025217. PubMed PMID: 12660384.
48. Shimizu A, O'Brien KP, Sjöblom T, Pietras K, Buchdunger E, Collins VP, Heldin CH, Dumanski JP, Ostman A. The dermatofibrosarcoma protuberans-associated collagen type Ialpha1/platelet-derived growth factor (PDGF) B-chain fusion gene generates a transforming protein that is processed to functional PDGF-BB. Cancer Res. 1999;59(15):3719-23. PubMed PMID: 10446987.
49. Ben-Hamo R, Efroni S. Biomarker robustness reveals the PDGF network as driving disease outcome in ovarian cancer patients in multiple studies. BMC Syst Biol. 2012;6:3. doi: 10.1186/1752-0509-6-3. PubMed PMID: 22236809; PubMed Central PMCID: PMCPMC3298526.
50. Galimberti S, Ferreri MI, Simi P, Azzarà A, Baratè C, Fazzi R, Cecconi N, Cervetti G, Guerrini F, Petrini M. Platelet-derived growth factor beta receptor (PDGFRB) gene is rearranged in a significant percentage of myelodysplastic syndromes with normal karyotype. Br J Haematol. 2009;147(5):763-6. doi: 10.1111/j.1365-2141.2009.07878.x. PubMed PMID: 19758395.
51. Andrae J, Gallini R, Betsholtz C. Role of platelet-derived growth factors in physiology and medicine. Genes Dev. 2008;22(10):1276-312. doi: 22/10/1276 [pii] 10.1101/gad.1653708. PubMed PMID: 18483217; PubMed Central PMCID: PMCPMC2732412.
52. Ross R, Glomset J, Kariya B, Harker L. A platelet-dependent serum factor that stimulates the proliferation of arterial smooth muscle cells in vitro. Proc Natl Acad Sci U S A. 1974;71(4):1207-10. PubMed PMID: 4208546; PubMed Central PMCID: PMCPMC388193.
53. Kohler N, Lipton A. Platelets as a source of fibroblast growth-promoting activity. Exp Cell Res. 1974;87(2):297-301. PubMed PMID: 4370268.
54. Westermark B, Wasteson A. A platelet factor stimulating human normal glial cells. Exp Cell Res. 1976;98(1):170-4. PubMed PMID: 1253836.
55. Antoniades HN. Human platelet-derived growth factor (PDGF): purification of PDGF-I and PDGF-II and separation of their reduced subunits. Proc Natl Acad Sci U S A. 1981;78(12):7314-7. PubMed PMID: 6950377; PubMed Central PMCID: PMCPMC349256.

56. Raines EW, Ross R. Platelet-derived growth factor. I. High yield purification and evidence for multiple forms. J Biol Chem. 1982;257(9):5154-60. PubMed PMID: 7068680.
57. Hammacher A, Hellman U, Johnsson A, Ostman A, Gunnarsson K, Westermark B, Wasteson A, Heldin CH. A major part of platelet-derived growth factor purified from human platelets is a heterodimer of one A and one B chain. J Biol Chem. 1988;263(31):16493-8. PubMed PMID: 2460450.
58. Li X, Pontén A, Aase K, Karlsson L, Abramsson A, Uutela M, Bäckström G, Hellström M, Boström H, Li H, Soriano P, Betsholtz C, Heldin C, Alitalo K, Ostman A, Eriksson U. PDGF-C is a new protease-activated ligand for the PDGF alpha-receptor. Nat Cell Biol. 2000;2(5):302-9. doi: 10.1038/35010579. PubMed PMID: 10806482.
59. Gilbertson DG, Duff ME, West JW, Kelly JD, Sheppard PO, Hofstrand PD, Gao Z, Shoemaker K, Bukowski TR, Moore M, Feldhaus AL, Humes JM, Palmer TE, Hart CE. Platelet-derived growth factor C (PDGF-C), a novel growth factor that binds to PDGF alpha and beta receptor. J Biol Chem. 2001;276(29):27406-14. doi: M101056200 [pii] 10.1074/jbc.M101056200. PubMed PMID: 11297552.
60. LaRochelle WJ, Jeffers M, McDonald WF, Chillakuru RA, Giese NA, Lokker NA, Sullivan C, Boldog FL, Yang M, Vernet C, Burgess CE, Fernandes E, Deegler LL, Rittman B, Shimkets J, Shimkets RA, Rothberg JM, Lichenstein HS. PDGF-D, a new protease-activated growth factor. Nat Cell Biol. 2001;3(5):517-21. doi: 35074593 [pii]10.1038/35074593. PubMed PMID: 11331882.
61. Bergsten E, Uutela M, Li X, Pietras K, Ostman A, Heldin CH, Alitalo K, Eriksson U. PDGF-D is a specific, protease-activated ligand for the PDGF beta-receptor. Nat Cell Biol. 2001;3(5):512-6. doi: 35074588 [pii] 10.1038/35074588. PubMed PMID: 11331881.
62. Reigstad LJ, Sande HM, Fluge Ø, Bruland O, Muga A, Varhaug JE, Martinez A, Lillehaug JR. Platelet-derived growth factor (PDGF)-C, a PDGF family member with a vascular endothelial growth factor-like structure. J Biol Chem. 2003;278(19):17114-20. doi: M301728200 [pii] 10.1074/jbc.M301728200. PubMed PMID: 12598536.
63. Williams LT, Tremble P, Antoniades HN. Platelet-derived growth factor binds specifically to receptors on vascular smooth muscle cells and the binding becomes nondissociable. Proc Natl Acad Sci U S A. 1982;79(19):5867-70. PubMed PMID: 6310551; PubMed Central PMCID: PMCPMC347011.
64. Bowen-Pope DF, Ross R. Platelet-derived growth factor. II. Specific binding to cultured cells. J Biol Chem. 1982;257(9):5161-71. PubMed PMID: 6279659.
65. Fredriksson L, Li H, Eriksson U. The PDGF family: four gene products form five dimeric isoforms. Cytokine Growth Factor Rev. 2004;15(4):197-204. doi: S1359610104000176 [pii] 10.1016/j.cytogfr.2004.03.007. PubMed PMID: 15207811.
66. Bork P, Beckmann G. The CUB domain. A widespread module in developmentally regulated proteins. J Mol Biol. 1993;231(2):539-45. doi: S0022-2836(83)71305-7 [pii] 10.1006/jmbi.1993.1305. PubMed PMID: 8510165.

67. Gaboriaud C, Gregory-Pauron L, Teillet F, Thielens NM, Bally I, Arlaud GJ. Structure and properties of the Ca(2+)-binding CUB domain, a widespread ligand-recognition unit involved in major biological functions. Biochem J. 2011;439(2):185-93. doi: BJ20111027 [pii] 10.1042/BJ20111027. PubMed PMID: 21954942.

68. Creanga A, Glenn TD, Mann RK, Saunders AM, Talbot WS, Beachy PA. Scube/You activity mediates release of dually lipid-modified Hedgehog signal in soluble form. Genes Dev. 2012;26(12):1312-25. doi: 10.1101/gad.191866.112. PubMed PMID: 22677548; PubMed Central PMCID: PMCPMC3387659.

69. Hollway GE, Maule J, Gautier P, Evans TM, Keenan DG, Lohs C, Fischer D, Wicking C, Currie PD. Scube2 mediates Hedgehog signalling in the zebrafish embryo. Dev Biol. 2006;294(1):104-18. doi: S0012-1606(06)00130-8 [pii]10.1016/j.ydbio.2006.02.032. PubMed PMID: 16626681.
70. Giger RJ, Urquhart ER, Gillespie SK, Levengood DV, Ginty DD, Kolodkin AL. Neuropilin-2 is a receptor for semaphorin IV: insight into the structural basis of receptor function and specificity. Neuron. 1998;21(5):1079-92. PubMed PMID: 9856463.
71. Lee HX, Mendes FA, Plouhinec JL, De Robertis EM. Enzymatic regulation of pattern: BMP4 binds CUB domains of Tolloids and inhibits proteinase activity. Genes Dev. 2009;23(21):2551-62. doi: 10.1101/gad.1839309. PubMed PMID: 19884260; PubMed Central PMCID: PMCPMC2779747.
72. Hartigan N, Garrigue-Antar L, Kadler KE. Bone morphogenetic protein-1 (BMP-1). Identification of the minimal domain structure for procollagen C-proteinase activity. J Biol Chem. 2003;278(20):18045-9. doi: 10.1074/jbc.M211448200. PubMed PMID: 12637537.
73. Teillet F, Gaboriaud C, Lacroix M, Martin L, Arlaud GJ, Thielens NM. Crystal structure of the CUB1-EGF-CUB2 domain of human MASP-1/3 and identification of its interaction sites with mannan-binding lectin and ficolins. J Biol Chem. 2008;283(37):25715-24. doi: 10.1074/jbc.M803551200. PubMed PMID: 18596036.
74. Christensen EI, Nielsen R, Birn H. From bowel to kidneys: the role of cubilin in physiology and disease. Nephrol Dial Transplant. 2013;28(2):274-81. doi: 10.1093/ndt/gfs565. PubMed PMID: 23291372.
75. Dijkmans J, Xu J, Masure S, Dhanaraj S, Gosiewska A, Geesin J, Sprengel J, Harris S, Verhasselt P, Gordon R, Yon J. Characterization of platelet-derived growth factor-C (PDGF-C): expression in normal and tumor cells, biological activity and chromosomal localization. The international journal of biochemistry & cell biology. 2002;34(4):414-26. PubMed PMID: 118.
76. Pontén A, Li X, Thorén P, Aase K, Sjöblom T, Ostman A, Eriksson U. Transgenic overexpression of platelet-derived growth factor-C in the mouse heart induces cardiac fibrosis, hypertrophy, and dilated cardiomyopathy. Am J Pathol. 2003;163(2):673-82. doi: S0002-9440(10)63694-2 [pii]10.1016/S0002-9440(10)63694-2. PubMed PMID: 12875986; PubMed Central PMCID: PMCPMC1868211.
77. Klinghoffer RA, Hamilton TG, Hoch R, Soriano P. An allelic series at the PDGFalphaR locus indicates unequal contributions of distinct signaling pathways during development. Dev Cell. 2002;2(1):103-13. doi: S1534580701001034 [pii]. PubMed PMID: 11782318.
78. Tallquist MD, French WJ, Soriano P. Additive effects of PDGF receptor beta signaling pathways in vascular smooth muscle cell development. PLoS Biol. 2003;1(2):E52. doi: 10.1371/journal.pbio.0000052. PubMed PMID: 14624252; PubMed Central PMCID: PMCPMC261889.
79. Crosby JR, Seifert RA, Soriano P, Bowen-Pope DF. Chimaeric analysis reveals role of Pdgf receptors in all muscle lineages. Nat Genet. 1998;18(4):385-8. doi: 10.1038/ng0498-385. PubMed PMID: 9537425.
80. Soriano P. The PDGF alpha receptor is required for neural crest cell development and for normal patterning of the somites. Development. 1997;124(14):2691-700. PubMed PMID: 9226440.
81. McKinnon RD, Waldron S, Kiel ME. PDGF alpha-receptor signal strength controls an RTK rheostat that integrates phosphoinositol 3'-kinase and phospholipase Cgamma pathways during oligodendrocyte maturation. J Neurosci. 2005;25(14):3499-508. doi: 10.1523/JNEUROSCI.5049-04.2005. PubMed PMID: 15814780.
82. Murtie JC, Zhou YX, Le TQ, Vana AC, Armstrong RC. PDGF and FGF2 pathways regulate distinct oligodendrocyte lineage responses in experimental demyelination with

spontaneous remyelination. Neurobiol Dis. 2005;19(1-2):171-82. doi:10.1016/j.nbd.2004.12.006. PubMed PMID: 15837572.
83. Andrae J, Ehrencrona H, Gallini R, Lal M, Ding H, Betsholtz C. Analysis of mice lacking the heparin-binding splice isoform of PDGF-A. Mol Cell Biol. 2013. doi: 10.1128/MCB.00749-13. PubMed PMID: 23938297.
84. Schmahl J, Raymond C, Soriano P. PDGF signaling specificity is mediated through multiple immediate early genes. Nat Genet. 2007;39(1):52-60. doi: ng1922 [pii]10.1038/ng1922. PubMed PMID: 17143286.
85. Boström H, Willetts K, Pekny M, Levéen P, Lindahl P, Hedstrand H, Pekna M, Hellström M, Gebre-Medhin S, Schalling M, Nilsson M, Kurland S, Törnell J, Heath JK, Betsholtz C. PDGF-A signaling is a critical event in lung alveolar myofibroblast development and alveogenesis. Cell. 1996;85(6):863-73. doi: S0092-8674(00)81270-2 [pii]. PubMed PMID: 8681381.
86. Levéen P, Pekny M, Gebre-Medhin S, Swolin B, Larsson E, Betsholtz C. Mice deficient for PDGF B show renal, cardiovascular, and hematological abnormalities. Genes Dev. 1994;8(16):1875-87. PubMed PMID: 7958863.
87. Ding H, Wu X, Bostrom H, Kim I, Wong N, Tsoi B, O'Rourke M, Koh GY, Soriano P, Betsholtz C, Hart TC, Marazita ML, Field LL, Tam PP, Nagy A. A specific requirement for PDGF-C in palate formation and PDGFR-alpha signaling. Nature genetics. 2004;36(10):1111-6. PubMed PMID: 121.
88. Johnsson A, Heldin CH, Wasteson A, Westermark B, Deuel TF, Huang JS, Seeburg PH, Gray A, Ullrich A, Scrace G. The c-sis gene encodes a precursor of the B chain of platelet-derived growth factor. EMBO J. 1984;3(5):921-8. PubMed PMID: 6329745; PubMed Central PMCID: PMCPMC557452.
89. Hart CE, Forstrom JW, Kelly JD, Seifert RA, Smith RA, Ross R, Murray MJ, Bowen-Pope DF. Two classes of PDGF receptor recognize different isoforms of PDGF. Science. 1988;240(4858):1529-31. PubMed PMID: 2836952.
90. Soriano P. Abnormal kidney development and hematological disorders in PDGF beta-receptor mutant mice. Genes Dev. 1994;8(16):1888-96. PubMed PMID: 7958864.
91. Tallquist MD, Soriano P. Cell autonomous requirement for PDGFRalpha in populations of cranial and cardiac neural crest cells. Development. 2003;130(3):507-18. PubMed PMID: 12490557.
92. Fredriksson L, Li H, Eriksson U. The PDGF family: four gene products form five dimeric isoforms. Cytokine & growth factor reviews. 2004;15(4):197-204. PubMed PMID: 127.
93. Eitner F, Bücher E, van Roeyen C, Kunter U, Rong S, Seikrit C, Villa L, Boor P, Fredriksson L, Bäckström G, Eriksson U, Ostman A, Floege J, Ostendorf T. PDGF-C is a proinflammatory cytokine that mediates renal interstitial fibrosis. J Am Soc Nephrol. 2008;19(2):281-9. doi: ASN.2007030290 [pii]10.1681/ASN.2007030290. PubMed PMID: 18184860; PubMed Central PMCID: PMCPMC2396746.
94. Fredriksson L, Nilsson I, Su EJ, Andrae J, Ding H, Betsholtz C, Eriksson U, Lawrence DA. Platelet-Derived Growth Factor C Deficiency in C57BL/6 Mice Leads to Abnormal Cerebral Vascularization, Loss of Neuroependymal Integrity, and Ventricular Abnormalities. Am J Pathol. 2012. doi: S0002-9440(11)01100-X [pii]10.1016/j.ajpath.2011.12.006. PubMed PMID: 22230248.
95. Fredriksson L, Nilsson I, Su EJ, Andrae J, Ding H, Betsholtz C, Eriksson U, Lawrence DA. Platelet-derived growth factor C deficiency in C57BL/6 mice leads to abnormal cerebral vascularization, loss of neuroependymal integrity, and ventricular abnormalities. Am J Pathol. 2012;180(3):1136-44. doi: 10.1016/j.ajpath.2011.12.006. PubMed PMID: 22230248; PubMed Central PMCID: PMCPMC3349890.

96. Betsholtz C, Johnsson A, Heldin CH, Westermark B, Lind P, Urdea MS, Eddy R, Shows TB, Philpott K, Mellor AL. cDNA sequence and chromosomal localization of human platelet-derived growth factor A-chain and its expression in tumour cell lines. Nature. 1986;320(6064):695-9. doi: 10.1038/320695a0. PubMed PMID: 3754619.
97. Sauer MK, Donoghue DJ. Identification of nonessential disulfide bonds and altered conformations in the v-sis protein, a homolog of the B chain of platelet-derived growth factor. Mol Cell Biol. 1988;8(3):1011-8. PubMed PMID: 2835654; PubMed Central PMCID: PMCPMC363243.
98. Kenney WC, Haniu M, Herman AC, Arakawa T, Costigan VJ, Lary J, Yphantis DA, Thomason AR. Formation of mitogenically active PDGF-B dimer does not require interchain disulfide bonds. J Biol Chem. 1994;269(16):12351-9. PubMed PMID: 8163539.
99. Kreysing J, Ostman A, van de Poll M, Bäckström G, Heldin CH. Identification of three amino acid residues in the B-chain of platelet-derived growth factor with different importance for binding to PDGF alpha- and beta-receptors. FEBS Lett. 1996;385(3):181-4. doi: 0014-5793(96)00349-3 [pii]. PubMed PMID: 8647246.
100. Fenstermaker RA, Poptic E, Bonfield TL, Knauss TC, Corsillo L, Piskurich JF, Kaetzel CS, Jentoft JE, Gelfand C, DiCorleto PE. A cationic region of the platelet-derived growth factor (PDGF) A-chain (Arg159-Lys160-Lys161) is required for receptor binding and mitogenic activity of the PDGF-AA homodimer. J Biol Chem. 1993;268(14):10482-9. PubMed PMID: 8486701.
101. Andersson M, Ostman A, Kreysing J, Bäckström G, Van de Poll M, Heldin CH. Involvement of loop 2 of platelet-derived growth factor-AA and -BB in receptor binding. Growth Factors. 1995;12(2):159-64. PubMed PMID: 8679250.
102. Kibbe WA. OligoCalc: an online oligonucleotide properties calculator. Nucleic Acids Res. 2007;35(Web Server issue):W43-6. doi: 10.1093/nar/gkm234. PubMed PMID: 17452344; PubMed Central PMCID: PMCPMC1933198.
103. Crouthamel MH, Kelly EJ, Ho RJ. Development and characterization of transgenic mouse models for conditional gene knockout in the blood-brain and blood-CSF barriers. Transgenic Res. 2012;21(1):113-30. doi: 10.1007/s11248-011-9512-z. PubMed PMID: 21538071; PubMed Central PMCID: PMCPMC3192922.
104. Sambrook J, Russell DW. Calcium-phosphate-mediated Transfection of Eukaryotic Cells with Plasmid DNAs. CSH Protoc. 2006;2006(1). doi: 10.1101/pdb.prot3871. PubMed PMID: 22485343.
105. Campbell JS, Riehle KJ, Brooling JT, Bauer RL, Mitchell C, Fausto N. Proinflammatory cytokine production in liver regeneration is Myd88-dependent, but independent of Cd14, Tlr2, and Tlr4. J Immunol. 2006;176(4):2522-8. PubMed PMID: 16456013.
106. Sundberg JP, Taylor D, Lorch G, Miller J, Silva KA, Sundberg BA, Roopenian D, Sperling L, Ong D, King LE, Everts H. Primary follicular dystrophy with scarring dermatitis in C57BL/6 mouse substrains resembles central centrifugal cicatricial alopecia in humans. Vet Pathol. 2011;48(2):513-24. doi: 10.1177/0300985810379431. PubMed PMID: 20861494; PubMed Central PMCID: PMCPMC3101716.
107. Hamilton TG, Klinghoffer RA, Corrin PD, Soriano P. Evolutionary divergence of platelet-derived growth factor alpha receptor signaling mechanisms. Mol Cell Biol. 2003;23(11):4013-25. PubMed PMID: 12748302; PubMed Central PMCID: PMCPMC155222.
108. Anisimov A, Leppänen VM, Tvorogov D, Zarkada G, Jeltsch M, Holopainen T, Kaijalainen S, Alitalo K. The basis for the distinct biological activities of vascular endothelial growth factor receptor-1 ligands. Sci Signal. 2013;6(282):ra52. doi: 10.1126/scisignal.2003905. PubMed PMID: 23821770.
109. Kiba A, Yabana N, Shibuya M. A set of loop-1 and -3 structures in the novel vascular endothelial growth factor (VEGF) family member, VEGF-ENZ-7, is essential for the activation of

VEGFR-2 signaling. J Biol Chem. 2003;278(15):13453-61. doi: 10.1074/jbc.M210931200. PubMed PMID: 12551914.
110. Thielens NM, Bersch B, Hernandez JF, Arlaud GJ. Structure and functions of the interaction domains of C1r and C1s: keystones of the architecture of the C1 complex. Immunopharmacology. 1999;42(1-3):3-13. PubMed PMID: 10408360.
111. Nakamura F, Goshima Y. Structural and functional relation of neuropilins. Adv Exp Med Biol. 2002;515:55-69. PubMed PMID: 12613543.
112. Mahoney DJ, Mikecz K, Ali T, Mabilleau G, Benayahu D, Plaas A, Milner CM, Day AJ, Sabokbar A. TSG-6 regulates bone remodeling through inhibition of osteoblastogenesis and osteoclast activation. J Biol Chem. 2008;283(38):25952-62. doi: M802138200 [pii] 10.1074/jbc.M802138200. PubMed PMID: 18586671; PubMed Central PMCID: PMCPMC2533787.

113. Lee HX, Mendes FA, Plouhinec JL, De Robertis EM. Enzymatic regulation of pattern: BMP4 binds CUB domains of Tolloids and inhibits proteinase activity. Genes Dev. 2009;23(21):2551-62. doi: 23/21/2551 [pii]10.1101/gad.1839309. PubMed PMID: 19884260; PubMed Central PMCID: PMCPMC2779747.
114. Starr SP, Raines D. Cirrhosis: diagnosis, management, and prevention. Am Fam Physician. 2011;84(12):1353-9. PubMed PMID: 22230269.
115. Olson LE, Soriano P. Increased PDGFRalpha activation disrupts connective tissue development and drives systemic fibrosis. Dev Cell. 2009;16(2):303-13. doi: S1534-5807(08)00513-3 [pii]10.1016/j.devcel.2008.12.003. PubMed PMID: 19217431; PubMed Central PMCID: PMCPMC2664622.
116. Chong JJ, Reinecke H, Iwata M, Torok-Storb B, Stempien-Otero A, Murry CE. Progenitor cells identified by PDGFR-alpha expression in the developing and diseased human heart. Stem Cells Dev. 2013;22(13):1932-43. doi: 10.1089/scd.2012.0542. PubMed PMID: 23391309; PubMed Central PMCID: PMCPMC3685392.
117. Antoniades HN, Bravo MA, Avila RE, Galanopoulos T, Neville-Golden J, Maxwell M, Selman M. Platelet-derived growth factor in idiopathic pulmonary fibrosis. J Clin Invest. 1990;86(4):1055-64. doi: 10.1172/JCI114808. PubMed PMID: 2170444; PubMed Central PMCID: PMCPMC296832.
118. Floege J, Eitner F, Alpers CE. A new look at platelet-derived growth factor in renal disease. J Am Soc Nephrol. 2008;19(1):12-23. doi: 10.1681/ASN.2007050532. PubMed PMID: 18077793.
119. Zymek P, Bujak M, Chatila K, Cieslak A, Thakker G, Entman ML, Frangogiannis NG. The role of platelet-derived growth factor signaling in healing myocardial infarcts. J Am Coll Cardiol. 2006;48(11):2315-23. doi: 10.1016/j.jacc.2006.07.060. PubMed PMID: 17161265.
120. Abdollahi A, Li M, Ping G, Plathow C, Domhan S, Kiessling F, Lee LB, McMahon G, Gröne HJ, Lipson KE, Huber PE. Inhibition of platelet-derived growth factor signaling attenuates pulmonary fibrosis. J Exp Med. 2005;201(6):925-35. doi: 10.1084/jem.20041393. PubMed PMID: 15781583; PubMed Central PMCID: PMCPMC2213091.
121. Chen YT, Chang FC, Wu CF, Chou YH, Hsu HL, Chiang WC, Shen J, Chen YM, Wu KD, Tsai TJ, Duffield JS, Lin SL. Platelet-derived growth factor receptor signaling activates pericyte-myofibroblast transition in obstructive and post-ischemic kidney fibrosis. Kidney Int. 2011;80(11):1170-81. doi: 10.1038/ki.2011.208. PubMed PMID: 21716259.
122. Hoch RV, Soriano P. Roles of PDGF in animal development. Development. 2003;130(20):4769-84. doi: 130/20/4769 [pii] 10.1242/dev.00721. PubMed PMID: 12952899.

123. Mellgren AM, Smith CL, Olsen GS, Eskiocak B, Zhou B, Kazi MN, Ruiz FR, Pu WT, Tallquist MD. Platelet-derived growth factor receptor beta signaling is required for efficient epicardial cell migration and development of two distinct coronary vascular smooth muscle cell populations. Circ Res. 2008;103(12):1393-401. doi: 10.1161/CIRCRESAHA.108.176768. PubMed PMID: 18948621; PubMed Central PMCID: PMCPMC2757035.
124. Olson LE, Soriano P. PDGFRβ signaling regulates mural cell plasticity and inhibits fat development. Dev Cell. 2011;20(6):815-26. doi: 10.1016/j.devcel.2011.04.019. PubMed PMID: 21664579; PubMed Central PMCID: PMCPMC3121186.
125. Chen H, Gu X, Liu Y, Wang J, Wirt SE, Bottino R, Schorle H, Sage J, Kim SK. PDGF signalling controls age-dependent proliferation in pancreatic β-cells. Nature. 2011;478(7369):349-55. doi: nature10502 [pii]10.1038/nature10502. PubMed PMID: 21993628.
126. Bonner JC. Regulation of PDGF and its receptors in fibrotic diseases. Cytokine Growth Factor Rev. 2004;15(4):255-73. doi: S1359610104000164 [pii] 10.1016/j.cytogfr.2004.03.006. PubMed PMID: 15207816.
127. Iwayama T, Olson LE. Involvement of PDGF in fibrosis and scleroderma: recent insights from animal models and potential therapeutic opportunities. Curr Rheumatol Rep. 2013;15(2):304. doi: 10.1007/s11926-012-0304-0. PubMed PMID: 23307576.
128. Campbell JS, Johnson MM, Bauer RL, Hudkins KL, Gilbertson DG, Riehle KJ, Yeh MM, Alpers CE, Fausto N. Targeting stromal cells for the treatment of platelet-derived growth factor C-induced hepatocellular carcinogenesis. Differentiation. 2007;75(9):843-52. doi: S0301-4681(09)60176-6 [pii] 10.1111/j.1432-0436.2007.00235.x. PubMed PMID: 17999742.
129. Junqueira LC, Bignolas G, Brentani RR. Picrosirius staining plus polarization microscopy, a specific method for collagen detection in tissue sections. Histochem J. 1979;11(4):447-55. PubMed PMID: 91593.
130. Argast GM, Campbell JS, Brooling JT, Fausto N. Epidermal growth factor receptor transactivation mediates tumor necrosis factor-induced hepatocyte replication. J Biol Chem. 2004;279(33):34530-6. doi: M405703200 [pii]10.1074/jbc.M405703200. PubMed PMID: 15199050.
131. Ikura Y, Morimoto H, Ogami M, Jomura H, Ikeoka N, Sakurai M. Expression of platelet-derived growth factor and its receptor in livers of patients with chronic liver disease. J Gastroenterol. 1997;32(4):496-501. PubMed PMID: 9250897.
132. Wong L, Yamasaki G, Johnson RJ, Friedman SL. Induction of beta-platelet-derived growth factor receptor in rat hepatic lipocytes during cellular activation in vivo and in culture. J Clin Invest. 1994;94(4):1563-9. doi: 10.1172/JCI117497. PubMed PMID: 7929832; PubMed Central PMCID: PMCPMC295310.
133. Pinzani M, Milani S, Herbst H, DeFranco R, Grappone C, Gentilini A, Caligiuri A, Pellegrini G, Ngo DV, Romanelli RG, Gentilini P. Expression of platelet-derived growth factor and its receptors in normal human liver and during active hepatic fibrogenesis. Am J Pathol. 1996;148(3):785-800. PubMed PMID: 8774134; PubMed Central PMCID: PMCPMC1861723.
134. Tiribelli C, Melato M, Crocè LS, Giarelli L, Okuda K, Ohnishi K. Prevalence of hepatocellular carcinoma and relation to cirrhosis: comparison of two different cities of the world--Trieste, Italy, and Chiba, Japan. Hepatology. 1989;10(6):998-1002. PubMed PMID: 2555298.
135. Borkham-Kamphorst E, Kovalenko E, van Roeyen CR, Gassler N, Bomble M, Ostendorf T, Floege J, Gressner AM, Weiskirchen R. Platelet-derived growth factor isoform expression in carbon tetrachloride-induced chronic liver injury. Lab Invest. 2008;88(10):1090-100. doi: labinvest200871 [pii] 10.1038/labinvest.2008.71. PubMed PMID: 18663351.
136. Breitkopf K, Roeyen C, Sawitza I, Wickert L, Floege J, Gressner AM. Expression patterns of PDGF-A, -B, -C and -D and the PDGF-receptors alpha and beta in activated rat

hepatic stellate cells (HSC). Cytokine. 2005;31(5):349-57. doi: S1043-4666(05)00193-6 [pii] 10.1016/j.cyto.2005.06.005. PubMed PMID: 16039137.
137. Johnson S, Rabinovitch P. Ex vivo imaging of excised tissue using vital dyes and confocal microscopy. Curr Protoc Cytom. 2012;Chapter 9:Unit 9.39. doi: 10.1002/0471142956.cy0939s61. PubMed PMID: 22752953; PubMed Central PMCID: PMCPMC3401092.
138. Rockey DC, Boyles JK, Gabbiani G, Friedman SL. Rat hepatic lipocytes express smooth muscle actin upon activation in vivo and in culture. J Submicrosc Cytol Pathol. 1992;24(2):193-203. PubMed PMID: 1600511.
139. Yamaoka K, Nouchi T, Marumo F, Sato C. Alpha-smooth-muscle actin expression in normal and fibrotic human livers. Dig Dis Sci. 1993;38(8):1473-9. PubMed PMID: 8344103.
140. Heldin CH, Westermark B. Mechanism of action and in vivo role of platelet-derived growth factor. Physiol Rev. 1999;79(4):1283-316. PubMed PMID: 10508235.
141. Friedman SL, Arthur MJ. Activation of cultured rat hepatic lipocytes by Kupffer cell conditioned medium. Direct enhancement of matrix synthesis and stimulation of cell proliferation via induction of platelet-derived growth factor receptors. J Clin Invest. 1989;84(6):1780-5. doi: 10.1172/JCI114362. PubMed PMID: 2556445; PubMed Central PMCID: PMCPMC304055.
142. Krampert M, Heldin CH, Heuchel RL. A gain-of-function mutation in the PDGFR-beta alters the kinetics of injury response in liver and skin. Lab Invest. 2008;88(11):1204-14. doi: 10.1038/labinvest.2008.81. PubMed PMID: 18762776.
143. Bell RD, Winkler EA, Sagare AP, Singh I, LaRue B, Deane R, Zlokovic BV. Pericytes control key neurovascular functions and neuronal phenotype in the adult brain and during brain aging. Neuron. 2010;68(3):409-27. doi: 10.1016/j.neuron.2010.09.043. PubMed PMID: 21040844; PubMed Central PMCID: PMCPMC3056408.
144. Uhlen M, Oksvold P, Fagerberg L, Lundberg E, Jonasson K, Forsberg M, Zwahlen M, Kampf C, Wester K, Hober S, Wernerus H, Björling L, Ponten F. Towards a knowledge-based Human Protein Atlas. Nat Biotechnol. 2010;28(12):1248-50. doi: 10.1038/nbt1210-1248. PubMed PMID: 21139605.
145. Teo YL, Ho HK, Chan A. Risk of tyrosine kinase inhibitors-induced hepatotoxicity in cancer patients: A meta-analysis. Cancer Treat Rev. 2013;39(2):199-206. doi: 10.1016/j.ctrv.2012.09.004. PubMed PMID: 23099278.
146. Hasinoff BB, Patel D. The lack of target specificity of small molecule anticancer kinase inhibitors is correlated with their ability to damage myocytes in vitro. Toxicol Appl Pharmacol. 2010;249(2):132-9. doi: 10.1016/j.taap.2010.08.026. PubMed PMID: 20832415.
147. Janssen BJ, Malinauskas T, Weir GA, Cader MZ, Siebold C, Jones EY. Neuropilins lock secreted semaphorins onto plexins in a ternary signaling complex. Nat Struct Mol Biol. 2012;19(12):1293-9. doi: 10.1038/nsmb.2416. PubMed PMID: 23104057; PubMed Central PMCID: PMCPMC3590443.
148. Andrae J, Ehrencrona H, Gallini R, Lal M, Ding H, Betsholtz C. Analysis of mice lacking the heparin-binding splice isoform of platelet-derived growth factor a. Mol Cell Biol. 2013;33(20):4030-40. doi: 10.1128/MCB.00749-13. PubMed PMID: 23938297.
149. Gronwald RG, Grant FJ, Haldeman BA, Hart CE, O'Hara PJ, Hagen FS, Ross R, Bowen-Pope DF, Murray MJ. Cloning and expression of a cDNA coding for the human platelet-derived growth factor receptor: evidence for more than one receptor class. Proc Natl Acad Sci U S A. 1988;85(10):3435-9. PubMed PMID: 2835772; PubMed Central PMCID: PMCPMC280226.
150. Kelly JD, Haldeman BA, Grant FJ, Murray MJ, Seifert RA, Bowen-Pope DF, Cooper JA, Kazlauskas A. Platelet-derived growth factor (PDGF) stimulates PDGF receptor subunit dimerization and intersubunit trans-phosphorylation. J Biol Chem. 1991;266(14):8987-92. PubMed PMID: 1709159.

151. de Jong LA, Uges DR, Franke JP, Bischoff R. Receptor-ligand binding assays: technologies and applications. J Chromatogr B Analyt Technol Biomed Life Sci. 2005;829(1-2):1-25. doi: 10.1016/j.jchromb.2005.10.002. PubMed PMID: 16253574.
152. Shim AH, Liu H, Focia PJ, Chen X, Lin PC, He X. Structures of a platelet-derived growth factor/propeptide complex and a platelet-derived growth factor/receptor complex. Proc Natl Acad Sci U S A. 2010;107(25):11307-12. doi: 1000806107 [pii]10.1073/pnas.1000806107. PubMed PMID: 20534510; PubMed Central PMCID: PMCPMC2895058.
153. Fischer WH, Schubert D. Characterization of a novel platelet-derived growth factor-associated protein. J Neurochem. 1996;66(5):2213-6. PubMed PMID: 8780057.
154. Zemskov EA, Loukinova E, Mikhailenko I, Coleman RA, Strickland DK, Belkin AM. Regulation of platelet-derived growth factor receptor function by integrin-associated cell surface transglutaminase. J Biol Chem. 2009;284(24):16693-703. doi: 10.1074/jbc.M109.010769. PubMed PMID: 19386600; PubMed Central PMCID: PMCPMC2713562.
155. Martin IV, Borkham-Kamphorst E, Zok S, van Roeyen CR, Eriksson U, Boor P, Hittatiya K, Fischer HP, Wasmuth HE, Weiskirchen R, Eitner F, Floege J, Ostendorf T. Platelet-derived growth factor (PDGF)-C neutralization reveals differential roles of PDGF receptors in liver and kidney fibrosis. Am J Pathol. 2013;182(1):107-17. doi: 10.1016/j.ajpath.2012.09.006. PubMed PMID: 23141925.
156. Ganat YM, Silbereis J, Cave C, Ngu H, Anderson GM, Ohkubo Y, Ment LR, Vaccarino FM. Early postnatal astroglial cells produce multilineage precursors and neural stem cells in vivo. J Neurosci. 2006;26(33):8609-21. doi: 10.1523/JNEUROSCI.2532-06.2006. PubMed PMID: 16914687.
157. Hernández-Gea V, Ghiassi-Nejad Z, Rozenfeld R, Gordon R, Fiel MI, Yue Z, Czaja MJ, Friedman SL. Autophagy releases lipid that promotes fibrogenesis by activated hepatic stellate cells in mice and in human tissues. Gastroenterology. 2012;142(4):938-46. doi: 10.1053/j.gastro.2011.12.044. PubMed PMID: 22240484; PubMed Central PMCID: PMCPMC3439519.
158. Schuler M, Dierich A, Chambon P, Metzger D. Efficient temporally controlled targeted somatic mutagenesis in hepatocytes of the mouse. Genesis. 2004;39(3):167-72. doi: 10.1002/gene.20039. PubMed PMID: 15282742.
159. Motoike T, Markham DW, Rossant J, Sato TN. Evidence for novel fate of Flk1+ progenitor: contribution to muscle lineage. Genesis. 2003;35(3):153-9. doi: 10.1002/gene.10175. PubMed PMID: 12640619.
160. Clausen BE, Burkhardt C, Reith W, Renkawitz R, Förster I. Conditional gene targeting in macrophages and granulocytes using LysMcre mice. Transgenic Res. 1999;8(4):265-77. PubMed PMID: 10621974.
161. Ferns GA, Sprugel KH, Seifert RA, Bowen-Pope DF, Kelly JD, Murray M, Raines EW, Ross R. Relative platelet-derived growth factor receptor subunit expression determines cell migration to different dimeric forms of PDGF. Growth Factors. 1990;3(4):315-24. PubMed PMID: 2175209.
162. Chen W, Delrow J, Corrin P, Frazier J, Soriano P. Identification and validation of PDGF transcriptional targets by microarray-coupled gene-trap mutagenesis. Nat Genet. 2004;36(3):304-12. doi: ng1306 [pii]10.1038/ng1306. PubMed PMID: 14981515.
163. Klinghoffer RA, Mueting-Nelsen PF, Faerman A, Shani M, Soriano P. The two PDGF receptors maintain conserved signaling in vivo despite divergent embryological functions. Mol Cell. 2001;7(2):343-54. PubMed PMID: 11239463.
164. Fang L, Yan Y, Komuves LG, Yonkovich S, Sullivan CM, Stringer B, Galbraith S, Lokker NA, Hwang SS, Nurden P, Phillips DR, Giese NA. PDGF C is a selective alpha platelet-derived

growth factor receptor agonist that is highly expressed in platelet alpha granules and vascular smooth muscle. Arterioscler Thromb Vasc Biol. 2004;24(4):787-92. PubMed PMID: 15061151.
165. Kaplan DR, Chao FC, Stiles CD, Antoniades HN, Scher CD. Platelet alpha granules contain a growth factor for fibroblasts. Blood. 1979;53(6):1043-52. PubMed PMID: 444648.
166. Raines EW. PDGF and cardiovascular disease. Cytokine Growth Factor Rev. 2004;15(4):237-54. doi: S1359610104000140 [pii]10.1016/j.cytogfr.2004.03.004. PubMed PMID: 15207815.
167. Breitkopf K, Roeyen C, Sawitza I, Wickert L, Floege J, Gressner AM. Expression patterns of PDGF-A, -B, -C and -D and the PDGF-receptors alpha and beta in activated rat hepatic stellate cells (HSC). Cytokine. 2005;31(5):349-57. doi: S1043-4666(05)00193-6 [pii] 10.1016/j.cyto.2005.06.005. PubMed PMID: 16039137.

168. Ding H, Wu X, Boström H, Kim I, Wong N, Tsoi B, O'Rourke M, Koh G, Soriano P, Betsholtz C, Hart T, Marazita M, Field L, Tam P, Nagy A. A specific requirement for PDGF-C in palate formation and PDGFR-alpha signaling. Nat Genet. 2004;36(10):1111-6. doi: ng1415 [pii] 10.1038/ng1415. PubMed PMID: 15361870.